

Optimization and Characterization of the Antimalarial Activity of *N*-Aryl Acetamides that are Susceptible to Mutations in ROM8 and CSC1

William Nguyen, Coralie Boulet, Madeline G. Dans, Katie Loi, Kate E. Jarman, Claudia B. G. Barnes, Tomas Yeo, Tanaya Sheth, Partha Mukherjee, Arnish Chakraborty, Mufuliat T. Famodimu, Michael J. Delves, Harry Pollard, Colin J. Sutherland, Rachael Coyle, Nicole Sevileno, Nonlawat Boonyalai, Marcus C. S. Lee, Tayla Rabie, Lyn-Marié Birkholtz, Delphine Baud, Stephen Brand, Mrityika Chowdury, Tania F. de Koning-Ward, David A. Fidock, Paul R. Gilson, and Brad E. Sleebs*



Cite This: <https://doi.org/10.1021/acs.jmedchem.5c01471>



Read Online

ACCESS |



Metrics & More

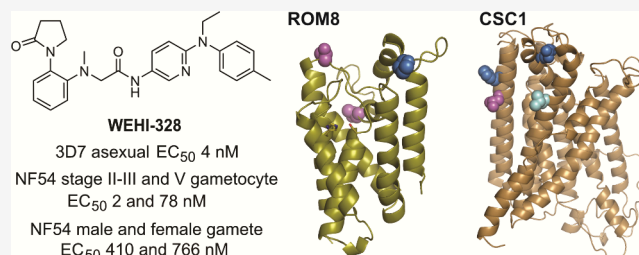


Article Recommendations



Supporting Information

ABSTRACT: New antimalarials are needed due to the threat of emerging resistance against existing antimalarial therapies. A phenotypic screen uncovered the *N*-aryl acetamide class that inhibits the development of *P. falciparum* asexual ring-stage parasites. The structure–activity relationship of this class was investigated, and key modifications were introduced that produced WEHI-326 with potent antimalarial activity. Enhancing the metabolic stability of this class will be a future challenge to achieve efficacy in a malaria mouse model. WEHI-326 was found to have a moderate barrier to resistance and a moderate rate of asexual kill, potently inhibited gametocyte and gamete development, and in turn, blocked the transmission of parasites to the mosquito. Forward genetics and cross-resistance profiling determined that parasites resistant to *N*-aryl acetamides had mutations in rhomboid protease 8 (ROM8) and the putative cation channel, CSC1. WEHI-326 will be an important tool in unraveling the role of ROM8 and CSC1 in *P. falciparum* development.



INTRODUCTION

Malaria is a devastating disease that causes significant human morbidity and mortality. Malaria is caused by the *Plasmodium* parasite, of which *P. falciparum* is the most prevalent, accounting for the most cases and deaths. Only recently, the first vaccines to prevent malaria have been approved; however, they are relatively expensive, require cold-chain, do not give complete protection, and immunity is short-lived.^{1,2} The treatment of malaria has historically been reliant on quinoline-based antimalarials but the over-reliance on this drug class has seen the emergence of resistance, reducing their effectiveness and widespread use.³ Artemisinin combination therapies (ACTs) are now the frontline therapy against malaria, although resistance has emerged in Southeast Asia⁴ and more recently in sub-Saharan Africa,⁵ delaying the clearance of parasitemia in patients treated with ACTs.

At the turn of the century, academia and industry worked together collaboratively to mass-screen compound libraries against the malaria parasite to uncover new starting points for antimalarial development. From this endeavor, several new chemotypes were developed with novel mechanisms of action that target multiple stages of the parasite lifecycle.^{6,7} The most

promising antimalarial candidates that are aligned with target product profile criteria⁸ have entered human clinical trials and some have shown promising efficacy in human challenge models and field trials.⁹ Clinical assessment of other candidates has been halted due to pharmacokinetic or safety issues, and concerning resistant parasites were detected in patients treated with compounds that target PfATP4 and DHODH.⁶ The emergence of resistance with clinically used antimalarials and the attrition rate of candidates in clinical trials underscores the need to uncover and develop new starting antimalarial chemotypes that ideally have new mechanisms of action and target multiple stages of the parasite's lifecycle.

The lifecycle of the malaria parasite broadly consists of the liver stage, asexual blood stage, and the sexual blood stage or

Received: May 30, 2025

Revised: June 26, 2025

Accepted: July 2, 2025

transmission stage that are closely aligned with, respectively, prophylaxis, curative and mass-administered transmission control antimalarial target candidate, and product profiles.⁸ The asexual blood stage is the most important in developing a curative treatment and has several steps that can be interrupted for antimalarial design. The process in which the merozoite form of the parasite enters the host red blood cell is governed by several intricate steps that involve numerous interactions with proteins on the surface of the red blood cell and the merozoite.^{10,11} Once inside the red blood cell, the parasite develops into a ring stage form and then transitions through a trophozoite and then a schizont stage over 48 h. The merozoites then exit from the schizont and the red blood cell—a process that requires the maturation of many effector proteins.¹² Given the critical nature of the invasion of and egress from the red blood cell, compounds that block these key events would be reasonable candidates for antimalarial development. For example, plasmepsin IX and X inhibitors that prevent the maturation of invasion and egress ligands and stop invasion and egress¹³ have recently transitioned to human clinical trials.¹⁴

To uncover compounds that inhibit invasion and egress, an assay was developed that utilizes parasites that express nanoluciferase to detect merozoite egress and invasion and subsequent ring-stage development.¹⁵ This assay was used to screen the Medicines for Malaria Venture (MMV) Pathogen Box that contains compounds selected based on their known activity against various infectious pathogens including malaria.¹⁶ A cohort of these compounds have unknown mechanisms of action making them intriguing starting points to explore their mode of action. The screen of the Pathogen Box uncovered several hit compounds that either impacted parasite egress or invasion.¹⁵ Several of the hit compounds have been investigated in prior studies including the sulfonyl piperazine class that targets the actin-myosin invasion engine of the parasite,^{17,18} and the amino acetamide class that engages the lipid transport protein PfSTART1, which is important for early ring stage development.^{19,20} MMV020512 (**1**), which is from the *N*-aryl acetamide structural class (Figure 1), was also

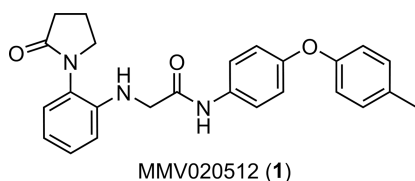


Figure 1. Structure of MMV020512 (**1**).

identified from the screen. MMV020512 (**1**) exhibited modest activity in a 72 h asexual parasite assay (EC_{50} 0.810 μ M) and exhibited low cytotoxicity against human HepG2 cells (CC_{50} 14.3 μ M). Further phenotyping established that MMV020512 (**1**) modestly inhibited the growth of ring stage and trophozoite parasites, and was likely not just specific for merozoite invasion or egress from the red blood cell.¹⁵ The *N*-aryl acetamide series had not been previously explored from an antimalarial development nor a mechanism of action standpoint, making it a worthy scaffold to further investigate.

Here we establish the structure–activity relationship toward optimizing the antimalarial activity of the *N*-aryl acetamide series while monitoring the human HepG2 cell cytotoxicity. We also assessed the in vitro ADME properties to determine

the suitability of the scaffold for administration into a malaria mouse model and its antimalarial development potential. We utilized forward genetics to uncover genetic determinants responsible for the observed parasite resistance. We then profiled analogs against resistant parasites to further confirm protein targets responsible for parasite resistance. Finally, we characterized the activity of the *N*-aryl acetamide series across the lifecycle of the parasite and suggest possible future therapeutic and tool compound applications for this compound class.

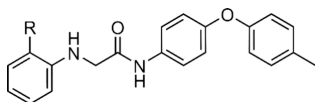
RESULTS AND DISCUSSION

Structure–Activity Relationship. We sought to establish the importance of functionality on the *N*-aryl acetamide scaffold for antimalarial activity by evaluating compounds against the *P. falciparum* 3D7 asexual stage parasite over 72 h using lactate dehydrogenase (LDH) as a maker for parasite growth. The cytotoxicity of compounds was also monitored against human HepG2 cells using Cell Titer Glo as a measure of cell growth. Metabolic stability and aqueous solubility of selected compounds were also assessed to determine their suitability for dosing in a mouse efficacy model.

We first investigated the importance of the lactam moiety on antimalarial activity. Exchanging the 5-membered lactam on analog MMV020512 (**1**) (EC_{50} 0.810 μ M) for a 6-membered lactam (**2**) gave a 3-fold loss in antimalarial activity (EC_{50} 2.50 μ M) (Table 1). Replacement of the 5-membered lactam with a pyridone, or a 5-membered or 6-membered cyclic sulfonamide (**3–5**) resulted in a loss of activity (EC_{50} >10 μ M). The cyclic carbamate variant **6** exhibited similar antiparasitic activity (EC_{50} 0.958 μ M) to compound **1**. The inclusion of *N*-pyrrolidine, *N*-pyrazole, and 2-methoxy *N*-pyrazole groups in analogs **7**, **8**, and **10** also resulted in a loss in activity (EC_{50} >10 μ M), signifying the carbonyl on the lactam was important for antiparasitic activity. The *N*-triazole analog **9** was the exception, exhibiting a 2-fold loss in antimalarial activity (EC_{50} 1.93 μ M) compared to compound **1**. These data suggest that the 5-membered lactam appeared optimal for antimalarial activity. Modest human HepG2 activity (CC_{50} 8.6–15.0 μ M) was observed for lactam analogs **1**, **2**, and **6**, while the cytotoxicity was ablated (CC_{50} >40 μ M) with the *N*-triazole analog **9**.

The substitution on the pendant aryl ring was next explored. It was shown that the analog **11** with no substitution was inactive (EC_{50} >10 μ M) (Table 2), signifying that the 4-methyl substitution on compound **1** was important for antimalarial activity. Analogs **12**, **13**, **15**, and **16** with 4-fluoro, 4-chloro, 4-nitrile and 4-methoxy were 2- to 4-fold less active (EC_{50} 1.40–4.15 μ M) than compound **1**, while analog **14** with a 4-trifluoromethyl group was inactive (EC_{50} >10 μ M). Analogs **17–20** with methyl or chloro substitution in the 2- or 3-positions were also inactive (EC_{50} >10 μ M). These data imply that the pendant aryl ring is sensitive to change, and substitution with groups that have a small steric volume in the 4-position is required for antimalarial activity. Analog **12** with 4-fluoro substitution had similar activity against human HepG2 cells (CC_{50} 5.3 μ M) compared to its antimalarial activity, while analogs **13** and **15** had greater selectivity windows (CC_{50} 16.8–>40 μ M).

The amino acetamide moiety was next examined. It was shown that the derivative **21** with *N*-methyl substitution gave a slight improvement in antimalarial activity (EC_{50} 0.503 μ M) relative to compound **1** (Table 3), whereas compound **22** with

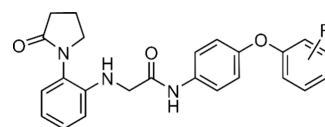
Table 1. Activity of Analogs with Modification to the *N*-Pyrrolidinone

compound	R	Pf parasite EC ₅₀ (SD) μM ^a	HepG2 CC ₅₀ (SD) μM ^b
1		0.810 (0.033)	14.3 (3.6)
2		2.50 (1.02)	15 (3.2)
3		>10	-
4		>10	-
5		>10	-
6		0.958 (0.321)	8.6 (1.0)
7		>10	-
8		>10	-
9		1.93 (0.94)	>40
10		>10	-

^aEC₅₀ data represent means and SDs for 3 or more experiments measuring LDH activity of *P. falciparum* 3D7 asexual parasites following exposure to compounds for 72 h. ^bCC₅₀ data represents mean and SD for 4 or more technical experiments measuring human HepG2 cell viability over 48 h using Cell Titer-Glo.

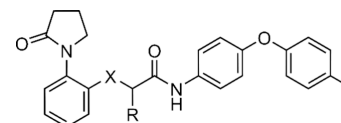
N-ethyl substitution exhibited a slight reduction in activity (EC₅₀ 1.16 μM). Replacing the amino functionality with oxygen (23) resulted in a 2-fold reduction in activity (EC₅₀ 1.57 μM). Analogs 24 and 25 with either methyl or dimethyl substitution on the acetamide alpha-carbon were both inactive (EC₅₀ >10 μM). These data suggest that amino acetamide moiety is tolerant of *N*-methyl substitution but not substitution on the acetamide backbone. Switching from the unsubstituted amino group to an oxygen or a substituted amine resulted in a significant reduction in activity against the human HepG2 cell line (CC₅₀ >40 μM). As a result, the *N*-methyl substitution was maintained on the *N*-amino acetamide for the remainder of the study.

We next probed the importance of the oxygen in the phenolic linker for antimalarial activity. The exchange of the phenolic oxygen for an *N*-methyl group (26) gave a 14-fold improvement in antimalarial activity (EC₅₀ 0.036 μM) (Table 4). Analogs 27 and 28 with an unsubstituted carbon or a methyl-substituted carbon exhibited approximately the same activity (EC₅₀ 0.728 and 0.455 μM) as compound 21, whereas

Table 2. Activity of Analogs with Varying Substitution on the Terminal Phenoxy Ring

compound	R	Pf parasite EC ₅₀ (SD) μM ^a	HepG2 CC ₅₀ (SD) μM ^b
1	4-Me	0.810 (0.033)	14.3 (3.6)
11 (WEHI-907)	H	>10	-
12	4-F	3.08 (1.66)	5.3 (0.7)
13	4-Cl	1.67 (0.75)	16.8 (2.4)
14	4-CF ₃	>10	-
15	4-CN	1.40 (0.17)	>40
16	4-OMe	4.15 (1.56)	-
17	3-Me	>10	-
18	3-Cl	>10	>40
19	2-Me	>10	-
20	2-Cl	>10	-

^aEC₅₀ data represent means and SDs for 3 or more experiments measuring LDH activity of *P. falciparum* 3D7 asexual parasites following exposure to compounds for 72 h. ^bCC₅₀ data represents mean and SD for 4 or more technical experiments measuring human HepG2 cell viability over 48 h using Cell Titer-Glo.

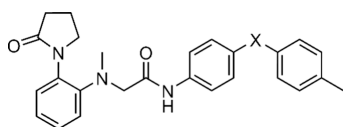
Table 3. Activity of Analogs with Variations to the *N*-Acetamide Moiety

compound	X	R	Pf parasite EC ₅₀ (SD) μM ^a	HepG2 CC ₅₀ (SD) μM ^b
1	NH	H	0.810 (0.033)	14.3 (3.6)
21	NMe	H	0.503 (0.255)	>40
22	NEt	H	1.16 (0.29)	>40
23	O	H	1.57 (0.55)	>40
24	NH	Me	>10	-
25	NH	(DiMe)	>10	-

^aEC₅₀ data represent means and SDs for 3 or more experiments measuring LDH activity of *P. falciparum* 3D7 asexual parasites following exposure to compounds for 72 h. ^bCC₅₀ data represents mean and SD for 4 or more technical experiments measuring human HepG2 cell viability over 48 h using Cell Titer-Glo.

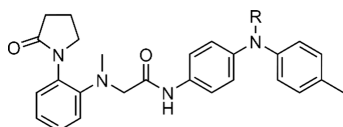
analog 29 with a dimethyl substituted carbon was 2-fold more potent (EC₅₀ 0.215 μM). Moreover, analog 30 with a hydroxy-substituted carbon was 10-fold less active (EC₅₀ 4.83 μM), suggesting polar groups on this moiety were not tolerated. None of the analogs 26–30 exhibited toxicity toward the human HepG2 cell line (CC₅₀ >40 μM).

Given the *N*-methyl group in place of the phenolic linker significantly increased antimalarial activity, we further examined other *N*-substitutions in this position. Analogs 31–33 (WEHI-326) with an *N*-ethyl, *N*-*n*-propyl, or *N*-isopropyl group lead to slight incremental increases in antimalarial activity (EC₅₀ 0.019–0.005 μM) (Table 5) compared to the *N*-methyl derivative 26. Analogs 34–36 with *N*-substitution larger than an isopropyl group were equipotent (EC₅₀ 0.031–0.035 μM) compared to the *N*-methyl progenitor 26, although

Table 4. Activity of Analogs with Modification of the Aryl Linking Atom

compound	X	Pf parasite EC ₅₀ (SD) μM ^a	HepG2 CC ₅₀ μM ^b
21	O	0.503 (0.255)	>40
26	NMe	0.036 (0.005)	>40
27	CH ₂	0.728 (0.196)	>40
28	CH(Me)	0.455 (0.159)	>40
29	C(Me) ₂	0.215 (0.070)	>40
30	CH(OH)	4.83 (1.19)	>40

^aEC₅₀ data represent means and SDs for 3 or more experiments measuring LDH activity of *P. falciparum* 3D7 asexual parasites following exposure to compounds for 72 h. ^bCC₅₀ data represents mean and SD for 4 or more technical experiments measuring human HepG2 cell viability over 48 h using Cell Titer-Glo.

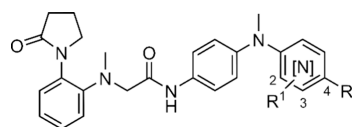
Table 5. Activity of Analogs with Varying Substitution on the Aryl Linking Nitrogen

compound	R	Pf parasite EC ₅₀ (SD) μM ^a	HepG2 CC ₅₀ (SD) μM ^b
26	Me	0.036 (0.005)	>40
31	Et	0.019 (0.010)	>40
32	nPr	0.010 (0.002)	27 (1.4)
33 (WEHI-326)	iPr	0.005 (0.001)	>40
34	cyPen	0.035 (0.010)	>40
35	iBu	0.031 (0.009)	>40
36	nBu	0.035 (0.007)	>40
37	secBu	0.014 (0.005)	>40

^aEC₅₀ data represent means and SDs for 3 or more experiments measuring LDH activity of *P. falciparum* 3D7 asexual parasites following exposure to compounds for 72 h. ^bCC₅₀ data represents mean and SD for 4 or more technical experiments measuring human HepG2 cell viability over 48 h using Cell Titer-Glo.

analog 37 was the exception exhibiting a 2-fold increase in activity (EC₅₀ 0.014 μM). These modifications were not accompanied by an increase in human HepG2 cytotoxicity (CC₅₀ >40 μM), nor did WEHI-326 (55) exhibit hemolysis of nonparasitized red blood cells (Figure S14).

With the incorporation of an *N*-methyl group on both the *N*-acetamide and the biaryl linker moieties, we examined the effects of pendent aryl ring disubstitution on antimalarial activity. Noting the 4-chloro or 4-methyl substitution (26 and 38) were important for antimalarial activity (EC₅₀ 0.036 and 0.053 μM), 4-substitution was maintained while varying substitution in the 2- or 3-position. It was found that analogs 39–44 with combinations of fluoro or chloro in the 2- or the 3-position with a 4-substituent were all relatively equipotent (EC₅₀ 0.020–0.084 μM) (Table 6). Endocyclic nitrogens were next trialed in the 2- and 3-positions of the pendant ring, although these analogs, 45 and 46, exhibited 100-fold and 15-fold decreases in antimalarial activity (EC₅₀ 4.00 and 0.543

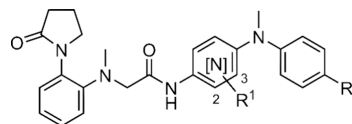
Table 6. Activity of Analogs with Modifications to the Terminal Aryl Ring

compound	R ¹	R ²	Pf parasite EC ₅₀ (SD) μM ^a	HepG2 CC ₅₀ μM ^b
26	H	Me	0.036 (0.005)	>40
38	H	Cl	0.053 (0.017)	>40
39	2-F	Me	0.020 (0.006)	>40
40	3-F	Me	0.026 (0.004)	>40
41	3-Cl	Me	0.031 (0.005)	>40
42	3-Cl	Cl	0.061 (0.015)	>40
43	3-F	Cl	0.084 (0.013)	>40
44	3-F	F	0.051 (0.016)	>40
45	2-N	Me	4.00 (0.23)	>40
46	3-N	Me	0.543 (0.142)	>40

^aEC₅₀ data represent means and SDs for 3 or more experiments measuring LDH activity of *P. falciparum* 3D7 asexual parasites following exposure to compounds for 72 h. ^bCC₅₀ data represents mean for 4 or more technical experiments measuring HepG2 viability over 48 h using Cell Titer-Glo.

μM), demonstrating the preference for hydrophobic substitution on the pendant ring system.

We next explored substitutions on the central aryl ring system while maintaining an *N*-methyl group on both the *N*-acetamide and the biaryl linker moieties. It was shown that the analog 48 with chloro substitution in the 2-position of the central aryl ring exhibited a 10-fold decrease in antiparasitic activity (EC₅₀ 0.338 μM), but strikingly, the analog 47 with a 2-fluoro substituent gave a 10-fold increase in antimalarial activity (EC₅₀ 0.003 μM) compared to the progenitor 26 (Table 7). Derivatives 49 and 50, with a fluoro and chloro in the 2-position of the central ring, both exhibited significantly decreased antimalarial activity (EC₅₀ 0.623 and 0.418 μM). The inclusion of an endocyclic nitrogen was also examined at

Table 7. Activity of Analogs with Modification to the Central Aryl Ring

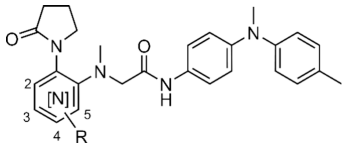
compound	R ¹	R ²	Pf parasite EC ₅₀ (SD) μM ^a	HepG2 CC ₅₀ μM ^b
26	-	Me	0.036 (0.005)	>40
38	-	Cl	0.053 (0.017)	>40
47	2-F	Me	0.003 (0.002)	>40
48	2-Cl	Cl	0.338 (0.160)	>40
49	3-F	Me	0.623 (0.125)	>40
50	3-Cl	Cl	0.418 (0.188)	>40
51	2-N	Me	0.101 (0.007)	>40
52	3-N	Me	0.013 (0.001)	>40

^aEC₅₀ data represent means and SDs for 3 or more experiments measuring LDH activity of *P. falciparum* 3D7 asexual parasites following exposure to compounds for 72 h. ^bCC₅₀ data represents mean for 4 or more technical experiments measuring human HepG2 cell viability over 48 h using Cell Titer-Glo.

these positions. Analog **51** with an endocyclic nitrogen in the 2-position was 3-fold less active (EC_{50} 0.101 μ M) than **26**, whereas analog **52** an endocyclic nitrogen in the 3-position gave a 3-fold increase in antimalarial activity (EC_{50} 0.013 μ M).

We then examined the effect of synthetically tractable modifications on the lactam aryl ring on antimalarial activity. Analogs **53** and **54** with fluoro substitution in the 3- and the 4-positions exhibited comparable antiparasitic potency (EC_{50} 0.016 and 0.034 μ M) to parent analog **26** (Table 8). Analog

Table 8. Activity of Analogs with Modification to the *N*-Pyrrolidinone Aryl Ring



compound	N	R	Pf parasite EC_{50} (SD) μ M ^a	HepG2 CC_{50} μ M ^b
26	-	-	0.036 (0.005)	>40
53	-	3-F	0.016 (0.005)	>40
54	-	4-F	0.034 (0.012)	>40
55	2-N	-	0.030 (0.006)	>40

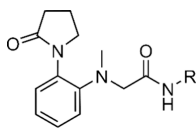
^a EC_{50} data represent means and SDs for 3 or more experiments measuring LDH activity of *P. falciparum* 3D7 asexual parasites following exposure to compounds for 72 h. ^b CC_{50} data represents mean for 4 or more technical experiments measuring HepG2 viability over 48 h using Cell Titer-Glo.

55 with an endocyclic nitrogen in the 2-position was also equipotent (EC_{50} 0.030 μ M). None of the analogs with central aryl ring or lactam aryl ring iterations exhibited measurable activity against the human HepG2 cell line (EC_{50} >40 μ M).

Finally, we combined the components of the central and pendant ring system that contributed to potent antimalarial activity aiming to achieve an additive effect on potency. Analogs **56** and **58** with the inclusion of a fluoro in the 2-position of the central aryl ring and an *N*-isopropyl substituted linker combined with either 3,4-dihalogen substitution or a 4-methyl group on the pendant aryl ring exhibited 5- to 20-fold increase in antimalarial activity (EC_{50} 0.001 and 0.002 μ M) compared to parent analogs **33** (WEHI-326) and **56** (Table 9), while the variant **59** with a 4-nitrile was considerably less active (EC_{50} 0.044 μ M). Derivatives **60** (WEHI-328)–**63** with the inclusion of an endocyclic nitrogen in the 3-position of the central ring system and with a similar set of halogen and methyl combinations on the pendant aryl ring, all exhibited potent antiparasitic activity (EC_{50} 0.001–0.004 μ M), while the variant **64** with the 4-nitrile was slightly less potent (EC_{50} 0.007 μ M). Notably, analogs with a combination of substituents did not exhibit adverse human HepG2 cell cytotoxicity.

Synthesis. The synthesis of the hit compound (**1**) and analogs (**11**–**20**) with iterations on the terminal aryl ring started from 2-bromoaniline (Scheme 1). Ullmann coupling conditions were applied to 2-bromoaniline using 2-pyrrolidinone to afford the *N*-lactam substituted aniline **65**. The amine functionality on **3** was then alkylated using *tert*-butyl bromoacetate in the presence of K_2CO_3 at an elevated temperature to yield the *N*-aryl amino acetate **66**. The *tert*-butyl ester on **66** was then protected under acidic conditions to provide the carboxylic acid **67**, which was then coupled to a

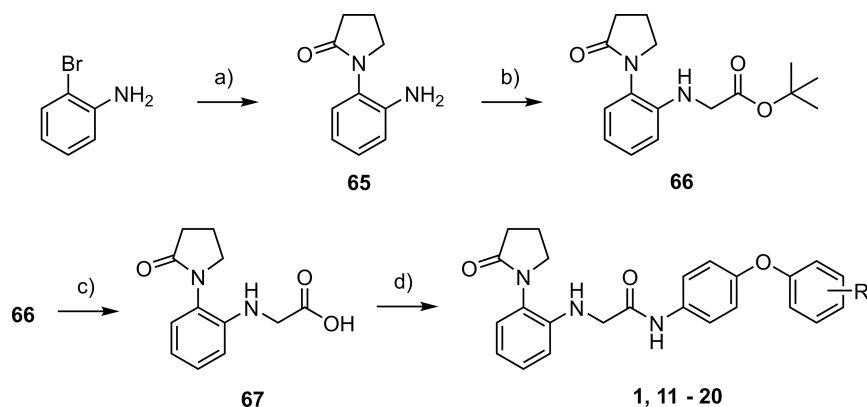
Table 9. Activity of Analogs with a Combination of Modifications to the Aryl Moieties



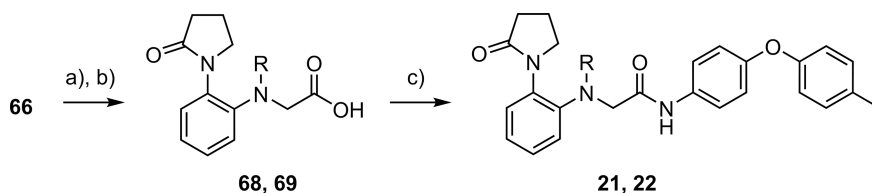
compound	R	Pf parasite EC_{50} (SD) μ M ^a	HepG2 CC_{50} (SD) μ M ^b
77 (WEHI-326)		0.005 (0.001)	>40
56		0.039 (0.010)	>40
57		0.001 (<0.001)	>40
58		0.002 (0.001)	>40
59		0.044 (0.011)	>40
60 (WEHI-328)		0.004 (<0.001)	>40
61		0.003 (0.001)	>40
62		0.001 (<0.001)	>40
63 (WEHI-264)		0.002 (0.001)	>40
64		0.007 (0.003)	>40

^a EC_{50} data represent means and SDs for 3 or more experiments measuring LDH activity of *P. falciparum* 3D7 asexual parasites following exposure to compounds for 72 h. ^b CC_{50} data represents mean and SD for 4 or more technical experiments measuring human HepG2 cell viability over 48 h using Cell Titer-Glo.

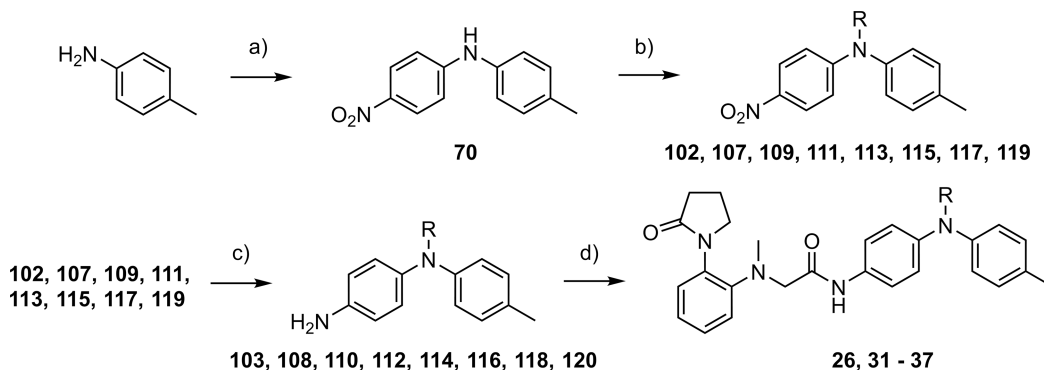
variety of substituted phenol 4-aryl amines to yield a series of *N*-aryl acetamide analogs (**1**, **11**–**20**). Alternatively, the amine functionality on intermediate **66** was alkylated with iodomethane with the addition of K_2CO_3 to give the *N*-methylated amino acetate *tert*-butyl ester that was subsequently deprotected using 4 N HCl in dioxane to afford the carboxylic acid (**68** and **69**) (Scheme 2). The carboxylic acid was then coupled with a range of substituted anilines to give an *N*-substituted analogs **21** and **22**.

Scheme 1. Synthetic Route to Access *N*-Aryl Acetamide Derivatives^a

^aReagents and conditions: (a) 2-bromoaniline, 2-pyrrolidinone, DMEDA, CuI, K₂CO₃, DMF, 80 °C; (b) *tert*-butyl bromoacetate, K₂CO₃, MeCN, 80 °C; (c) 4 M HCl in 1,4-dioxane, 20 °C; (d) HATU, substituted arylamine, DCM, 20 °C. For R groups refer to Table 2.

Scheme 2. Synthetic Route to Access *N*-Substituted Amino Acetamide Analogs^a

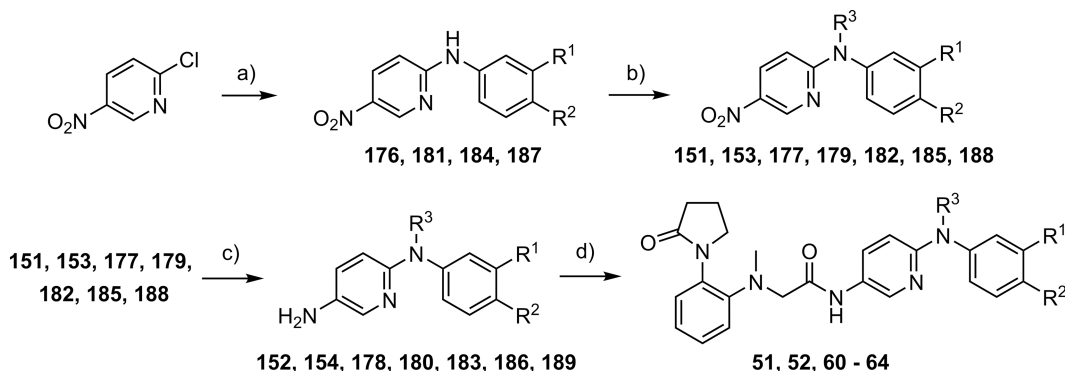
^aReagents and conditions: (a) alkyl halide, K₂CO₃, DMF, 30 °C; (b) 4 M HCl in 1,4-dioxane, 20 °C; (c) HATU, substituted arylamine, DCM, 20 °C. For R groups refer to Table 3.

Scheme 3. Synthesis of *N*-Substituted Biaryl Derivatives^a

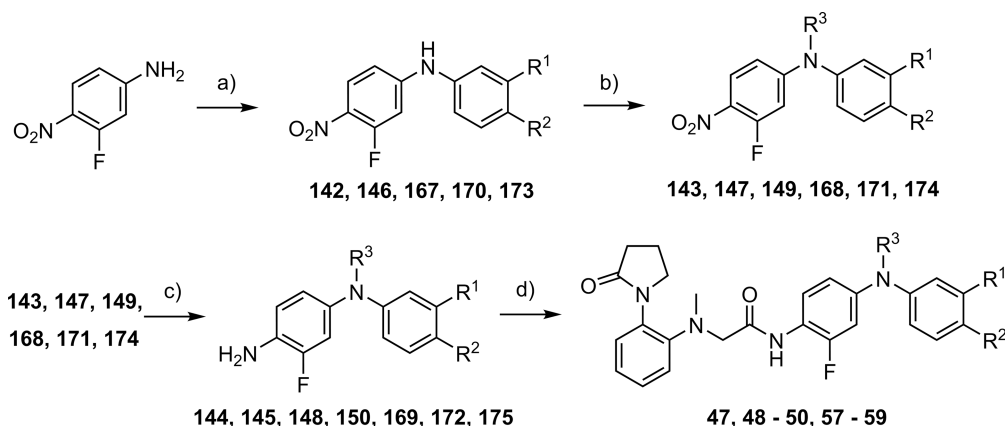
^aReagents and conditions: (a) 1-fluoro-4-nitrobenzene, K₂CO₃, DMSO, 130 °C; (b) alkyl halide, NaH, DMF, 30 °C; (c) Zn, NH₄Cl, H₂O/MeOH (1:1), 40 °C; or cat. Pd/C, EtOH, H₂, 30 °C; (d) 68, HATU, DIPEA, DCM, 20 °C. For R groups refer to Table 5.

To access *N*-substituted biaryl analogs (26, 31–37), the synthesis began with a nucleophilic substitution reaction between 1-fluoro-4-nitrobenzene and 4-methyl aniline at an elevated temperature to afford the *N*-aryl aniline 70 (Scheme 3). The aniline nitrogen was then alkylated with an alkyl halide in the presence of sodium hydride to yield the *N*-substituted aniline (102, 107, 109, 111, 113, 115, 117, 119). The nitro functionality on the aniline was then reduced using zinc dust and ammonium chloride to give the 4-amino aniline (103, 108, 110, 112, 114, 116, 118, 120). The 4-amino aniline was then reacted with the carboxylic acid 68 using HATU and Huning's base to afford a variety of *N*-substituted biaryl analogs (26, 31–37). Synthesis of analogs (51, 52, 60–64) with an endocyclic nitrogen in the central aryl ring followed a similar synthetic route except the synthesis began with a 2-chloro-

pyridine (Scheme 4). The 2-chloro pyridine was subject to a nucleophilic substitution reaction with a substituted aniline to yield the aryl-pyridine (176, 181, 184, 187), which was *N*-alkylated under basic conditions to give *N*-alkylated *N*-arylpyridine (151, 153, 177, 179, 182, 185, 188) and subsequently, the nitro functionality was reduced using Zn and ammonium chloride to give the 5-amino pyridyl intermediate (151, 153, 177, 179, 182, 185, 188). The 5-amino pyridine was reacted with the carboxylic acid 7 using HATU and Huning's base to yield *N*-aryl acetamide *N*-pyridyl analogs (51, 52, 60–64). Analogously, accessing analogs (47–50, 56–59) where the central ring is fluorinated followed the same synthetic pathway, starting from 3-fluoro-4-nitroaniline (Scheme 5). Using a Buchwald reaction, 3-fluoro-4-nitroaniline was reacted with a substituted aryl halide using catalytic

Scheme 4. Synthesis of *N*-Substituted Pyridyl Acetamide Derivatives^a

^aReagents and conditions: (a) substituted aniline, K₂CO₃, DMF, 120 °C; (b) alkyl halide, NaH, DMF, 30 °C; (c) Zn, NH₄Cl, H₂O/MeOH (1:1), 40 °C; or cat. Pd/C, EtOH, H₂, 30 °C; (d) **68**, HATU, DIPEA, DCM, 20 °C. For R¹, R², and R³ groups refer to Tables 7 and 9.

Scheme 5. Synthesis of Fluoro Substituted *N*-Aryl Acetamide Derivatives^a

^aReagents and conditions: (a) substituted aryl halide, Pd(OAc)₂, Xantphos, Cs₂CO₃, 1,4-dioxane, 100 °C; (b) alkyl halide, NaH, DMF, 30 °C; (c) Zn, NH₄Cl, H₂O/MeOH (1:1), 40 °C; (d) **68**, HATU, DIPEA, DCM, 20 °C. For R¹, R², and R³ groups refer to Tables 7 and 9.

palladium acetate and Xantphos under basic conditions to yield the *N*-aryl aniline intermediate (**142**, **146**, **167**, **170**, **173**). The *N*-aryl aniline was *N*-alkylated using sodium hydride and an alkyl halide and to give the *N*-alkylated aniline (**143**, **147**, **149**, **168**, **171**, **174**), and then the nitro functionality was reduced to afford (**144**, **145**, **148**, **150**, **169**, **172**, **175**). The carboxylic acid **7** was then reacted under amide coupling conditions to give the *N*-aryl acetamide analogs (**47–50**, **57–59**). Other syntheses to access intermediates and other bespoke analogs in Tables 1–9, which are too numerous to detail here, are outlined in Schemes S1–S11.

In Vitro ADME Analysis. We assessed the metabolic stability, aqueous solubility and experimental LogD of selected *N*-aryl acetamide analogs with varying structural modifications to determine the suitability for mouse efficacy studies and their potential for future development. The hit compound MMV020512 (**1**) was characterized by rapid turnover in human liver microsomes and rat hepatocytes (CL_{int} 102 μL/min/mg and 58 μL/min/10⁶ cells) (Table 10). Analog **9** also exhibited similar metabolic stability (CL_{int} 98 μL/min/mg and 46 μL/min/10⁶ cells) signifying that replacing the lactam with a triazole did not improve metabolic stability. Incorporation of an *N*-methyl amino acetamide (**21**) reduced metabolic stability (CL_{int} 383 μL/min/mg and >92 μL/min/10⁶ cells) possibly due to oxidative *N*-demethylation. Supporting this notion, replacing the amino acetamide with an oxy-acetamide (**23**)

resulted in improved metabolic stability (CL_{int} 132 μL/min/mg and 68 μL/min/10⁶ cells) relative to analog **21**. Analogs **26** and **29** with either a *N*-methyl or carbon biaryl linker also exhibited low metabolic stability (CL_{int} 347 and 263 μL/min/mg and >92 and 63 μL/min/10⁶ cells) that was similar to compound **21**. Switching the *N*-methyl biaryl linker to an *N*-isopropyl group (WEHI-326, **33**) did not mitigate metabolism (CL_{int} 319 μL/min/mg and >92 μL/min/10⁶ cells) possibly due to the high lipophilicity (eLogD 5.7). Inclusion of halogens to potentially mitigate oxidative metabolism of amino-substituted aryl rings (**43**, **54**, and **57**) did not improve metabolic stability (CL_{int} 218–273 μL/min/mg and 79–>92 μL/min/10⁶ cells), neither did the incorporation of endocyclic nitrogens to each of the aryl rings **52**, **55**, **60**, and **61** (CL_{int} 216–408 μL/min/mg and 86–>92 μL/min/10⁶ cells). Combinations of endocyclic nitrogen with halogens and a nitrile (**63** and **64**) also did not improve metabolic stability (CL_{int} 287 and 309 μL/min/mg and 62 and 92 μL/min/10⁶ cells).

The aqueous solubility of the hit compound MMV020512 (**1**) at physiological pH 7.4 was moderate-to-low (9.1 μM) (Table 10). Most analogs exhibited lower aqueous solubility than the hit compound, particularly those with higher eLogD values. There were several analogs **52**, **55**, **61**, and **64** with endocyclic nitrogens that possessed lower eLogD values (3.7–4.7) and concomitantly higher aqueous solubility (16–44

Table 10. Evaluation of Aqueous Solubility, In Vitro Metabolism and eLogD

compound	solubility pH 7.4 (μM) ^a	human liver microsome CL_{int} ($\mu\text{L}/\text{min}/\text{mg}$)	rat hepatocyte CL_{int} ($\mu\text{L}/\text{min}/10^6$ cells)	eLogD ^b
1	9.1	102	58	4.3
9	15	98	46	4.4
21	4.8	383	>92	4.6
23	4.2	132	68	4.8
26	7.2	347	>92	4.6
29	2.5	263	63	5.1
33				
(WEHI-326)	<2.5	319	>92	5.7
43	<2.5	218	79	5.7
52	44	216	>92	3.8
54	6.3	260	91	5.0
55	16	222	>92	4.1
57	4.3	273	92	5.2
60				
(WEHI-328)	3.4	408	>92	4.4
61	24	270	86	4.7
63				
(WEHI-264)	9.6	287	62	5.0
64	40	309	92	3.7

^aKinetic in PBS. ^bShake-flask method.

μM); however, there were exceptions—solubility was not improved with endocyclic nitrogen analogs **60** and **63** (3.4 and 9.6 μM). It was also observed that despite the high eLogD (5.7), WEHI-326 (**33**) exhibited moderate apical to basolateral Caco-2 permeability (1.09×10^{-6} cm/s), and reasonable basolateral to apical translocation (2.52×10^{-6} cm/s) (Table S1).

Overall, it is plausible that the high lipophilicity of the *N*-aryl acetamide series contributed to the low metabolic stability and aqueous solubility. The other contributing factor to low metabolic stability is the necessity of electron-rich diamino and oxy-amino substituted ring systems for antimalarial activity, which are known sites of oxidative metabolism.²¹ Endocyclic nitrogen incorporation and halogen substitution, which are known on occasions to strategically mitigate oxidative metabolism,²² did not improve the metabolic stability of the *N*-aryl acetamide scaffold. Endocyclic nitrogen inclusion, however, did lower the overall lipophilicity and improve aqueous solubility. We concluded that it would be a challenge to enhance the metabolic stability and aqueous solubility while retaining or enhancing the antiparasitic activity of the *N*-aryl acetamide class.

Minimum Inoculum of Resistance Profiling. The minimum inoculum of resistance (MIR) assay determines the risk of resistance onset by exposing a varying inoculum of parasites to a compound over 60 days.²³ Recrudescing

parasites are then phenotyped to determine EC₅₀ shift and risk of resistance and genotyped to establish the genetic determinants responsible for the resistance to the compound. The EC₅₀ and EC₉₀ WEHI-326 (**33**) against the *P. falciparum* Dd2-B2 clone were experimentally to be 3 nM and 9 nM, respectively (Tables 11 and S2 and Figure S2). One MIR single-step selection was set up by exposing 3.3×10^6 Dd2-B2 parasites in each well of a 24-well plate to $3 \times \text{EC}_{90}$ (27 nM) of WEHI-326 (**33**) for 60 days. Cultures were screened three times weekly by flow cytometry and smearing and wells were considered positive for recrudescence when the overall parasitemia reached 0.3% and parasites were observed by blood smear. Over 60 days, it was found that 12 out of 24 wells recrudescenced between days 14 and 53 (Table S2). Wells A3, A6, and C2 were selected to determine their EC₅₀, and a 182- to 843-fold shift in EC₅₀ values was observed (Table 11 and Figure S2). The MIR was calculated to be 4.0×10^7 (Table S2), which implies the *N*-aryl acetamide series has a moderate risk of resistance.^{23,24}

The recrudescence parasite populations in wells A3, A6, and C2 were then whole genome sequenced to uncover the genetic determinants responsible for the resistance in the MIR study. Single nucleotide polymorphisms (SNPs) were observed in all three samples (Tables S3–S5), with well A3 having a total of 4; the highest of all three samples. The four genes included PF3D7_0527900, PF3D7_0705500, PF3D7_0818200, and PF3D7_1250200. The first, second and fourth genes are putative, coding for ATP-dependent RNA helicase, inositol phosphate phosphatase and a calcium-permeable stress-gated cation channel 1 (CSC1)-like protein, respectively (Tables S4 and S5). The third gene codes for 14-3-3 protein. Well A6 presented with a SNP in PF3D7_1411200 coding for rhomboid protease, ROM8 (Tables S4 and S5). Well C2 had SNPs in PF3D7_1024600 and PF3D7_1250200, both putative genes coding for RAP protein and CSC1-like protein, respectively. All three wells yielded missense mutations. Notably, SNPs in CSC1 were found in both Dd2 A3 and C2 populations, and ROM8 in the Dd2 A6 population, implying that both proteins are likely responsible for the mechanism of resistance or action, though, further evidence was required to confirm whether one or both of these proteins were responsible for the resistance observed in the MIR study.

Cross-Resistance Profiling Using AReBar Assay. The profiles compounds for cross-resistance with unknown modes of action.²⁵ The platform utilizes 52 drug-resistant parasite lines, as well as two wildtype lines, each with a unique genomic barcode integrated into a nonessential locus (Table S6). The pooled parasite lines were exposed to the query compound at $3 \times \text{EC}_{50}$, and flow cytometry was used to monitor growth over the assay period (14 days). The subsequent amplicon sequencing of the pool provided barcode counts that represent the proportion of each line post-treatment, thus identifying any enriched cross-resistant line(s). WEHI-326 (**33**) was subjected

Table 11. Activity against WEHI-326-Resistant *P. falciparum* Strains from the MIR Study

compound	Dd2 EC ₅₀ (\pm SEM) μM ^a	Dd2 WEHI-326-resistant populations EC ₅₀ (\pm SEM) μM ^{a,b}		
		Dd2-Pop A3	Dd2-Pop A6	Dd2-Pop C2
WEHI-326 (33)	0.002 (<0.001)	1.93 (0.24)	0.750 (0.040)	0.417 (0.074)

^aEC₅₀ data represent mean and \pm SEM for 3 experiments measuring SYBR-green of *P. falciparum* 3D7 parasites following exposure to compounds for 72 h. ^bDd2-Pop A3 has a F957L mutation in CSC1; Dd2-Pop A6 has a P534S mutation in ROM8; Dd2-Pop C2 has a R823S mutation in CSC1.

to the AReBar platform, to determine if the *N*-aryl acetamide series was cross-resistant to any mutant lines in the resistome pool.

The resistome pool was exposed to 3× the EC₅₀ of WEHI-326 (33) (0.010 μM) for 14 days. Cumulative growth profiles for compound WEHI-326 (33), a no drug control as well as a positive control using GNF179²⁶ were measured by flow cytometry, with the WEHI-326 (33) treated pool exhibiting growth recovery after day 4 (Figure S3A). Barcode sequencing and differential analysis of the WEHI-326 (33) treated pool versus the day 14 control showed a single line enriched to 98.9% of the total population, with a significant expansion (Log fold change (LFC) > 2.5) of the parasite line, possessing a L800P mutation in CSC1 (Figure S3A–C, and Table S6). To confirm the CSC1 L800P mutant enrichment translates to a detectable shift in resistance compared to the Dd2 wild type, a dose–response assay was undertaken. WEHI-326 (33) showed an EC₅₀ shift of approximately 650-fold against the CSC1 L800P strain (EC₅₀ 3.24 μM) versus the parental Dd2 strain (Table 12 and Figure S4).

Table 12. Activity against the CSC1 Mutant *P. falciparum* Dd2 Strain from the AReBar Study

compound	Dd2 EC ₅₀ (±SEM) μM ^a	CSC1 mutant Dd2 strain EC ₅₀ (±SEM) μM ^{a,b}
WEHI-326 (33)	0.008 (0.002)	3.24 (0.34)

^aEC₅₀ data represent means for 2 technical experiments measuring SYBR-green of *P. falciparum* 3D7 parasites following exposure to compounds for 72 h. ^bDd2 CSC1 mutant strain has a L800P mutation in CSC1. Dose–response data are shown in Figure S6.

The CSC1 L800P mutation was initially uncovered in MMV407834-resistant parasites.²⁷ MMV407834 was originally unearthed in the high throughput screen of the GSK library against *P. falciparum* asexual stage parasites,²⁸ and antimalarial activities were later reported.²⁹ MMV407834 shares distant structural similarity with the *N*-aryl acetamide class, but based on structure–activity analyses are two distinct chemical series, although they share the same CSC1 resistance mechanism.

Mutations in CSC1 were detected in resistant parasite populations from both the MIR and AReBar studies on the *N*-aryl acetamide class supporting CSC1 as the mechanism of resistance or action. However, CSC1 was not detected in the Dd2 A6-resistant MIR population that had a mutation in ROM8, suggesting alternate mechanisms of resistance may be possible. To provide additional evidence on the mechanism, an

independent resistance study was performed on MMV020512 (mentioned in the next section).³⁰

Evaluation against ROM8-Resistant Parasites. Independent from the MIR and AReBar studies undertaken here, a parallel study performed resistance selection on MMV020512 (1) generating the resistant populations 3D7-Pop A, D, and E.³⁰ Whole genome sequencing of the resistant clonal populations revealed 3D7-Pop A had a T622 K mutation in ROM8, 3D7-Pop D had a L954F mutation in CSC1 (and a M1061I mutation in valine tRNA ligase), and 3D7-Pop E had a L562R mutation in ROM8,³⁰ supporting the genetic determinants uncovered in the MIR and AReBar studies on the *N*-aryl acetamide class.

To assess the level of cross-resistance, a selection of *N*-aryl acetamide analogs were evaluated against the MMV020512-resistant populations, 3D7-Pop A, D, and E.³⁰ The analogs 26, 38, 55, 62, and 63 exhibited an approximately 15- to 50-fold reduction in activity against the MMV020512-resistant 3D7-Pop A, D, and E populations (EC₅₀ 0.006–0.643 μM) relative to the parental 3D7 strain (EC₅₀ 0.0002–0.012 μM) (Table 13 and Figure S5). MMV1845852, which belongs to the same structural class as MMV407834, and is a putative inhibitor of CSC1,^{27,29} was used as a control and exhibited an approximately 3-fold shift in activity (EC₅₀ 0.135–0.164 μM) against all MMV020512-resistant 3D7-Pop A, D, and E populations compared to the parental 3D7 strain (EC₅₀ 0.045 μM). Curiously, MMV1845852 has the same level of cross-resistance against Pop A and E as it does against Pop D, which has a mutation in CSC1, signifying that ROM8 and CSC1 may regulate or interact with one another. Collectively, these data imply that during the optimization of the *N*-aryl acetamide class, the susceptibility to CSC1 and ROM8 mutations was maintained.

***P. falciparum* ROM8 and CSC1.** ROM8 is one of 10 rhomboid proteases expressed by the *P. falciparum* parasite of which ROM4, 6, 7, and 8 are essential to asexual stage development.^{31,32} Of the essential rhomboid proteases, ROM4 is the most widely studied and processes ligands that are found on the surface of the merozoite during the invasion of the red blood cell.^{33,34} There are no reports on the function of ROM8 in *Plasmodium* parasites, although ancestral gene orthology predicts it is located on the parasite membrane, whereby the catalytic dyad consisting of catalytic serine and an activating histidine are extracellularly exposed. CSC1 is a putative calcium channel expressed by *Plasmodium* parasites and it is essential for parasite development, as indicated by piggyBac transposon insertional mutagenesis.³⁵ CSC1 is predicted by

Table 13. Evaluation of Compounds against MMV020512-Resistant *P. falciparum* Strains

compound	3D7 EC ₅₀ (SD) μM ^a	3D7 MMV020512-resistant populations EC ₅₀ (SD) μM ^{a,b}		
		3D7-Pop A	3D7-Pop D	3D7-Pop E
MMV020512 (1) ^c	0.338	5.13	10.0	6.05
26	0.003 (0.002)	0.078 (0.031)	0.167 (0.032)	0.158 (0.024)
38	0.012 (0.008)	0.187 (0.078)	0.263 (0.004)	0.423 (0.076)
55	0.007 (0.007)	0.274 (0.191)	0.252 (0.082)	0.643 (0.481)
62	0.0002 (<0.0001)	0.009 (0.010)	0.008 (0.008)	0.006 (0.007)
63	0.0005 (0.0002)	0.011 (0.005)	0.011 (0.004)	0.017 (0.013)
MMV1845852	0.045 (0.010)	0.140 (0.034)	0.135 (0.053)	0.615 (0.666)

^aEC₅₀ data represent means and SDs for 3 experiments measuring LDH activity of *P. falciparum* 3D7 parasites following exposure to compounds for 72 h. ^b3D7-Pop A has a T622 K mutation in ROM8; 3D7-Pop D has a L954F mutation in CSC1; 3D7-Pop E has a L562R mutation in ROM8.³⁰ MMV1845852 was used as a putative control CSC1 inhibitor.^{27,29} ^cData taken from Boulet et al.³⁰ Error values are shown in Figure S5.

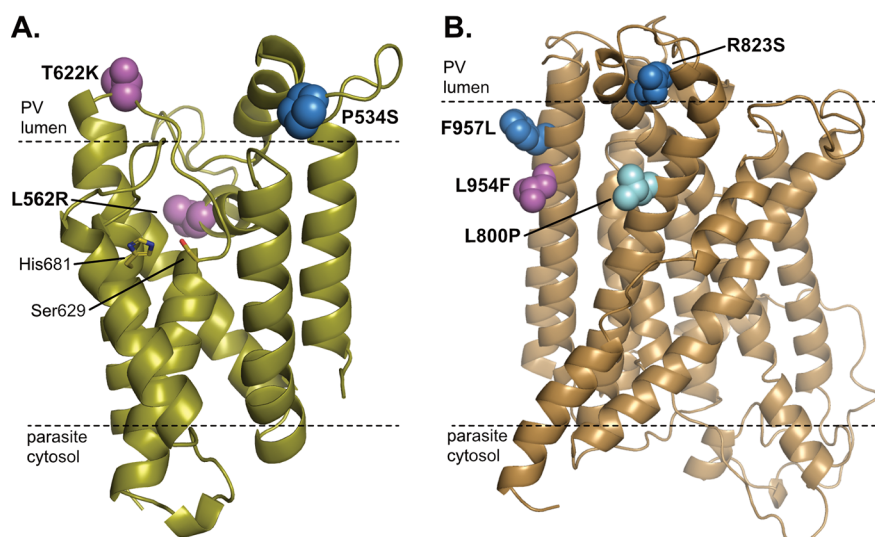


Figure 2. Homology models of *P. falciparum* ROM8 and CSC1 showing the mutations found in MIR, AReBar and MMV020512-resistance studies. **A.** A homology model of *P. falciparum* ROM8 catalytic transmembrane domain showing the location of T622K and L562R mutations (purple) from MMV020512-resistant 3D7-Pop A and D parasites respectively, and the P534S mutation (blue) from WEHI-326-resistant Dd2-Pop A6 parasites from the MIR study. The homology model of *P. falciparum* ROM8 was created from the X-ray structure of *Escherichia coli* GlpG (PDB: 6XRP).³⁴ Amino acids 1–506 and 696–738 are excluded for clarity. **B.** A homology model of *P. falciparum* CSC1 showing the location of the L945F mutation from (purple) from MMV020512-resistant 3D7-Pop D parasites, the L800P mutation (cyan) from the resistant parasite strain from the AReBar study, and the R823S and F957L mutations (blue) from WEHI-326-resistant Dd2-A3 and -C2 parasites respectively from the MIR study. The homology model of *P. falciparum* CSC1 transmembrane domain was created from the X-ray structure of *Arabidopsis thaliana* OSCA (PDB: 8GRN).³⁷ Amino acids 181–686 and 966–1039 were excluded for clarity. The dotted line in both ROM8 and CSC1 models indicates the approximate transmembrane regions and predicted orientation relative to the parasitophorous vacuole (PV) and parasite cytosol.

gene ancestry to be located on the parasite membrane,³⁶ but nothing else is known about this channel.

Mapping of Resistant Mutations to Homology Models of ROM8 and CSC1. Mutations in CSC1 and ROM8 were detected in *N*-aryl acetamide-resistant parasites from three independent studies. To determine if the detected mutations for each of these proteins are in close proximity to one another, these mutations were mapped to either CSC1 or ROM8. Presently, there are no X-ray structures of *P. falciparum* CSC1 or ROM8, or from other *Plasmodium* or related Apicomplexa species, and therefore homology models were created of both *P. falciparum* 3D7 CSC1 and ROM8. The homology model of *P. falciparum* ROM8 (Figure 2A) was generated from the X-ray structure of the *Escherichia coli* GlpG (PDB: 6XRP).³⁴ The homology model of the *P. falciparum* CSC1 transmembrane domain (Figure 2B) was constructed from the X-ray structure of *Arabidopsis thaliana* hyperosmolality-gated Ca^{2+} permeable channel 1 (OSCA1) (PDB: 8GRN).³⁷

The location of T622K and L562R mutations from MMV020512-resistant 3D7-Pop A and D parasites and the P534S mutation from WEHI-326-resistant Dd2-A6 parasites from the MIR study are located around the edge of the catalytic cleft of ROM8, which is predicted to face into the parasitophorous vacuole lumen (Figure 2A). Given the location of the mutations, the aryl *N*-acetamide class may bind in the catalytic cleft of ROM8. There are reports that lactams covalently react with the catalytic serine of rhomboid proteases to inhibit their function,^{38,39} and therefore the lactam moiety of the *N*-aryl acetamide series could also react and inhibit the proteolytic function of ROM8. Further research is required to confirm the inhibitory mechanism.

The L945F mutation from MMV020512-resistant 3D7-Pop D parasites, the L800P mutation from the resistant parasite

strain from the AReBar study, and the R823S and F957L mutations from WEHI-326-resistant Dd2-A3 and -C2 parasites from the MIR study all clustered to a region of CSC1 located in the transmembrane domain orientated toward the parasitophorous vacuole (Figure 2B). The homologous OSCA1 mechanically senses Ca^{2+} hyperosmolality and is predicted to operate as a dimer.⁴⁰ Curiously, the CSC1 mutations are located in the same region where the two OSCA monomers are predicted to interact,⁴⁰ suggesting a possible binding site whereby aryl *N*-acetamide series could inhibit the function of CSC1.

The ROM8 and CSC1 mutations are all located on or toward the PV-facing region of each protein. It is not known if ROM8 and CSC1 interact with one another. There is evidence that the rhomboid-related protein 2 (RHBDL2) processes a motif on the calcium release-activated calcium (CRAC) channel, Orai1 to regulate its function.⁴¹ It is possible that binding of aryl *N*-acetamide series to the ROM8 catalytic cleft inhibits CSC1 processing by ROM8 or prevents it from interacting with CSC1. Overall, further research is required to consolidate these hypotheses, and whether ROM8 and CSC1 are molecular targets or resistance mechanisms of the aryl *N*-acetamide series.

Asexual Stage Rate of Kill. An important criterion for an antimalarial used for treatment is the speed at which it kills the malaria parasite,⁸ which is intrinsically linked to its mechanism of action. We compared the rate of kill of an *N*-aryl acetamide analog with clinically used antimalarials in a parasite reduction ratio (PRR) assay.⁴² In this assay, synchronous *P. falciparum* 3D7 asexual stage parasites were exposed to 10 \times EC₅₀ of WEHI-326 (33) (0.010 μM) for 120 h where the media and the compound were exchanged every 24 h. Parasitemia was then allowed to recover over 28 days, and parasite levels were measured for each 24 h time point using an LDH growth assay.

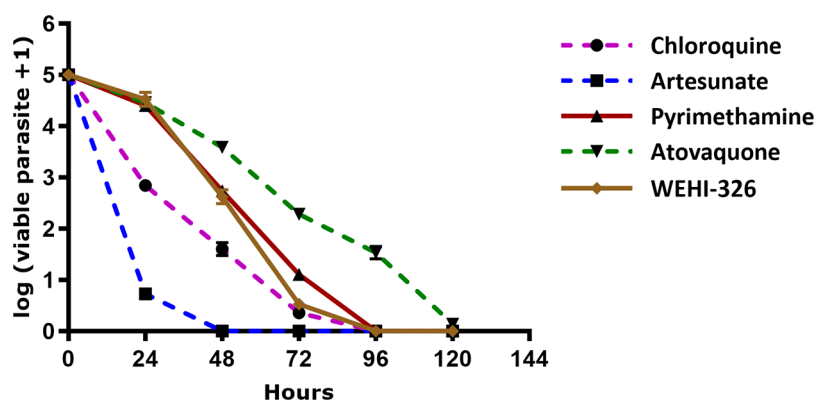


Figure 3. Activity of WEHI-326 (33) was benchmarked against antimalarial drugs in a parasite reduction ratio assay. Data represent the means and SDs of 3 replicate experiments using *P. falciparum* 3D7 parasites using an LDH assay.

WEHI-326 had a 24 h lag phase with a LogPRR of 3.99 and a parasite clearance time (PCT_{99.9%}) of 55.2 h (Figure 3). Parasites were completely cleared by WEHI-326 after 96 h. WEHI-326 (33) was observed to exhibit a moderate killing profile similar to pyrimethamine.

Table 14. Impact of Selected Compounds on the Transition from Invasion to Ring Stage and Egress from the Schizont and the Red Blood Cell

compound	invasion to ring stage EC ₅₀ (SD) μM^a	schizont egress EC ₅₀ μM^a
WEHI-326 (33)	0.006 (0.001)	>10
WEHI-328 (60)	0.005 (0.001)	>10

^aEC₅₀ data represent means and SD of $n = 3$ experiments (each conducted in technical duplicate) measuring the bioluminescence of *P. falciparum* parasites expressing nanoluciferase (nano-Luc) following exposure of compound. Late-stage nano-Luc-expressing schizonts were treated with serially diluted compound for 4 h, during which time merozoite egress and reinvasion occurred. Egress was quantified by measuring the bioluminescent signal intensity of nano-Luc released into the culture medium during drug treatment. After the 4 h egress and invasion window, drugs were removed and parasites were grown until the following trophozoite stage (24 h), at which stage nano-Luc is strongly expressed. The bioluminescent signal intensity of trophozoite lysates indicated the success of invasion during the treatment window.

Inhibition of Invasion to Ring Establishment in Asexual Stage Parasites. MMV020512 (1) was previously shown to impact invasion to ring stage development and schizont egress in an assay that measures the bioluminescence of parasites that express nanoluciferase.¹⁵ To determine if optimized *N*-aryl acetamide analogs inhibit the transition from invasion to ring stage, we assessed selected analogs in the nanoluciferase assay. It was shown that both WEHI-326 (33)

and WEHI-328 (60) potentially inhibited ring stage development (EC₅₀ 0.006 and 0.005 μM) (Table 14 and Figure S6). There was only a partial effect on schizont egress (Figure S6), and therefore an EC₅₀ value was not measurable (Table 14). This asexual stage phenotype was initially reported with MMV020512 (1)¹⁵ and signifies the optimized *N*-aryl acetamide class analogs retain the asexual ring stage killing phenotype.

Transmission Stage Activity. Establishing the activity of an antimalarial across the lifecycle of the malaria parasite is important for assessing its potential to meet a particular target candidate and product profile.⁸ We profiled the activity of selected *N*-aryl acetamide analogs against gametocytes and gametes, which are forms of the parasite that constitute the transmission stage. The activity against both immature (stage II–III) and mature (stage V) gametocytes was determined using transgenic *P. falciparum* lines expressing luciferase, which is used to detect parasite viability over 48 h.⁴³ In the dual gamete formation assay (DGFA), stage V gametocytes were incubated for 48 h with test compounds before gametogenesis triggered by exposure to xanthurenic acid and a decrease in temperature from 37 to 20 °C, which simulates the mosquito midgut environment and induces male and female gametogenesis. Male gametocyte viability was assessed by successful male gamete formation detected by brightfield microscopy capture of the moving exflagellation centers. Female gametocyte viability was measured by successful female gamete formation using fluorescence microscopy to detect cells labeled using a female gamete-specific αPfs25 antibody coupled to a Cy3 fluorophore.⁴⁴ Both analogs 33 (WEHI-326) and 60 (WEHI-328) showed potent activity against immature gametocytes (EC₅₀ 0.006 and 0.002 μM) and against mature gametocytes (EC₅₀ 0.123 and 0.078 μM) (Table 15 and Figure S7). As a point of reference, lumefantrine has EC₅₀ values of 0.009 and 2.38 μM against immature and mature gametocytes

Table 15. *P. falciparum* NF54 Transmission Activity of Selected Compounds

compound	Transmission stage			
	stage II–III gametocytes EC ₅₀ μM ($\pm\text{SEM}$) ^a	stage V gametocytes EC ₅₀ μM ($\pm\text{SEM}$) ^a	male gamete EC ₅₀ μM^b	female gamete EC ₅₀ μM^b
WEHI-326 (33)	0.006 (0.001)	0.123 (0.018)	0.354	0.464
WEHI-328 (60)	0.002 (<0.001)	0.078 (0.015)	0.410	0.766

^aEC₅₀ data represents means and \pm SEM of $n = 3$ experiments measuring the bioluminescence of NF54-Pfs16-GFP-luc or 3D7elo1-pfs16-CBG99 gametocytes following exposure of compound for 48 h. ^bData represents means from 4 replicate experiments using NF54 parasites in a DGFA. Dose–response curves with error values are shown in Figures S7 and S8.

in this assay.⁴³ Both analogs 33 (WEHI-326) and 60 (WEHI-328) also showed moderate activity against both male and female stage V gametocyte functionality (EC_{50} 0.354 and 0.410 μ M; EC_{50} 0.464 and 0.766 μ M) (Table 15 and Figure S8).

Given the *N*-aryl acetamide analogs showed potent activity against both stage V gametocytes and gametes in vitro, we next confirmed the ability of WEHI-326 (33) to block transmission of the parasite from infected blood to the mosquito in a standard membrane feeding assay. In this model, blood infected with stage V gametocytes was exposed to WEHI-326 (33), methylene blue or vehicle control and then the infected blood was immediately fed to *Anopheles stephensi* mosquitoes. Seven days post the blood meal, the mosquito midguts were dissected, and the oocysts were counted by microscopy. WEHI-326 (33) at both 500 and 100 nM was shown to significantly reduce the number of oocysts per midgut relative to the vehicle control (Figure 4 and Figure S9).

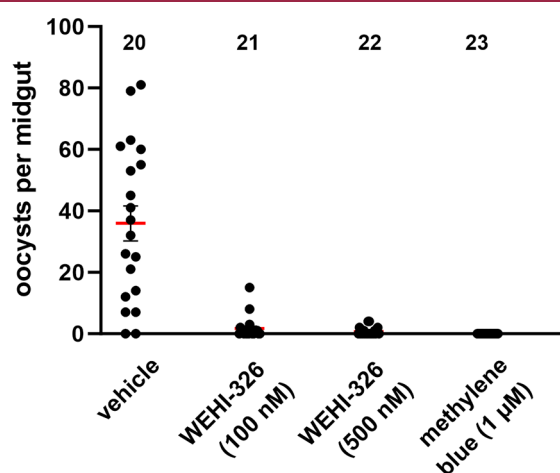


Figure 4. Activity of WEHI-326 (33) in a standard membrane feeding assay. Oocyst counts from midguts dissected from *Anopheles stephensi* mosquitoes 7 days post a blood meal infected with *P. falciparum* NF54 stage V gametocytes treated with compound at the indicated concentration. Numbers indicate the total number of mosquito midguts dissected per treatment group. Red bars indicate average oocyst intensity and error bars represent SEM. WEHI-326 (33) at both 100 and 500 nM compared to the vehicle: Wilcoxon $P < 0.0001$. The repeat experiment is shown in Figure S9.

Table 16. Evaluation of WEHI-326 (33) in a 4-Day *P. berghei* Mouse Model^a

compound	WEHI-326 (33)	artesunate
dose (mg/kg)	50	30
% parasitemia ^b	15.6	0.8
% reduction in parasitemia ^c	20.5	95.9

^a*P. berghei* ANKA parasites were injected into the tail vein to infect mice on day 0. Compounds WEHI-326 (33) were administered 50 mg/kg q.d. by oral gavage 2 h after infection (day 0) and then on days 1, 2, and 3. Parasitemia of blood samples was measured by microscopy. ^bAverage % parasitemia for 4 mice on day 4. ^cAverage % reduction in parasitemia versus the vehicle control for 4 mice on day 4. Figure S10A shows average data and error.

Methylene blue, a complete blocking control, at 1 μ M completely reduced oocyst midgut count. These data suggest that the *N*-aryl acetamide series has potential in combination therapy that is mass-administered in a malaria-endemic area to prevent transmission of the disease.

Efficacy in a *P. berghei* 4-Day Mouse Model. The in vitro antimalarial potency of the frontrunner analog WEHI-326 (33) was deemed suitable for efficacy evaluation in a *P. berghei* 4-day mouse model. In this model, mice are infected with *P. berghei* ANKA parasites, and then 2 h after the infection WEHI-326 (33) at 50 mg/kg, artesunate at 30 mg/kg and vehicle are administered by oral gavage. Compound administration was repeated 24, 48, and 72 h after parasite infection. Blood samples were taken from day 1 to day 8 and parasitemia was measured by microscopy. WEHI-326 (33) did not substantially reduce parasitemia relative to the vehicle control (Table 16 and Figure S10A). In comparison, artesunate reduced parasitemia by 98.7%. The mice treated with 50 mg/kg of WEHI-326 (33) were healthy and maintained their body weights (Figure S10B), demonstrating the safety of WEHI-326 (33). The systemic exposure of WEHI-326 (33) after oral administration was characterized by fast and moderate absorption (T_{max} 0.67 h; C_{max} 1.0 μ g/mL), low systemic exposure (AUC_{0-inf} 2.71 h* μ g/mL) and moderate-to-fast elimination (terminal half-life 1.48 h and Cl 125.4 mL/min/kg) (Figure S11 and Table S7). These data imply that the poor efficacy of WEHI-326 (33) in the *P. berghei* mouse model was due to the moderate and short systemic half-life associated with its high metabolic turnover and low aqueous solubility (Table 10). Further development of the *N*-aryl acetamide series is required to improve the metabolic stability and low aqueous solubility to achieve greater oral efficacy in malaria mouse models.

CONCLUSION

A screen of the MMV Pathogen Box to detect inhibitors of invasion/ring stage formation uncovered MMV020512 (1), which has an *N*-aryl acetamide scaffold.¹⁵ In exploration of the SAR we were able to establish that the lactam, amino acetamide, phenoxy aryl and the 4-methyl group were sensitive to change, signifying that the entire compound structure was required for activity. The incorporation of an *N*-substituted biaryl linker and *N*-methylation of the amino acetamide were key drivers of antimalarial potency; however, the overall lipophilicity was likely a contributing factor to the low metabolic stability and aqueous solubility. Endocyclic nitrogens and fluorine atoms were tolerated in certain positions of the scaffold, but these iterations did not improve metabolic stability. However, the addition of an endocyclic nitrogen did enhance aqueous solubility. Overall, we modified the *N*-aryl acetamide framework to drive antimalarial activity to single-digit nanomolar potency, but improving metabolic stability and aqueous solubility while maintaining antimalarial activity will be a challenge in future development.

The *N*-aryl acetamide class was found to have a moderate rate of resistance onset calculated from the MIR study.^{23,24} Parasites with mutations in antimalarial targets or resistance mechanisms from the AReBar study were not cross-resistant to the *N*-aryl acetamide series, except for the L800P CSC1 parasite strain, which is resistant to MMV407834.²⁷ The *N*-aryl acetamide series was found to have a moderate rate of asexual stage parasite kill akin to pyrimethamine. The *N*-aryl acetamide series did not affect liver stage development (data not shown) but was shown to kill both immature and mature gametocytes and disrupt the functionality of both male and female stage V gametocytes. Accordingly, WEHI-326 (33) was shown to block transmission of the parasite from infected blood to the mosquito, suggesting a potential application in a therapy mass

administered in malaria-endemic communities to prevent seasonal transmission of malaria—provided the metabolic stability of this compound series was improved.⁸ WEHI-326 (33) was shown to have low efficacy in a *P. berghei* mouse model, and this was attributed to its low metabolic stability and low aqueous solubility resulting in low and short systemic exposure in vivo. Species differentiation could also be a contributing factor in that WEHI-326 (33) may have reduced activity against *P. berghei* forms of the target proteins, and therefore WEHI-326 (33) may exhibit greater efficacy in the *P. falciparum* humanized mouse model. Notably, there is a high conservation of amino acids around the clefts where the resistant mutations are located in both CSC1 and ROM8 between *P. falciparum* and *P. berghei* (Figure S12 and S13), although it cannot be completely dismissed that a small number of nonconserved amino acids may impact the binding of compounds to either or both of these targets. Evaluation against *P. berghei* parasites in vitro is required to assess this hypothesis. Ultimately, further optimization of the metabolic stability and aqueous solubility is required to achieve efficacy in mouse models, although we expect that this will be challenging.

A forward genetic study using the MIR platform detected mutations in both ROM8 and CSC1 in parasite populations resistant to WEHI-326 (33). Mutations in ROM8 and CSC1 were also detected in MMV020512-resistant parasites in an independent study,³⁰ and another study using the AREBar platform⁴⁵ uncovered WEHI-326 (33) had reduced activity against a parasite line with a mutation in CSC1. Homology modeling revealed the ROM8 mutations were located around the periphery of the substrate binding cleft, while CSC1 mutations were clustered to a transmembrane domain oriented toward the parasitophorous vacuole. Structural and functional studies on each protein are required to understand the relevance of each mutation. It is possible that the *N*-aryl acetamide inhibits ROM8 by binding to the catalytic cleft and that the *N*-lactam moiety covalently binds the catalytic serine, as reported with other rhomboid proteases.^{38,39} CSC1 is a putative calcium ion channel and homology modeling suggests it may function as a homodimer, whereby the resistance mutations are located along the interface of the homodimer, suggesting a possible binding site for the *N*-aryl acetamide and a molecular mechanism by which to modulate the ion transport function of CSC1. Both ROM8 and CSC1 are essential for parasite development,^{31,32,35} however, their role in parasite development is unknown. Functional data on orthologous proteins found in humans, RHBDL2 and CRAC,⁴¹ suggest that ROM8 may process an activation motif on CSC1 to regulate its function. An alternate hypothesis is that both CSC1 and ROM8 have independent functions, whereby CSC1 could act as a drug efflux pump transporting compounds out of the parasite cytosol and ROM8 could process invasion ligands analogous to ROM4.³³ Complementary structural and functional phenotypic studies utilizing tool compounds such as WEHI-326 (33) will be required in future investigations to unravel the essential roles of both ROM8 and CSC1 in asexual and transmission stage parasite development.

EXPERIMENTAL SECTION

Chemistry. *General Chemistry Methods.* NMR spectra were recorded on a Bruker AscendTM 300. Chemical shifts are reported in ppm on the δ scale and referenced to the appropriate solvent peak. MeOD, DMSO-*d*₆, D₂O, and CDCl₃ contain H₂O. Chromatography was performed with silica gel 60 (particle size 0.040–0.063 μ m) using

an automated CombiFlash Rf purification system. LCMS were recorded on an Agilent LCMS system comprised of an Agilent G6120B Mass Detector, 1260 Infinity G1312B Binary pump, 1260 Infinity G1367E HiPALS autosampler and 1260 Infinity G4212B Diode Array Detector. Conditions for LCMS were as follows, column: Luna Omega 3 μ m PS C18 100 Å, LC Column 50 \times 2.1 mm at 20 °C, injection volume 2 μ L, gradient: 5–100% B over 3 min (solvent A: H₂O 0.1% formic acid; solvent B: ACN 0.1% formic acid), flow rate: 1.5 mL/min, detection: 254 nm, acquisition time: 4.3 min. Unless otherwise noted, all compounds were found to be >95% pure by this method. HRMS were acquired through The Bio21 Mass Spectrometry and Proteomics Facility using a Thermo Scientific nano-LC Q Exactive Plus Mass spectrometer.

N-[4-(4-Methylphenoxy)phenyl]-2-[2-(2-oxopyrrolidin-1-yl)anilino]-acetamide (1). General Method A: 67 (25 mg, 0.092 mmol), 4-(4-methylphenoxy)aniline (46 mg, 0.23 mmol), HATU (53 mg, 0.14 mmol), and DIPEA (0.048 mL, 0.28 mmol) were stirred in DCM (2 mL) for 2 h and quenched with 5% citric acid (1 mL). The reaction was then diluted with more DCM (10 mL) and washed with sat NaHCO₃ (10 mL), washed with brine (10 mL), dried with anhydrous MgSO₄, filtered, and concentrated. The crude material was then purified by column chromatography eluting with a gradient of 100% DCM to 100% EtOAc to afford crude. The crude material was then purified by reverse phase preparatory HPLC using a gradient of 95% water/ACN to 100% ACN to afford 1 as a white solid (20 mg, 52%). ¹H NMR (300 MHz, CDCl₃): δ 9.45 (s, 1H), 7.58 (d, *J* = 9.0 Hz, 2H), 7.20 (t, *J* = 7.3 Hz, 1H), 7.03–7.15 (m, 3H), 6.71–6.94 (m, 6H), 4.49 (t, *J* = 6.9 Hz, 1H), 4.08 (d, *J* = 6.9 Hz, 2H), 3.92 (t, *J* = 6.9 Hz, 2H), 2.61–2.73 (m, 2H), 2.21–2.40 (m, 5H). ¹³C NMR (75 MHz, CDCl₃): δ 174.4, 168.8, 155.4, 153.5, 140.9, 133.6, 132.3, 130.1, 128.9, 124.5, 121.5, 119.2, 118.3, 118.3, 111.5, 50.5, 47.5, 31.7, 20.6, 19.3. LCMS, *m/z* 416.4 (100) [M + H]⁺. HRMS *m/z*: [M + H]⁺ calculated for C₂₅H₂₅N₃O₃, 416.1969; found 416.1969.

N-[4-(4-Methylphenoxy)phenyl]-2-[2-(2-oxo-1-piperidyl)anilino]-acetamide (2). General Method A was followed using 73 (18 mg, 0.064 mmol) and 4-(4-methylphenoxy)aniline (19 mg, 0.095 mmol) to afford 2 as a white solid (12 mg, 44%). ¹H NMR (300 MHz, CDCl₃): δ 9.33 (s, 1H), 7.52–7.63 (m, 2H), 7.06–7.24 (m, 4H), 6.79–6.92 (m, 5H), 6.73 (d, *J* = 8.17 Hz, 1H), 4.08–4.19 (m, 1H), 3.97–4.08 (m, 1H), 3.74–3.92 (m, 1H), 3.46–3.65 (m, 1H), 2.57–2.74 (m, 2H), 2.31 (s, 3H), 1.87–2.11 (m, 4H). LCMS, *m/z* 430.4 (100) [M + H]⁺. HRMS *m/z*: [M + H]⁺ calculated for C₂₆H₂₇N₃O₃, 430.2125; found 430.2122.

N-[4-(4-Methylphenoxy)phenyl]-2-[2-(2-oxo-1-pyridyl)anilino]-acetamide (3). General Method A was followed using 75 (18 mg, 0.064 mmol) and 4-(4-methylphenoxy)aniline (19 mg, 0.095 mmol) to afford 3 as a white solid (12 mg, 44%). ¹H NMR (300 MHz, CDCl₃): δ 8.81 (s, 1H), 8.10 (dd, *J* = 1.6, 4.9 Hz, 1H), 7.69–7.80 (m, 1H), 7.35–7.43 (m, 2H), 6.98–7.20 (m, 6H), 6.79–6.98 (m, 5H), 6.76 (dd, *J* = 1.1, 8.0 Hz, 1H), 4.70 (t, *J* = 6.0 Hz, 1H), 3.98 (d, *J* = 6.0 Hz, 2H), 2.33 (s, 3H). ¹³C NMR (75 MHz, CDCl₃): δ 168.6, 163.1, 155.0, 154.3, 147.8, 141.4, 139.9, 139.5, 132.7, 132.6, 130.2, 126.5, 121.9, 121.7, 119.2, 119.0, 118.7, 112.2, 48.3, 20.6. LCMS, *m/z* 426.2 (100) [M + H]⁺. HRMS *m/z*: [M + H]⁺ calculated for C₂₆H₂₃N₃O₃, 426.1812; found 426.1810.

2-[2-(1,1-Dioxo-1,2-thiazolidin-2-yl)anilino]-*N*-[4-(4-methylphenoxy)phenyl]acetamide (4). General Method A was followed using 78 (33 mg, 0.012 mmol) and 4-(4-methylphenoxy)aniline (49 mg, 0.24 mmol) to afford 4 as an off white solid (35 mg, 63%). ¹H NMR (300 MHz, CDCl₃): δ 8.74 (s, 1H), 7.48–7.61 (m, 2H), 7.27–7.33 (m, 1H), 7.24 (d, *J* = 7.6 Hz, 1H), 7.10 (d, *J* = 8.4 Hz, 2H), 6.81–6.94 (m, 5H), 6.72 (d, *J* = 8.1 Hz, 1H), 4.04 (s, 2H), 3.76 (t, *J* = 6.7 Hz, 2H), 3.45 (dd, *J* = 7.1, 8.5 Hz, 2H), 2.53–2.70 (m, 2H), 2.31 (s, 3H). ¹³C NMR (75 MHz, CDCl₃): δ 168.6, 155.2, 153.8, 144.5, 133.0, 132.5, 130.3, 130.1, 127.7, 121.3, 121.1, 119.1, 118.5, 118.4, 111.0, 48.6, 47.5, 46.8, 20.6, 19.3. LCMS, *m/z* 452.2 (100) [M + H]⁺. HRMS *m/z*: [M + H]⁺ calculated for C₂₄H₂₅N₃O₄S, 452.1639; found 452.1637.

2-[2-(1,1-Dioxothiazinan-2-yl)anilino]-*N*-[4-(4-methylphenoxy)phenyl]acetamide (5). General Method A was followed using 81 (25

mg, 0.078 mmol) and 4-(4-methylphenoxy)aniline (31 mg, 0.16 mmol) to afford **5** as clear solid crystals (26 mg, 72%). ¹H NMR (300 MHz, CDCl₃): δ 8.78 (s, 1H), 7.53 (d, *J* = 9.0 Hz, 2H), 7.34 (dd, *J* = 1.3, 7.8 Hz, 1H), 7.22 (t, *J* = 7.8 Hz, 1H), 7.1 (d, *J* = 8.4 Hz, 2H), 6.75–6.93 (m, 5H), 6.64 (d, *J* = 8.3 Hz, 1H), 5.24 (br. s., 1H), 4.04 (d, *J* = 4.7 Hz, 2H), 3.82–3.97 (m, 1H), 3.53 (d, *J* = 12.8 Hz, 1H), 3.19–3.41 (m, 2H), 2.35–2.50 (m, 2H), 2.31 (s, 3H), 1.87–2.12 (m, 2H). ¹³C NMR (75 MHz, CDCl₃): δ 168.5, 155.3, 153.7, 143.7, 133.2, 132.4, 130.1, 130.1, 127.1, 125.3, 121.4, 119.1, 118.4, 118.3, 110.4, 77.4, 77.2, 76.6, 53.6, 50.8, 47.2, 25.1, 24.1, 20.6. LCMS, *m/z* 466.2 (100) [M + H]⁺. HRMS *m/z*: [M + H]⁺ calculated for C₂₃H₂₇N₃O₄S, 466.1795; found 466.1794.

N-[4-(4-Methylphenoxy)phenyl]-2-[2-(2-oxooxazolidin-3-yl)anilino]-acetamide (**6**). General Method E: **83** (17 mg, 0.095 mmol), **84** (26 mg, 0.095 mmol), and potassium iodide (19 mg, 0.11 mmol) was dissolved in DMF (1 mL) and stirred at 60 °C for 2 h. The reaction was then concentrated and dissolved in EtOAc (10 mL) and washed with H₂O (10 mL), brine (10 mL), dried with anhydrous MgSO₄, filtered, and concentrated. The crude material was then purified by reverse phase preparatory HPLC using a gradient of 95% water/ACN to 100% ACN to afford **6** as a white solid (8.3 mg, 21%). ¹H NMR (300 MHz, CDCl₃): δ 9.14 (s, 1H), 7.45–7.65 (m, 2H), 7.16–7.27 (m, 2H), 7.11 (d, *J* = 8.3 Hz, 2H), 6.69–6.94 (m, 6H), 4.73 (br. s., 1H), 4.63 (t, *J* = 7.9 Hz, 2H), 3.94–4.27 (m, 4H), 2.33 (s, 3H). ¹³C NMR (75 MHz, CDCl₃): δ 168.6, 156.5, 155.3, 153.7, 141.5, 133.3, 132.4, 130.1, 129.4, 124.5, 123.0, 121.4, 119.1, 118.6, 118.4, 111.8, 63.0, 47.4, 47.1, 20.6. LCMS, *m/z* 418.4 (100) [M + H]⁺. HRMS *m/z*: [M + H]⁺ calculated for C₂₄H₂₃N₃O₄, 418.1761; found 418.1752.

N-[4-(4-Methylphenoxy)phenyl]-2-(2-pyrrolidin-1-yl)anilino)-acetamide (**7**). General Method A was followed using **87** (25 mg, 0.085 mmol) and 4-(4-methylphenoxy)aniline (42 mg, 0.21 mmol) to afford **7** as a white solid (8.1 mg, 24%). ¹H NMR (300 MHz, CDCl₃): δ 8.62 (s, 1H), 7.37–7.51 (m, 2H), 7.07–7.19 (m, 3H), 7.03 (dt, *J* = 1.4, 7.7 Hz, 1H), 6.91–6.98 (m, 2H), 6.80–6.91 (m, 3H), 6.63 (dd, *J* = 1.3, 8.0 Hz, 1H), 5.35 (br. s., 1H), 3.91 (s, 2H), 3.09 (t, *J* = 6.0 Hz, 4H), 2.31–2.39 (m, 3H), 1.99 (td, *J* = 3.3, 6.7 Hz, 4H). ¹³C NMR (75 MHz, CDCl₃): δ 169.2, 155.1, 154.2, 142.7, 138.0, 132.7, 130.2, 124.7, 121.6, 119.4, 119.4, 119.2, 118.6, 111.3, 51.9, 50.3, 24.2, 20.7. LCMS, *m/z* 402.2 (100) [M + H]⁺. HRMS *m/z*: [M + H]⁺ calculated for C₂₄H₂₃N₃O₄, 402.2176; found 401.2103.

N-[4-(4-Methylphenoxy)phenyl]-2-(2-pyrazol-1-yl)anilino)-acetamide (**8**). General Method A was followed using **90** (15 mg, 0.052 mmol) and 4-(4-methylphenoxy)aniline (17 mg, 0.087 mmol) to afford **8** as a white solid (8.1 mg, 24%). ¹H NMR (300 MHz, CDCl₃): δ 8.75 (s, 1H), 7.81 (t, *J* = 2.0 Hz, 2H), 7.44–7.53 (m, 2H), 7.22–7.31 (m, 2H), 7.11 (d, *J* = 8.3 Hz, 2H), 6.78–6.96 (m, 6H), 6.48–6.63 (m, 2H), 4.01 (d, *J* = 6.0 Hz, 2H), 2.32 (s, 3H). LCMS, *m/z* 399.4 (100) [M + H]⁺. HRMS *m/z*: [M + H]⁺ calculated for C₂₄H₂₃N₃O₄, 399.1816; found 399.1811.

N-[4-(4-Methylphenoxy)phenyl]-2-[2-(1,2,4-triazol-1-yl)anilino]-acetamide (**9**). General Method E was followed using **92** (15 mg, 0.094 mmol) and **100** (31 mg, 0.112 mmol) to afford **9** as a white solid (9 mg, 24%). ¹H NMR (300 MHz, CDCl₃): δ 8.46 (s, 1H), 8.39 (s, 1H), 8.24 (s, 1H), 7.42–7.50 (m, 2H), 7.33–7.42 (m, 1H), 7.12 (d, *J* = 8.4 Hz, 2H), 6.80–7.00 (m, 7H), 6.16 (s, 1H), 4.01 (d, *J* = 5.7 Hz, 2H), 2.33 (s, 3H). LCMS, *m/z* 400.4 (100) [M + H]⁺. HRMS *m/z*: [M + H]⁺ calculated for C₂₃H₂₁N₅O₂, 400.1768; found 400.1764.

2-[2-(5-Methoxy-pyrazol-1-yl)anilino]-*N*-[4-(4-methylphenoxy)phenyl]acetamide (**10**). General Method E was followed using **94** (15 mg, 0.0793 mmol) and **84** (22 mg, 0.079 mmol) to afford **10** as a yellow solid (14 mg, 40%). ¹H NMR (300 MHz, CDCl₃): δ 8.68 (s, 1H), 7.59 (d, *J* = 2.5 Hz, 1H), 7.42–7.53 (m, 2H), 7.17–7.26 (m, 2H), 7.12 (d, *J* = 8.17 Hz, 2H), 6.83–6.97 (m, 5H), 6.79 (d, *J* = 8.2 Hz, 1H), 6.52 (t, *J* = 5.9 Hz, 1H), 5.94 (d, *J* = 2.5 Hz, 1H), 4.02 (d, *J* = 5.9 Hz, 2H), 3.95 (s, 3H), 2.33 (s, 3H). LCMS, *m/z* 429.2 (100) [M + H]⁺. HRMS *m/z*: [M + H]⁺ calculated for C₂₅H₂₄N₄O₃, 429.1921; found 429.1911.

2-[2-(2-Oxopyrrolidin-1-yl)anilino]-*N*-(4-phenoxyphenyl)acetamide (**11**). General Method A was followed using **67** (20 mg, 0.074 mmol) and 4-phenoxyaniline (34 mg, 0.18 mmol) to afford **11** as a white

solid (11 mg, 37%). ¹H NMR (300 MHz, CDCl₃): δ 9.48 (s, 1H), 7.56–7.65 (m, 2H), 7.25–7.33 (m, 2H), 7.10–7.24 (m, 2H), 6.99–7.10 (m, 1H), 6.88–6.99 (m, 4H), 6.71–6.86 (m, 2H), 4.51 (t, *J* = 6.9 Hz, 1H), 4.08 (d, *J* = 7.0 Hz, 2H), 3.92 (t, *J* = 7.0 Hz, 2H), 2.62–2.75 (m, 2H), 2.24–2.40 (m, 2H). ¹³C NMR (75 MHz, CDCl₃): δ 174.4, 168.9, 157.9, 153.0, 140.9, 134.0, 129.6, 129.0, 124.5, 124.5, 122.7, 121.5, 119.7, 118.3, 118.1, 111.5, 50.5, 47.5, 31.7, 19.3. LCMS, *m/z* 402.2 (100) [M + H]⁺. HRMS *m/z*: [M + H]⁺ calculated for C₂₄H₂₃N₃O₃, 402.1812; found 402.1814.

N-[4-(4-Fluorophenoxy)phenyl]-2-[2-(2-oxopyrrolidin-1-yl)anilino]-acetamide (**12**). General Method A was followed using **67** (20 mg, 0.074 mmol) and 4-(4-fluorophenoxy)aniline (38 mg, 0.18 mmol) to afford **12** as a white solid (13 mg, 42%). ¹H NMR (300 MHz, CDCl₃): δ 9.50 (s, 1H), 7.60 (d, *J* = 9.0 Hz, 2H), 7.08–7.23 (m, 2H), 6.67–7.07 (m, 8H), 4.50 (t, *J* = 6.8 Hz, 1H), 4.08 (d, *J* = 6.8 Hz, 2H), 3.92 (t, *J* = 7.0 Hz, 2H), 2.68 (t, *J* = 8.0 Hz, 2H), 2.32 (quin, *J* = 7.5 Hz, 2H). ¹³C NMR (75 MHz, CDCl₃): δ 174.5, 169.0, 153.4, 140.9, 133.9, 129.0, 124.5, 121.6, 119.8, 119.6, 119.1, 118.4, 116.3, 115.9, 111.5, 77.4, 77.0, 76.6, 50.5, 47.5, 31.7, 19.3. LCMS, *m/z* 420.2 (100) [M + H]⁺. HRMS *m/z*: [M + H]⁺ calculated for C₂₄H₂₂FN₃O₃, 420.1718; found 420.1721.

N-[4-(4-Chlorophenoxy)phenyl]-2-[2-(2-oxopyrrolidin-1-yl)anilino]-acetamide (**13**). General Method A was followed using **67** (20 mg, 0.074 mmol) and 4-(4-chlorophenoxy)aniline (45 mg, 0.20 mmol) to afford **13** as a white solid (16 mg, 50%). ¹H NMR (300 MHz, CDCl₃): δ 9.53 (s, 1H), 7.62 (d, *J* = 9.0 Hz, 2H), 7.07–7.26 (m, 4H), 6.72–6.94 (m, 7H), 4.50 (t, *J* = 7.0 Hz, 1H), 4.08 (d, *J* = 6.8 Hz, 2H), 3.92 (t, *J* = 7.0 Hz, 2H), 2.68 (t, *J* = 8.0 Hz, 2H), 2.32 (quin, *J* = 7.5 Hz, 2H). ¹³C NMR (75 MHz, CDCl₃): δ 174.5, 169.0, 156.6, 152.5, 140.9, 134.4, 129.6, 129.0, 127.7, 124.5, 124.4, 121.6, 119.7, 119.2, 118.3, 111.5, 50.5, 47.5, 31.7, 19.3. LCMS, *m/z* 436.2 (100) [M + H]⁺. HRMS *m/z*: [M + H]⁺ calculated for C₂₄H₂₂ClN₃O₃, 436.1422; found 436.1425.

2-[2-(2-Oxopyrrolidin-1-yl)anilino]-*N*-[4-(4-(trifluoromethyl)phenoxy)phenyl]acetamide (**14**). General Method A was followed using **67** (20 mg, 0.074 mmol) and 4-(4-(trifluoromethyl)phenoxy)aniline (28 mg, 0.11 mmol) to afford **14** as clear solid crystals (5.0 mg, 14%). ¹H NMR (300 MHz, CDCl₃): δ 9.59 (s, 1H), 7.63–7.72 (m, 2H), 7.52 (d, *J* = 8.62 Hz, 2H), 7.09–7.24 (m, 2H), 6.90–7.04 (m, 4H), 6.71–6.84 (m, 2H), 4.48 (t, *J* = 7.1 Hz, 1H), 4.10 (d, *J* = 7.1 Hz, 2H), 3.94 (t, *J* = 7.0 Hz, 2H), 2.69 (t, *J* = 8.0 Hz, 2H), 2.33 (quin, *J* = 7.5 Hz, 2H). LCMS, *m/z* 470.2 (100) [M + H]⁺. HRMS *m/z*: [M + H]⁺ calculated for C₂₅H₂₂F₃N₃O₃, 470.1686; found 470.1685.

N-[4-(4-Cyanophenoxy)phenyl]-2-[2-(2-oxopyrrolidin-1-yl)anilino]-acetamide (**15**). General Method A was followed using **67** (20 mg, 0.074 mmol) and 4-(4-aminophenoxy)benzonitrile (39 mg, 0.18 mmol) to afford **15** as a white solid (4.8 mg, 15%). ¹H NMR (300 MHz, CDCl₃): δ 9.76 (s, 1H), 7.70 (d, *J* = 9.0 Hz, 2H), 7.50–7.59 (m, 2H), 7.13–7.25 (m, 2H), 6.92–6.98 (m, 4H), 6.82–6.91 (m, 2H), 4.12 (s, 2H), 3.95 (t, *J* = 7.0 Hz, 2H), 2.70 (t, *J* = 8.0 Hz, 2H), 2.34 (t, *J* = 7.5 Hz, 2H). ¹³C NMR (75 MHz, CDCl₃): δ 174.5, 169.2, 162.1, 150.4, 140.8, 135.6, 134.2, 134.0, 129.0, 124.5, 121.7, 121.2, 120.9, 118.3, 117.4, 111.4, 105.4, 77.4, 77.2, 76.6, 50.5, 47.4, 31.7, 19.3. LCMS, *m/z* 427.0 (100) [M + H]⁺. HRMS *m/z*: [M + H]⁺ calculated for C₂₅H₂₂N₄O₃, 427.1765; found 427.1770.

N-[4-(4-Methoxyphenoxy)phenyl]-2-[2-(2-oxopyrrolidin-1-yl)anilino]-acetamide (**16**). General Method A was followed using **67** (20 mg, 0.074 mmol) and 4-(4-methoxyphenoxy)aniline (40 mg, 0.18 mmol) to afford **16** as a white solid (18.4 mg, 58%). ¹H NMR (300 MHz, CDCl₃): δ 9.43 (s, 1H), 7.46–7.63 (m, 2H), 7.07–7.24 (m, 2H), 6.65–6.96 (m, 8H), 4.51 (br. s., 1H), 4.07 (br. s., 2H), 3.92 (t, *J* = 7.0 Hz, 2H), 3.79 (s, 3H), 2.67 (t, *J* = 8.0 Hz, 2H), 2.31 (quin, *J* = 7.5 Hz, 2H). ¹³C NMR (75 MHz, CDCl₃): δ 174.4, 168.9, 155.6, 154.4, 150.9, 141.0, 133.3, 129.0, 124.5, 124.5, 121.5, 120.1, 118.4, 114.8, 111.6, 55.7, 50.5, 47.5, 31.7, 19.3. LCMS, *m/z* 432.2 (100) [M + H]⁺. HRMS *m/z*: [M + H]⁺ calculated for C₂₅H₂₅N₃O₄, 432.1918; found 432.1918.

N-[4-(3-Methylphenoxy)phenyl]-2-[2-(2-oxopyrrolidin-1-yl)anilino]-acetamide (**17**). General Method A was followed using **67** (20 mg,

0.074 mmol) and 4-(3-methylphenoxy)aniline (29 mg, 0.15 mmol) to afford **17** as a white solid (19.5 mg, 64%). ^1H NMR (300 MHz, CDCl_3): δ 9.58 (s, 1H), 7.55–7.65 (m, 2H), 7.09–7.25 (m, 3H), 6.79–6.98 (m, 5H), 6.67–6.79 (m, 2H), 4.10 (s, 2H), 3.93 (t, J = 7.0 Hz, 2H), 2.62–2.75 (m, 2H), 2.24–2.39 (m, 5H). LCMS, m/z 416.0 (100) $[\text{M} + \text{H}]^+$. HRMS m/z : $[\text{M} + \text{H}]^+$ calculated for $\text{C}_{25}\text{H}_{25}\text{N}_3\text{O}_3$, 416.1969; found 416.1973.

N-[4-(3-Chlorophenoxy)phenyl]-2-[2-(2-oxopyrrolidin-1-yl)anilino]-acetamide (**18**). General Method A was followed using **67** (20 mg, 0.074 mmol) and 4-(3-chlorophenoxy)aniline (32 mg, 0.15 mmol) to afford **18** as a white solid (4.3 mg, 13%). ^1H NMR (300 MHz, CDCl_3): δ 9.66 (br. s., 1H), 7.56–7.71 (m, 2H), 7.09–7.26 (m, 3H), 6.98–7.06 (m, 1H), 6.75–6.98 (m, 6H), 4.11 (s, 2H), 3.94 (t, J = 7.0 Hz, 2H), 2.63–2.74 (m, 2H), 2.33 (quin, J = 7.5 Hz, 2H). LCMS, m/z 435.8 (100) $[\text{M} + \text{H}]^+$. HRMS m/z : $[\text{M} + \text{H}]^+$ calculated for $\text{C}_{24}\text{H}_{22}\text{ClN}_3\text{O}_3$, 436.1422; found 436.1428.

N-[4-(2-Methylphenoxy)phenyl]-2-[2-(2-oxopyrrolidin-1-yl)anilino]-acetamide (**19**). General Method A was followed using **67** (20 mg, 0.074 mmol) and 4-(2-methylphenoxy)aniline (41 mg, 0.20 mmol) to afford **19** as a white solid (17 mg, 56%). ^1H NMR (300 MHz, CDCl_3): δ 9.43 (s, 1H), 7.50–7.62 (m, 2H), 7.06–7.25 (m, 4H), 6.97–7.06 (m, 1H), 6.68–6.88 (m, 5H), 4.52 (br. s., 1H), 4.06 (d, J = 4.8 Hz, 2H), 3.91 (t, J = 7.0 Hz, 2H), 2.59–2.75 (m, 2H), 2.31 (quin, J = 7.5 Hz, 2H), 2.22 (s, 3H). ^{13}C NMR (75 MHz, CDCl_3): δ 174.5, 168.9, 155.0, 154.0, 141.0, 133.1, 131.3, 129.6, 129.0, 127.0, 124.6, 124.5, 123.6, 121.6, 119.0, 118.3, 117.9, 111.6, 50.5, 47.5, 31.6, 19.3, 16.1. LCMS, m/z 416.2 (100) $[\text{M} + \text{H}]^+$. HRMS m/z : $[\text{M} + \text{H}]^+$ calculated for $\text{C}_{25}\text{H}_{25}\text{N}_3\text{O}_3$, 416.1969; found 416.1969.

N-[4-(2-Chlorophenoxy)phenyl]-2-[2-(2-oxopyrrolidin-1-yl)anilino]-acetamide (**20**). General Method A was followed using **67** (20 mg, 0.074 mmol) and 4-(2-chlorophenoxy)aniline (41 mg, 0.18 mmol) to afford **20** as a white solid (18 mg, 57%). ^1H NMR (300 MHz, CDCl_3): δ 9.50 (s, 1H), 7.54–7.68 (m, 2H), 7.42 (dd, J = 1.6, 7.9 Hz, 1H), 7.07–7.24 (m, 3H), 6.98–7.07 (m, 1H), 6.70–6.93 (m, 5H), 4.07 (s, 2H), 3.92 (t, J = 7.0 Hz, 2H), 2.61–2.76 (m, 2H), 2.32 (quin, J = 7.5 Hz, 2H). LCMS, m/z 436.2 (100) $[\text{M} + \text{H}]^+$. HRMS m/z : $[\text{M} + \text{H}]^+$ calculated for $\text{C}_{24}\text{H}_{22}\text{ClN}_3\text{O}_3$, 436.1422; found 436.1426.

2-[*N*-Methyl-2-(2-oxopyrrolidin-1-yl)anilino]-*N*-[4-(4-methylphenoxy)phenyl]acetamide (**21**). General Method A was followed using **68** (25 mg, 0.088 mmol) and 4-(4-methylphenoxy)aniline (44 mg, 0.22 mmol) to afford **21** as a white solid (28 mg, 74%). ^1H NMR (300 MHz, CDCl_3): δ 9.96 (s, 1H), 7.62–7.69 (m, 2H), 7.01–7.29 (m, 6H), 6.82–6.97 (m, 4H), 3.75–4.02 (m, 4H), 2.81 (s, 3H), 2.56–2.66 (m, 2H), 2.19–2.34 (m, 5H). LCMS, m/z 430.2 (100) $[\text{M} + \text{H}]^+$. HRMS m/z : $[\text{M} + \text{H}]^+$ calculated for $\text{C}_{26}\text{H}_{27}\text{N}_3\text{O}_3$, 430.2125; found 430.2126.

2-[*N*-Ethyl-2-(2-oxopyrrolidin-1-yl)anilino]-*N*-[4-(4-methylphenoxy)phenyl]acetamide (**22**). General Method A was followed using **69** (10 mg, 0.034 mmol) and 4-(4-methylphenoxy)aniline (13 mg, 0.066 mmol) to afford **22** as a white solid (13.2 mg, 89%). ^1H NMR (300 MHz, CDCl_3): δ 10.09 (s, 1H), 7.55–7.68 (m, 2H), 7.14–7.24 (m, 2H), 6.98–7.14 (m, 4H), 6.76–6.95 (m, 4H), 3.91 (br. s., 4H), 3.04 (d, J = 7.1 Hz, 2H), 2.52–2.69 (m, 2H), 2.17–2.45 (m, 5H), 1.11 (t, J = 7.1 Hz, 3H). ^{13}C NMR (75 MHz, CDCl_3): δ 173.5, 168.4, 155.5, 153.3, 146.0, 134.1, 132.2, 131.7, 130.0, 128.5, 126.4, 123.0, 121.7, 120.1, 119.0, 118.3, 55.6, 50.6, 49.9, 31.7, 20.6, 19.3, 12.2. LCMS, m/z 444.2 (100) $[\text{M} + \text{H}]^+$. HRMS m/z : $[\text{M} + \text{H}]^+$ calculated for $\text{C}_{27}\text{H}_{29}\text{N}_3\text{O}_3$, 444.2282; found 444.2273.

N-[4-(4-Methylphenoxy)phenyl]-2-[2-(2-oxopyrrolidin-1-yl)phenoxy]-acetamide (**23**). General Method A was followed using **99** (15 mg, 0.064 mmol) and 4-(4-methylphenoxy)aniline (15 mg, 0.076 mmol) to afford **23** as a white solid (26.1 mg, 98%). ^1H NMR (300 MHz, CDCl_3): δ 9.93 (s, 1H), 7.61–7.74 (m, 2H), 7.20–7.26 (m, 1H), 6.96–7.14 (m, 4H), 6.88–6.95 (m, 2H), 6.81–6.88 (m, 2H), 4.75 (s, 2H), 3.87 (t, J = 7.0 Hz, 2H), 2.59–2.76 (m, 2H), 2.16–2.39 (m, 5H). ^{13}C NMR (75 MHz, CDCl_3): δ 174.8, 166.3, 155.3, 153.6, 151.3, 133.6, 132.3, 130.0, 128.8, 127.1, 126.3, 121.7, 121.5, 119.1, 118.3, 111.4, 66.5, 50.9, 31.6, 20.6, 19.0. LCMS, m/z 417.2 (100) $[\text{M} + \text{H}]^+$. HRMS m/z : $[\text{M} + \text{H}]^+$ calculated for $\text{C}_{25}\text{H}_{24}\text{N}_2\text{O}_4$, 417.1809; found 417.1801.

N-[4-(4-Methylphenoxy)phenyl]-2-[2-(2-oxopyrrolidin-1-yl)anilino]-propenamide (**24**). **65** (25 mg, 0.14 mmol), **100** (57 mg, 0.17 mmol), and K_2CO_3 (59 mg, 0.43 mmol) were dissolved in MeCN (2 mL) and stirred at 90 °C for 12 h. The crude material was then purified by column chromatography eluting with a gradient of 100% DCM to 80% EtOAc/DCM to afford crude. The crude material was then purified by reverse phase preparatory HPLC using a gradient of 95% water/ACN to 100% ACN to afford **24** as a white solid (3.3 mg, 5.4%). ^1H NMR (300 MHz, CDCl_3): δ 9.49 (s, 1H), 7.51–7.61 (m, 2H), 7.04–7.21 (m, 4H), 6.68–6.96 (m, 6H), 4.02–4.23 (m, 3H), 3.79 (d, J = 9.8 Hz, 1H), 2.61–2.79 (m, 2H), 2.25–2.40 (m, 5H), 1.59–1.65 (m, 3H). LCMS, m/z 430.3 (100) $[\text{M} + \text{H}]^+$. HRMS m/z : $[\text{M} + \text{H}]^+$ calculated for $\text{C}_{26}\text{H}_{27}\text{N}_3\text{O}_3$, 430.2125; found 430.2126.

2-Methyl-*N*-[4-(4-methylphenoxy)phenyl]-2-[2-(2-oxopyrrolidin-1-yl)anilino]propenamide (**25**). Sodium hydride (6.20 mg, 0.178 mmol) was added to a stirred solution of **65** (22.8 mg, 0.13 mmol) in THF (1 mL) and stirred for 10 min. **101** (30.0 mg, 0.086 mmol) was then added and the reaction stirred at 50 °C for 16 h. The reaction was quenched with 5% citric acid (1 mL) and concentrated. The residue was then dissolved in EtOAc (10 mL), which was washed with saturated NaHCO_3 (10 mL), brine (10 mL), dried with anhydrous MgSO_4 , filtered, and concentrated. The crude material was then purified by column chromatography eluting with a gradient of 100 DCM% to 50% EtOAc/DCM to afford **25** as a white solid (8.1 mg, 21%). ^1H NMR (300 MHz, CDCl_3): δ d 9.31 (s, 1H), 7.44 (d, J = 8.9 Hz, 2H), 7.09 (dd, J = 2.5, 8.1 Hz, 4H), 6.86 (t, J = 9.0 Hz, 4H), 6.61–6.80 (m, 2H), 4.21 (s, 1H), 3.90 (t, J = 7.0 Hz, 2H), 2.60–2.74 (m, 2H), 2.20–2.38 (m, 5H), 1.65 (s, 6H). ^{13}C NMR (75 MHz, CDCl_3): δ 174.6, 174.0, 155.4, 153.4, 140.4, 134.0, 132.3, 130.1, 128.5, 125.2, 124.8, 121.4, 119.1, 118.3, 118.2, 114.5, 58.7, 50.5, 31.5, 27.1, 20.6, 19.2. LCMS, m/z 444.4 (100) $[\text{M} + \text{H}]^+$. HRMS m/z : $[\text{M} + \text{H}]^+$ calculated for $\text{C}_{27}\text{H}_{29}\text{N}_3\text{O}_3$, 444.2282; found 444.2273.

N-[4-(*N*,4-Dimethylanilino)phenyl]-2-[*N*-methyl-2-(2-oxopyrrolidin-1-yl)anilino]acetamide (**26**). General Method A was followed using **68** (10 mg, 0.035 mmol) and **103** (10 mg, 0.049 mmol) to afford **26** as a gray solid (12.5 mg, 80%). ^1H NMR (300 MHz, CDCl_3): δ 9.78 (s, 1H), 7.51–7.63 (m, 2H), 7.08–7.26 (m, 3H), 7.05 (d, J = 8.2 Hz, 3H), 6.85–6.95 (m, 4H), 3.75–3.99 (m, 4H), 3.23 (s, 3H), 2.80 (s, 3H), 2.52–2.65 (m, 2H), 2.16–2.32 (m, 5H). ^{13}C NMR (75 MHz, CDCl_3): δ 173.8, 167.7, 147.5, 146.9, 145.5, 132.3, 131.1, 130.3, 129.7, 128.6, 126.6, 122.9, 121.1, 120.9, 120.0, 119.1, 59.8, 50.8, 42.7, 40.4, 31.5, 20.6, 19.3. LCMS, m/z 443.4 (100) $[\text{M} + \text{H}]^+$. HRMS m/z : $[\text{M} + \text{H}]^+$ calculated for $\text{C}_{27}\text{H}_{30}\text{N}_4\text{O}_2$, 443.2442; found 443.2431.

2-[*N*-Methyl-2-(2-oxopyrrolidin-1-yl)anilino]-*N*-[4-(*p*-tolylmethyl)phenyl]acetamide (**27**). Triethylsilane (0.016 mL, 0.10 mmol) was slowly to a solution of **104** (15 mg, 0.034 mmol) in TFA (1 mL) at 0 °C. The reaction was then allowed to warm to 20 °C and stirred for 16 h. The solvent was removed in vacuo and the residue dissolved in EtOAc (2 mL) and washed with saturated NaHCO_3 (2 \times 3 mL), brine, dried with anhydrous MgSO_4 , filtered, and concentrated. The crude material was then purified by column chromatography eluting with a gradient of 100% DCM to 50% EtOAc/DCM to afford **27** as a white solid (11.3 mg, 78%). ^1H NMR (300 MHz, CDCl_3): δ 9.82 (s, 1H), 7.61 (d, J = 8.4 Hz, 2H), 7.13–7.26 (m, 2H), 6.99–7.13 (m, 8H), 3.73–4.00 (m, 6H), 2.78 (s, 3H), 2.51–2.60 (m, 2H), 2.31 (s, 3H), 2.13–2.29 (m, 2H). ^{13}C NMR (75 MHz, CDCl_3): δ 173.8, 167.9, 147.4, 138.2, 136.8, 136.5, 135.4, 131.1, 129.1, 129.0, 128.7, 128.5, 126.5, 123.0, 120.0, 119.1, 77.4, 76.6, 59.9, 50.7, 42.6, 40.9, 31.5, 21.0, 19.2. LCMS, m/z 428.2 (100) $[\text{M} + \text{H}]^+$. HRMS m/z : $[\text{M} + \text{H}]^+$ calculated for $\text{C}_{27}\text{H}_{29}\text{N}_3\text{O}_2$, 428.2333; found 428.2320.

2-[*N*-Methyl-2-(2-oxopyrrolidin-1-yl)anilino]-*N*-[4-(1-(*p*-tolyl)ethyl)phenyl]acetamide (**28**). General Method A was followed using **68** (20 mg, 0.070 mmol) and **105** (18 mg, 0.084 mmol) to afford **28** as a white solid (15.2 mg, 49%). ^1H NMR (300 MHz, CDCl_3): δ 9.82 (s, 1H), 7.60 (d, J = 8.5 Hz, 2H), 6.91–7.26 (m, 10H), 4.06 (q, J = 7.2 Hz, 1H), 3.88 (t, J = 6.9 Hz, 2H), 3.83 (s, 2H), 2.78 (s, 3H), 2.51–2.62 (m, 2H), 2.15–2.39 (m, 5H), 1.58 (d, J = 7.3 Hz, 3H). ^{13}C NMR (75 MHz, CDCl_3): δ 173.7, 167.9, 147.4, 143.5, 142.0, 136.3, 135.3, 131.1, 128.9, 128.5, 127.8, 127.4, 126.5, 122.9, 119.9, 119.1, 59.8, 50.7, 43.8, 42.6, 31.5, 21.9, 20.9, 19.2. LCMS, m/z

442.4 (100) $[M + H]^+$. HRMS m/z : $[M + H]^+$ calculated for $C_{28}H_{31}N_3O_2$, 442.2489; found 442.2478.

2-[*N*-Methyl-2-(2-oxopyrrolidin-1-yl)anilino]-*N*-[4-[1-methyl-1-(*p*-tolyl)ethyl]phenyl]acetamide (**29**). General Method A was followed using **68** (15 mg, 0.053 mmol) and **106** (14 mg, 0.064 mmol) to afford **29** as a white solid (16.6 mg, 69%). 1H NMR (300 MHz, $CDCl_3$): δ 9.84 (s, 1H), 7.58 (d, J = 8.7 Hz, 2H), 7.20–7.26 (m, 1H), 6.96–7.20 (m, 10H), 3.76–3.97 (m, 4H), 2.78 (s, 3H), 2.45–2.67 (m, 2H), 2.31 (s, 3H), 2.11–2.30 (m, 2H), 1.62 (s, 6H). ^{13}C NMR (75 MHz, $CDCl_3$): δ 173.7, 167.9, 147.7, 147.4, 146.2, 135.9, 134.9, 131.1, 128.6, 128.5, 127.0, 126.6, 126.5, 122.9, 119.6, 119.1, 50.7, 42.7, 42.2, 31.5, 30.7, 20.8, 19.2. LCMS, m/z 456.4 (100) $[M + H]^+$. HRMS m/z : $[M + H]^+$ calculated for $C_{29}H_{33}N_3O_2$, 456.2646; found 456.2639.

N-[4-(Hydroxy(*p*-tolyl)methyl)phenyl]-2-[*N*-methyl-2-(2-oxopyrrolidin-1-yl)anilino]acetamide (**30**). Sodium borohydride (10 mg, 0.27 mmol) was added portion wise to a solution of **104** (20 mg, 0.045 mmol) in 3:1 mixture of EtOH/ H_2O (2 mL) and allowed to stir at 20 °C for 2 h. The EtOH was then removed in vacuo and the solution acidified (pH 5) with 1 M HCl. The crude solid was then filtered and purified by reverse phase preparatory HPLC using a gradient of 95% water/ACN to 100% ACN to afford **30** as a white solid (7.6 mg, 38%). 1H NMR (300 MHz, $CDCl_3$): δ 9.90 (s, 1H), 7.66 (d, J = 8.5 Hz, 2H), 7.18–7.30 (m, 5H), 6.98–7.18 (m, 5H), 5.75 (s, 1H), 3.89 (t, J = 6.8 Hz, 2H), 3.83 (s, 2H), 2.77 (s, 3H), 2.49–2.64 (m, 2H), 2.32 (s, 3H), 2.17–2.30 (m, 2H). LCMS, m/z 444.2 (100) $[M + H]^+$. HRMS m/z : $[M + H]^+$ calculated for $C_{27}H_{29}N_3O_3$, 444.2282; found 444.2268.

N-[4-(*N*-Ethyl-4-methyl-anilino)phenyl]-2-[*N*-methyl-2-(2-oxopyrrolidin-1-yl)anilino]acetamide (**31**). General Method A was followed using **68** (20 mg, 0.070 mmol) and **108** (24 mg, 0.105 mmol) to afford **31** as a gray solid (13.8 mg, 43%). 1H NMR (300 MHz, $CDCl_3$): δ 9.79 (br. s., 1H), 7.57 (d, J = 9.0 Hz, 2H), 7.00–7.25 (m, 6H), 6.86 (d, J = 8.4 Hz, 2H), 6.91 (d, J = 8.8 Hz, 2H), 3.90 (t, J = 7.0 Hz, 2H), 3.84 (s, 2H), 3.69 (q, J = 7.1 Hz, 2H), 2.80 (s, 3H), 2.52–2.63 (m, 2H), 2.18–2.33 (m, 6H), 1.17 (t, J = 7.1 Hz, 3H). LCMS, m/z 457.4 (100) $[M + H]^+$. HRMS m/z : $[M + H]^+$ calculated for $C_{28}H_{32}N_4O_2$, 457.2598; found 457.2588.

2-[*N*-methyl-2-(2-oxopyrrolidin-1-yl)anilino]-*N*-[4-(4-methyl-*N*-propyl-anilino)phenyl]acetamide (**32**). General Method A was followed using **68** (13 mg, 0.046 mmol) and **110** (11 mg, 0.046 mmol) to afford **32** as a gray solid (14.9 mg, 69%). 1H NMR (300 MHz, MeOD): δ 9.85 (s, 1H), 7.39 (d, J = 9.0 Hz, 2H), 7.26 (dd, J = 2.4, 7.8 Hz, 2H), 7.14 (d, J = 7.5 Hz, 1H), 7.02–7.11 (m, 3H), 6.76–6.90 (m, 4H), 3.93 (t, J = 7.1 Hz, 2H), 3.81 (s, 2H), 3.46–3.64 (m, 2H), 2.82 (s, 3H), 2.46–2.59 (m, 2H), 2.27 (s, 3H), 2.15–2.25 (m, 2H), 1.50–1.74 (m, 2H), 0.91 (t, J = 7.4 Hz, 3H). 1H NMR (300 MHz, $CDCl_3$): δ 9.77 (br. s., 1H), 7.56 (d, J = 8.8 Hz, 2H), 6.99–7.25 (m, 6H), 6.84 (d, J = 8.4 Hz, 2H), 6.89 (d, J = 8.8 Hz, 2H), 3.73–4.00 (m, 4H), 3.48–3.66 (m, 2H), 2.80 (s, 3H), 2.50–2.64 (m, 2H), 2.11–2.33 (m, 5H), 1.53–1.69 (m, 2H), 0.90 (t, J = 7.4 Hz, 3H). ^{13}C NMR (75 MHz, $CDCl_3$): δ 173.8, 167.7, 147.4, 145.9, 144.5, 132.1, 131.1, 129.9, 129.6, 128.6, 126.6, 122.9, 121.4, 121.1, 120.4, 119.1, 59.7, 54.1, 50.7, 42.7, 31.5, 20.5, 19.2, 11.4. LCMS, m/z 471.4 (100) $[M + H]^+$. HRMS m/z : $[M + H]^+$ calculated for $C_{29}H_{34}N_4O_2$, 471.2755; found 471.2748.

N-[4-(*N*-Isopropyl-4-methyl-anilino)phenyl]-2-[*N*-methyl-2-(2-oxopyrrolidin-1-yl)anilino]acetamide (**33**). General Method A was followed using **68** (15 mg, 0.053 mmol) and **112** (15 mg, 0.063 mmol) to afford **33** as a white solid (22.1 mg, 89%). 1H NMR (300 MHz, $CDCl_3$): δ 9.79 (s, 1H), 7.59 (d, J = 8.9 Hz, 2H), 6.96–7.26 (m, 6H), 6.62–6.88 (m, 4H), 4.24 (td, J = 6.6, 13.2 Hz, 1H), 3.90 (t, J = 6.9 Hz, 2H), 3.83 (s, 2H), 2.79 (s, 3H), 2.50–2.64 (m, 2H), 2.14–2.35 (m, 5H), 1.11 (d, J = 6.6 Hz, 6H). ^{13}C NMR (75 MHz, $CDCl_3$): δ 173.7, 167.7, 147.5, 144.2, 142.3, 132.8, 131.1, 130.3, 129.6, 128.5, 126.6, 123.6, 122.8, 122.1, 120.9, 119.1, 59.7, 50.7, 47.8, 42.7, 31.5, 20.9, 20.5, 19.2. LCMS, m/z 471.4 (100) $[M + H]^+$. HRMS m/z : $[M + H]^+$ calculated for $C_{29}H_{34}N_4O_2$, 471.2755; found 471.2756.

N-[4-(*N*-Cyclopentyl-4-methyl-anilino)phenyl]-2-[*N*-methyl-2-(2-oxopyrrolidin-1-yl)anilino]acetamide (**34**). General Method A was followed using **68** (15 mg, 0.053 mmol) and **114** (15 mg, 0.058 mmol) to afford **34** as a white solid (5.3 mg, 20%). 1H NMR (300 MHz, $CDCl_3$): δ 9.79 (br. s., 1 H) 7.59 (d, J = 8.8 Hz, 2H), 7.00–7.25 (m, 6H), 6.76 (d, J = 7.4 Hz, 2H), 6.82 (d, J = 7.8 Hz, 2H), 4.18 (t, J = 7.7 Hz, 1H), 3.71–4.00 (m, 4H), 2.79 (s, 3H), 2.50–2.63 (m, 2H), 2.17–2.34 (m, 5H), 1.92 (dd, J = 11.4, 6.9 Hz, 2H) 1.48 (m, 6H). LCMS, m/z 497.4 (100) $[M + H]^+$. HRMS m/z : $[M + H]^+$ calculated for $C_{31}H_{36}N_4O_2$, 497.2911; found 497.2903.

N-[4-(*N*-Isobutyl-4-methyl-anilino)phenyl]-2-[*N*-methyl-2-(2-oxopyrrolidin-1-yl)anilino]acetamide (**35**). General Method A was followed using **68** (15 mg, 0.053 mmol) and **116** (15 mg, 0.058 mmol) to afford **35** as a white solid (24.6 mg, 96%). 1H NMR (300 MHz, $CDCl_3$): δ 9.77 (s, 1H), 7.52–7.60 (m, 2H), 7.13–7.26 (m, 2H), 6.98–7.13 (m, 4H), 6.80–6.93 (m, 4H), 3.90 (t, J = 6.9 Hz, 2H), 3.83 (s, 2H), 3.42 (d, J = 7.3 Hz, 2H), 2.79 (s, 3H), 2.53–2.62 (m, 2H), 2.19–2.31 (m, 5H), 1.99 (td, J = 6.8, 13.6 Hz, 1H), 0.92 (d, J = 6.6 Hz, 6H). ^{13}C NMR (75 MHz, $CDCl_3$): δ 173.7, 167.6, 147.4, 146.7, 145.1, 132.1, 131.1, 129.9, 129.6, 128.5, 126.5, 122.8, 121.6, 121.0, 120.6, 119.0, 60.3, 59.7, 50.7, 42.7, 31.5, 27.0, 20.5, 20.4, 19.2. LCMS, m/z 485.4 (100) $[M + H]^+$. HRMS m/z : $[M + H]^+$ calculated for $C_{30}H_{36}N_4O_2$, 485.2911; found 485.2905.

N-[4-(*N*-Butyl-4-methyl-anilino)phenyl]-2-[*N*-methyl-2-(2-oxopyrrolidin-1-yl)anilino]acetamide (**36**). General Method A was followed using **68** (15 mg, 0.053 mmol) and **118** (15 mg, 0.058 mmol) to afford **36** as an off white solid (21.2 mg, 83%). 1H NMR (300 MHz, $CDCl_3$): δ 9.79 (s, 1H), 7.49–7.63 (m, 2H), 6.99–7.26 (m, 6H), 6.84 (d, J = 8.4 Hz, 2H), 6.89 (d, J = 8.9 Hz, 2H), 3.90 (t, J = 6.9 Hz, 2H), 3.84 (s, 2H), 3.52–3.67 (m, 2H), 2.79 (s, 3H), 2.53–2.64 (m, 2H), 2.16–2.32 (m, 5H), 1.60 (t, J = 7.7 Hz, 2H), 1.25–1.40 (m, 2H), 0.91 (t, J = 7.3 Hz, 3H). ^{13}C NMR (75 MHz, $CDCl_3$): δ 173.7, 167.7, 147.4, 145.9, 144.4, 132.0, 131.0, 129.9, 129.6, 128.5, 126.5, 122.8, 121.4, 121.1, 120.3, 119.0, 59.7, 52.1, 50.7, 42.7, 31.5, 29.5, 20.5, 20.2, 19.2, 13.9. LCMS, m/z 485.4 (100) $[M + H]^+$. HRMS m/z : $[M + H]^+$ calculated for $C_{30}H_{36}N_4O_2$, 485.2911; found 485.2905.

2-[*N*-Methyl-2-(2-oxopyrrolidin-1-yl)anilino]-*N*-[4-(4-methyl-*N*-sec-butyl-anilino)phenyl]acetamide (**37**). General Method A was followed using **68** (16 mg, 0.056 mmol) and **120** (16 mg, 0.062 mmol) to afford **37** as a white solid (20.4 mg, 75%). 1H NMR (300 MHz, $CDCl_3$): δ 9.79 (s, 1H), 7.48–7.64 (m, 2H), 6.95–7.28 (m, 6H), 6.66–6.89 (m, 4H), 3.86–4.00 (m, 3H), 3.85 (s, 2H), 2.76–2.84 (m, 3H), 2.53–2.65 (m, 2H), 2.18–2.37 (m, 5H), 1.70 (dd, J = 6.8, 14.1 Hz, 1H), 1.19–1.40 (m, 2H), 1.12 (d, J = 6.6 Hz, 2H), 0.96 (t, J = 7.4 Hz, 3H). LCMS, m/z 485.4 (100) $[M + H]^+$. HRMS m/z : $[M + H]^+$ calculated for $C_{30}H_{36}N_4O_2$, 485.2911; found 485.2902.

N-[4-(4-Chloro-*N*-methyl-anilino)phenyl]-2-[*N*-methyl-2-(2-oxopyrrolidin-1-yl)anilino]acetamide (**38**). General Method A was followed using **68** (20 mg, 0.070 mmol) and **121** (29 mg, 0.13 mmol) to afford **38** as a gray solid (20.3 mg, 62%). 1H NMR (300 MHz, $CDCl_3$): δ 9.98 (s, 1H), 7.59–7.68 (m, 2H), 7.16–7.26 (m, 2H), 7.04–7.15 (m, 4H), 6.97–7.04 (m, 2H), 6.69–6.84 (m, 2H), 3.80–4.03 (m, 4H), 3.22 (s, 3H), 2.81 (s, 3H), 2.61 (t, J = 8.03 Hz, 2H), 2.27 (t, J = 7.54 Hz, 2H). LCMS, m/z 463.2 (100) $[M + H]^+$. HRMS m/z : $[M + H]^+$ calculated for $C_{26}H_{27}ClN_4O_2$, 497.1895; found 463.1894.

N-[4-(2-Fluoro-*N*,4-dimethyl-anilino)phenyl]-2-[*N*-methyl-2-(2-oxopyrrolidin-1-yl)anilino]acetamide (**39**). General Method A was followed using **68** (9 mg, 0.032 mmol) and **124** (8.0 mg, 0.035 mmol) to afford **39** as an off white solid (11.3 mg, 78%). 1H NMR (300 MHz, $CDCl_3$): δ 9.62 (s, 1H), 7.42–7.63 (m, J = 9.1 Hz, 2H), 7.19–7.26 (m, 1H), 6.99–7.19 (m, 4H), 6.82–6.99 (m, 2H), 6.56–6.71 (m, J = 8.89 Hz, 2H), 3.87 (t, J = 6.9 Hz, 2H), 3.79 (s, 2H), 3.21 (s, 3H), 2.78 (s, 3H), 2.49–2.59 (m, 2H), 2.34 (s, 3H), 2.21 (quin, J = 7.5 Hz, 2H). ^{13}C NMR (75 MHz, $CDCl_3$): δ 173.9, 167.5, 158.3 (d, J = 247.5 Hz), 147.7, 145.5, 136.6 (d, J = 7.5 Hz), 133.3 (d, J = 11.3 Hz), 133.3, 131.1, 129.9, 128.5, 128.1 (d, J = 2.3 Hz), 126.6, 125.2 (d, J = 3.0 Hz), 122.9, 120.9, 119.2, 117.4 (d, J = 19.5 Hz), 114.6, 60.0, 50.7, 42.4, 39.7, 39.7, 31.4, 20.9, 19.2. LCMS, m/z 461.4 (100) $[M + H]^+$. HRMS m/z : $[M + H]^+$ calculated for $C_{27}H_{29}FN_4O_2$, 461.2347; found 461.2340.

N-[4-(3-Fluoro-*N*,4-dimethyl-anilino)phenyl]-2-[*N*-methyl-2-(2-oxopyrrolidin-1-yl)anilino]acetamide (**40**). General Method A was followed using **68** (15 mg, 0.053 mmol) and **127** (14.5 mg, 0.063 mmol) to afford **40** as a white solid (21.4 mg, 88%). ¹H NMR (300 MHz, CDCl₃): δ 9.91 (s, 1H), 7.60–7.68 (m, 2H), 7.14–7.26 (m, 2H), 6.92–7.14 (m, 6H), 6.46–6.58 (m, 2H), 3.74–4.02 (m, 4H), 3.21 (s, 3H), 2.80 (s, 3H), 2.50–2.66 (m, 2H), 2.26 (t, *J* = 7.5 Hz, 2H), 2.09–2.20 (m, 3H). LCMS, *m/z* 461.4 (100) [M + H]⁺. ¹³C NMR (75 MHz, CDCl₃): δ 173.7, 167.9, 161.7 (d, *J* = 242.3 Hz), 148.9 (d, *J* = 9.8 Hz), 147.3, 144.5, 134.1, 131.2 (d, *J* = 6.8 Hz), 131.1, 128.6, 126.5, 123.8, 122.9, 121.2, 119.0, 114.8 (d, *J* = 17.3 Hz), 112.6 (d, *J* = 3.0 Hz), 104.0 (d, *J* = 25.5 Hz), 59.6, 50.7, 42.8, 40.3, 31.5, 19.3, 13.6 (d, *J* = 3.8 Hz). HRMS *m/z*: [M + H]⁺ calculated for C₂₇H₂₉FN₄O₂, 461.2347; found 461.2339.

N-[4-(3-Chloro-*N*,4-dimethyl-anilino)phenyl]-2-[*N*-methyl-2-(2-oxopyrrolidin-1-yl)anilino]acetamide (**41**). General Method A was followed using **68** (15 mg, 0.053 mmol) and **129** (16 mg, 0.063 mmol) to afford **41** as a white solid (19.6 mg, 78%). ¹H NMR (300 MHz, CDCl₃): δ 9.92 (s, 1H), 7.60–7.68 (m, 2H), 7.15–7.26 (m, 2H), 6.92–7.15 (m, 5H), 6.86 (d, *J* = 2.4 Hz, 1H), 6.66 (dd, *J* = 2.4, 8.4 Hz, 1H), 3.87–3.95 (m, 2H), 3.86 (s, 2H), 3.21 (s, 3H), 2.80 (s, 3H), 2.55–2.64 (m, 2H), 2.17–2.33 (m, 5H). ¹³C NMR (75 MHz, CDCl₃): δ 173.7, 167.9, 148.4, 147.3, 144.4, 134.5, 134.0, 131.0, 130.9, 128.6, 126.5, 126.4, 123.4, 122.9, 121.2, 119.0, 117.7, 116.1, 59.5, 50.7, 42.8, 40.3, 31.5, 19.2, 18.9. LCMS, *m/z* 477.4 (100) [M + H]⁺. HRMS *m/z*: [M + H]⁺ calculated for C₂₇H₂₉ClN₄O₂, 477.2052; found 477.2043.

N-[4-(3,4-Dichloro-*N*-methyl-anilino)phenyl]-2-[*N*-methyl-2-(2-oxopyrrolidin-1-yl)anilino]acetamide (**42**). General Method A was followed using **68** (15 mg, 0.053 mmol) and **130** (15 mg, 0.055 mmol) to afford **42** as a white solid (23.3 mg, 89%). ¹H NMR (300 MHz, CDCl₃): δ 10.06 (s, 1H), 7.71 (d, *J* = 8.8 Hz, 2H), 6.98–7.28 (m, 7H), 6.84 (d, *J* = 2.8 Hz, 1H), 6.60 (dd, *J* = 2.8, 8.9 Hz, 1H), 3.75–4.12 (m, 4H), 3.22 (s, 3H), 2.82 (s, 3H), 2.55–2.72 (m, 2H), 2.20–2.37 (m, 2H). ¹³C NMR (75 MHz, CDCl₃): δ 173.7, 168.1, 148.8, 147.1, 143.4, 135.5, 132.5, 131.0, 130.1, 128.6, 126.4, 125.4, 122.9, 121.4, 120.8, 118.9, 116.6, 115.1, 77.4, 77.2, 76.6, 59.4, 50.8, 43.0, 40.3, 31.6, 19.3. LCMS, *m/z* 497.2 (100) [M + H]⁺. HRMS *m/z*: [M + H]⁺ calculated for C₂₆H₂₆Cl₂N₄O₂, 497.1506; found 497.1505.

N-[4-(4-Chloro-3-fluoro-*N*-methyl-anilino)phenyl]-2-[*N*-methyl-2-(2-oxopyrrolidin-1-yl)anilino]acetamide (**43**). General Method A was followed using **68** (17 mg, 0.060 mmol) and **133** (18 mg, 0.072 mmol) to afford **43** as a white solid (26.5 mg, 92%). ¹H NMR (300 MHz, CDCl₃): δ 10.04 (s, 1H), 7.61–7.77 (m, 2H), 7.14–7.26 (m, 2H), 7.01–7.14 (m, 5H), 6.40–6.56 (m, 2H), 3.78–4.00 (m, 4H), 3.21 (s, 3H), 2.80 (s, 3H), 2.55–2.67 (m, 2H), 2.28 (t, *J* = 7.6 Hz, 2H). ¹³C NMR (75 MHz, CDCl₃): δ 173.7, 168.1, 158.4 (d, *J* = 243.8 Hz), 149.5 (d, *J* = 9.0 Hz), 147.1, 143.4, 135.7, 131.0, 130.1, 128.6, 126.5, 125.7, 122.9, 121.4, 118.9, 111.5 (d, *J* = 3.0 Hz), 109.0, 108.8 (d, *J* = 18.0 Hz), 103.3 (d, *J* = 25.0 Hz), 59.4, 50.8, 42.9, 40.3, 31.6, 19.3. LCMS, *m/z* 481.2 (100) [M + H]⁺. HRMS *m/z*: [M + H]⁺ calculated for C₂₆H₂₆ClFN₄O₂, 481.1801; found 481.1795.

N-[4-(3,4-Difluoro-*N*-methyl-anilino)phenyl]-2-[*N*-methyl-2-(2-oxopyrrolidin-1-yl)anilino]acetamide (**44**). General Method A was followed using **68** (20 mg, 0.070 mmol) and **135** (16 mg, 0.070 mmol) to afford **44** as a light purple solid (30.4 mg, 93%). ¹H NMR (300 MHz, CDCl₃): δ 9.96 (s, 1H), 7.58–7.72 (m, 2H), 7.14–7.26 (m, 2H), 6.86–7.14 (m, 5H), 6.62 (ddd, *J* = 2.9, 6.9, 13.1 Hz, 1H), 6.41–6.55 (m, 1H), 3.80–4.05 (m, 4H), 3.20 (s, 3H), 2.80 (s, 3H), 2.61 (t, *J* = 8.0 Hz, 2H), 2.27 (quin, *J* = 7.5 Hz, 2H). LCMS, *m/z* 465.2 (100). HRMS *m/z*: [M + H]⁺ calculated for C₂₆H₂₆F₂N₄O₂, 465.2097; found 465.2086.

N-[4-[Methyl-(5-methyl-2-pyridyl)amino]phenyl]-2-[*N*-methyl-2-(2-oxopyrrolidin-1-yl)anilino]acetamide (**45**). General Method A was followed using **68** (11 mg, 0.039 mmol) and **138** (9.0 mg, 0.043 mmol) to afford **45** as a dark gray solid (11.7 mg, 68%). ¹H NMR (300 MHz, CDCl₃): δ 10.02 (s, 1H), 7.96–8.08 (m, 1H), 7.64–7.78 (m, 2H), 6.96–7.27 (m, 7H), 6.45 (d, *J* = 8.6 Hz, 1H), 3.75–4.06 (m, 4H), 3.40 (s, 3H), 2.81 (s, 3H), 2.55–2.67 (m, 2H), 2.29 (t, *J* = 7.6

Hz, 2H), 2.19 (s, 3H). ¹³C NMR (75 MHz, CDCl₃): δ 173.7, 168.0, 157.3, 147.2, 142.9, 137.5, 135.7, 131.1, 128.6, 126.5, 126.4, 122.9, 121.6, 121.3, 119.0, 109.1, 59.5, 50.8, 42.9, 38.4, 31.6, 19.3, 17.3. LCMS, *m/z* 444.2 (100) [M + H]⁺. HRMS *m/z*: [M + H]⁺ calculated for C₂₆H₂₉N₅O₂, 444.2394; found 444.2385.

N-[4-[Methyl-(6-methyl-3-pyridyl)amino]phenyl]-2-[*N*-methyl-2-(2-oxopyrrolidin-1-yl)anilino]acetamide (**46**). General Method A was followed using **68** (15 mg, 0.053 mmol) and **141** (12 mg, 0.058 mmol) to afford **46** as an off white solid (12.1 mg, 52%). ¹H NMR (300 MHz, CDCl₃): δ 9.92 (br. s., 1H), 8.18 (d, *J* = 2.7 Hz, 1H), 7.65 (d, *J* = 8.9 Hz, 2H), 7.17–7.27 (m, 2H), 7.04–7.15 (m, 3H), 6.98 (d, *J* = 8.8 Hz, 3H), 3.84–3.97 (m, 4H), 3.26 (s, 3H), 2.81 (s, 3H), 2.56–2.65 (m, 2H), 2.49 (s, 3H), 2.22–2.33 (m, 2H). ¹³C NMR (75 MHz, CDCl₃): δ 173.7, 167.9, 149.2, 147.3, 144.2, 143.1, 139.3, 133.9, 131.1, 128.6, 126.5, 126.1, 123.0, 122.9, 122.4, 121.3, 119.0, 59.6, 50.8, 42.8, 40.2, 31.5, 23.2, 19.3. LCMS, *m/z* 444.2 (100) [M + H]⁺. HRMS *m/z*: [M + H]⁺ calculated for C₂₆H₂₉N₅O₂, 444.2394; found 444.2384.

N-[4-(*N*,4-Dimethylanilino)-2-fluoro-phenyl]-2-[*N*-methyl-2-(2-oxopyrrolidin-1-yl)anilino]acetamide (**47**). General Method A was followed using **68** (15 mg, 0.053 mmol) and **144** (16 mg, 0.069 mmol) to afford **47** as a white solid (19.9 mg, 82%). ¹H NMR (300 MHz, CDCl₃): δ 9.27 (s, 1H), 7.58–7.70 (m, 1H), 7.27–7.33 (m, 1H), 7.05–7.23 (m, 5H), 7.00 (d, *J* = 8.4 Hz, 2H), 6.52–6.63 (m, 2H), 3.77–3.93 (m, 4H), 3.24 (s, 3H), 2.82 (s, 3H), 2.48–2.62 (m, 2H), 2.33 (s, 3H), 2.21 (quin, *J* = 7.5 Hz, 2H). ¹³C NMR (75 MHz, CDCl₃): δ 174.7, 168.2, 158.2 (d, *J* = 242.0 Hz), 148.3, 147.6 (d, *J* = 9.8 Hz), 145.8, 133.3, 131.8, 130.0, 128.7, 127.7, 124.7, 123.7, 120.0, 116.6 (d, *J* = 12 Hz), 112.4, 104.1 (d, 23 Hz), 60.3, 50.7, 42.6, 40.4, 31.2, 20.8, 19.1. LCMS, *m/z* 461.4 (100) [M + H]⁺. HRMS *m/z*: [M + H]⁺ calculated for C₂₇H₂₉FN₄O₂, 461.2347; found 461.2338.

N-[2-Chloro-4-(4-chloro-*N*-methyl-anilino)phenyl]-2-[*N*-methyl-2-(2-oxopyrrolidin-1-yl)anilino]acetamide (**48**). General Method A was followed using **68** (14 mg, 0.049 mmol) and **145** (18 mg, 0.069 mmol) to afford **48** as a white solid (6.4 mg, 26%). ¹H NMR (300 MHz, CDCl₃): δ 9.51 (br. s., 1H), 7.84 (d, *J* = 7.8 Hz, 1H), 7.05–7.25 (m, 6H), 6.84–7.00 (m, 4H), 3.84 (d, *J* = 10.6 Hz, 4H), 3.26 (s, 3H), 2.90 (br. s., 3H), 2.50 (d, *J* = 7.3 Hz, 2H), 2.11–2.28 (m, 2H). ¹³C NMR (75 MHz, CDCl₃): δ 175.0, 168.4, 148.6, 147.0, 146.4, 131.9, 129.3, 128.8, 128.1, 127.9, 127.0, 126.6, 124.9, 123.9, 122.1, 120.6, 120.1, 119.2, 60.9, 50.9, 42.4, 40.4, 31.2, 19.0. LCMS, *m/z* 497.2 (100) [M + H]⁺. HRMS *m/z*: [M + H]⁺ calculated for C₂₆H₂₆Cl₂N₄O₂, 497.1506; found 497.1500.

N-[4-(*N*,4-Dimethylanilino)-3-fluoro-phenyl]-2-[*N*-methyl-2-(2-oxopyrrolidin-1-yl)anilino]acetamide (**49**). General Method A was followed using **68** (15 mg, 0.053 mmol) and **148** (13 mg, 0.058 mmol) to afford **49** as a white solid (24.1 mg, 99%). ¹H NMR (300 MHz, CDCl₃): δ 10.18 (s, 1H), 7.66 (dd, *J* = 2.3, 12.9 Hz, 1H), 7.37–7.46 (m, 1H), 7.15–7.26 (m, 2H), 7.02–7.15 (m, 3H), 6.93–7.02 (m, *J* = 8.4 Hz, 2H), 6.55–6.67 (m, *J* = 8.5 Hz, 2H), 4.00–3.85 (m, 4H), 3.19 (s, 3H), 2.79 (s, 3H), 2.55–2.70 (m, 2H), 2.17–2.35 (m, 5H). LCMS, *m/z* 461.4 (100) [M + H]⁺. HRMS *m/z*: [M + H]⁺ calculated for C₂₇H₂₉FN₄O₂, 461.2347; found 461.2340.

N-[3-Chloro-4-(4-chloro-*N*-methyl-anilino)phenyl]-2-[*N*-methyl-2-(2-oxopyrrolidin-1-yl)anilino]acetamide (**50**). General Method A was followed using **68** (7 mg, 0.025 mmol) and **150** (7 mg, 0.026 mmol) to afford **50** as a white solid (9.7 mg, 79%). ¹H NMR (300 MHz, CDCl₃): δ 10.26 (s, 1H), 7.96 (d, *J* = 2.3 Hz, 1H), 7.61 (dd, *J* = 2.4, 8.6 Hz, 1H), 7.13–7.26 (m, 2H), 7.01–7.13 (m, 5H), 6.34–6.52 (m, 2H), 3.92 (br. s., 4H), 3.16 (s, 3H), 2.79 (s, 3H), 2.61–2.71 (m, 2H), 2.30 (t, *J* = 7.6 Hz, 2H). ¹³C NMR (75 MHz, CDCl₃): δ 173.5, 168.4, 147.4, 146.7, 140.0, 138.0, 133.5, 131.0, 130.0, 128.6, 126.4, 123.0, 122.2, 122.1, 120.0, 118.8, 114.1, 59.1, 50.8, 43.2, 39.0, 31.7, 19.3. LCMS, *m/z* 497.2 (100) [M + H]⁺, 499.2. HRMS *m/z*: [M + H]⁺ calculated for C₂₆H₂₆Cl₂N₄O₂, 497.1506; found 497.1503.

N-[5-(*N*,4-Dimethylanilino)-2-pyridyl]-2-[*N*-methyl-2-(2-oxopyrrolidin-1-yl)anilino]acetamide (**51**). General Method A was followed using **68** (16 mg, 0.056 mmol) and **152** (16 mg, 0.073 mmol) to afford **51** as a dark gray solid (11.5 mg, 46%). ¹H NMR (300 MHz, CDCl₃): δ 9.68 (s, 1H), 7.95–8.10 (m, 2H), 7.25–7.31 (m, 3H), 7.18 (dd, *J* =

1.6, 7.9 Hz, 2H), 7.11 (d, J = 8.4 Hz, 3H), 6.89–6.98 (m, 2H), 3.86 (t, J = 7.1 Hz, 2H), 3.79 (s, 2H), 3.27 (s, 3H), 2.82 (s, 3H), 2.55–2.64 (m, 2H), 2.32 (s, 3H), 2.17–2.28 (m, 2H). ^{13}C NMR (75 MHz, CDCl_3): δ 175.0, 168.3, 148.6, 145.9, 144.5, 142.3, 139.0, 132.2, 132.0, 130.0, 128.7, 128.3, 128.1, 124.0, 121.3, 120.1, 114.3, 76.6, 61.0, 50.8, 42.7, 40.3, 31.2, 20.7, 18.9. LCMS, m/z 444.4 (100) $[\text{M} + \text{H}]^+$. HRMS m/z : $[\text{M} + \text{H}]^+$ calculated for $\text{C}_{26}\text{H}_{29}\text{N}_5\text{O}_2$, 444.2394; found 444.2385.

N-[6-(*N*,4-Dimethylanilino)-3-pyridyl]-2-[*N*-methyl-2-(2-oxopyrrolidin-1-yl)anilino]acetamide (**52**). General Method A was followed using **68** (16 mg, 0.056 mmol) and **153** (17 mg, 0.080 mmol) to afford **52** as a dark gray solid (17.3 mg, 69%). ^1H NMR (300 MHz, CDCl_3): δ 9.88 (s, 1H), 8.42 (d, J = 2.5 Hz, 1H), 7.69 (dd, J = 2.7, 9.1 Hz, 1H), 6.96–7.25 (m, 9H), 6.46 (d, J = 9.1 Hz, 1H), 3.80–3.97 (m, 4H), 3.40 (s, 3H), 2.78 (s, 3H), 2.53–2.64 (m, 2H), 2.35 (s, 3H), 2.26 (quin, J = 7.6 Hz, 2H). ^{13}C NMR (75 MHz, CDCl_3): δ 173.6, 168.0, 155.8, 147.2, 144.6, 139.9, 134.6, 131.1, 130.1, 130.0, 128.5, 126.5, 126.2, 125.7, 122.9, 119.1, 108.9, 59.2, 50.7, 42.9, 38.5, 31.5, 20.9, 19.3. LCMS, m/z 444.4 (100) $[\text{M} + \text{H}]^+$. HRMS m/z : $[\text{M} + \text{H}]^+$ calculated for $\text{C}_{26}\text{H}_{29}\text{N}_5\text{O}_2$, 444.2394; found 444.2385.

N-[4-(*N*,4-Dimethylanilino)phenyl]-2-[4-fluoro-*N*-methyl-2-(2-oxopyrrolidin-1-yl)anilino]acetamide (**53**). General Method A was followed using **157** (15 mg, 0.050 mmol) and **103** (11 mg, 0.050 mmol) to afford **53** as a gray solid (18.2 mg, 80%). ^1H NMR (300 MHz, CDCl_3): δ 9.72 (s, 1H), 7.57 (d, J = 8.9 Hz, 2H), 7.02–7.15 (m, 3H), 6.80–7.01 (m, 7H), 3.87 (t, J = 7.0 Hz, 2H), 3.78 (s, 2H), 3.24 (s, 3H), 2.75 (s, 3H), 2.49–2.64 (m, 2H), 2.11–2.37 (m, 5H). ^{13}C NMR (75 MHz, CDCl_3): δ 173.8, 167.5, 158.2 (d, J = 242.3 Hz), 156.6, 146.9, 145.6, 143.9, 132.4 (d, J = 9.0 Hz), 132.0, 130.4, 129.6, 120.9, 120.6, 120.2, 115.1 (d, J = 22 Hz), 113.7 (d, J = 22 Hz), 60.0, 50.6, 42.9, 40.4, 31.4, 20.6, 19.2. LCMS, m/z 461.4 (100) $[\text{M} + \text{H}]^+$. HRMS m/z : $[\text{M} + \text{H}]^+$ calculated for $\text{C}_{27}\text{H}_{29}\text{FN}_4\text{O}_2$, 461.2347; found 461.2338.

N-[4-(*N*,4-Dimethylanilino)phenyl]-2-[5-fluoro-*N*-methyl-2-(2-oxopyrrolidin-1-yl)anilino]acetamide (**54**). General Method A was followed using **160** (5 mg, 0.017 mmol) and **103** (5 mg, 0.022 mmol) to afford **54** as a gray solid (5.2 mg, 80%). ^1H NMR (300 MHz, CDCl_3): δ 9.60 (s, 1H), 7.51–7.65 (m, 2H), 7.00–7.16 (m, 3H), 6.84–6.99 (m, 4H), 6.81 (dd, J = 2.7, 10.7 Hz, 1H), 6.72 (ddd, J = 2.7, 7.4, 8.7 Hz, 1H), 3.85 (t, J = 6.8 Hz, 2H), 3.80 (s, 2H), 3.24 (s, 3H), 2.81 (s, 3H), 2.49–2.59 (m, 2H), 2.29 (s, 3H), 2.13–2.28 (m, 2H). ^{13}C NMR (75 MHz, CDCl_3): δ 174.1, 167.1, 149.4 (d, J = 9.0 Hz), 146.9, 145.7, 131.9, 130.5, 129.7, 128.0, 127.9, 126.6 (d, J = 3.0 Hz), 121.0, 120.6, 120.3, 109.3 (d, J = 23.0 Hz), 106.4 (d, J = 25.0 Hz), 59.7, 50.8, 42.2, 40.4, 31.3, 20.6, 19.1. LCMS, m/z 461.2 (100) $[\text{M} + \text{H}]^+$. HRMS m/z : $[\text{M} + \text{H}]^+$ calculated for $\text{C}_{27}\text{H}_{29}\text{FN}_4\text{O}_2$, 461.2347; found 461.2338.

N-[4-(*N*,4-Dimethylanilino)phenyl]-2-[methyl-2-(2-oxopyrrolidin-1-yl)-3-pyridyl]amino]acetamide (**55**). General Method A was followed using **164** (5 mg, 0.020 mmol) and **103** (4.5 mg, 0.021 mmol) to afford **55** as a dark gray solid (4.6 mg, 52%). ^1H NMR (300 MHz, CDCl_3): δ 10.08 (s, 1H), 8.09 (dd, J = 1.4, 4.6 Hz, 1H), 7.58 (d, J = 8.9 Hz, 2H), 7.34–7.44 (m, 1H), 7.16 (dd, J = 4.6, 8.2 Hz, 1H), 7.05 (d, J = 8.3 Hz, 2H), 6.87 (d, J = 8.5 Hz, 2H), 6.91 (d, J = 9.0 Hz, 2H), 4.11 (t, J = 6.9 Hz, 2H), 3.90 (s, 2H), 3.23 (s, 3H), 2.81 (s, 3H), 2.57–2.71 (m, 2H), 2.23–2.35 (m, 5H). LCMS, m/z 444.2 (100) $[\text{M} + \text{H}]^+$. HRMS m/z : $[\text{M} + \text{H}]^+$ calculated for $\text{C}_{26}\text{H}_{29}\text{N}_5\text{O}_2$, 444.2394; found 444.2385.

N-[4-(4-Chloro-3-fluoro-*N*-isopropyl-anilino)phenyl]-2-[*N*-methyl-2-(2-oxopyrrolidin-1-yl)anilino]acetamide (**56**). General Method A was followed using **68** (20 mg, 0.070 mmol) **166** (22 mg, 0.078 mmol) to afford **56** as an off white solid (30.4 mg, 85%). ^1H NMR (300 MHz, CDCl_3): δ 10.02 (s, 1H), 7.68 (d, J = 8.8 Hz, 2H), 7.07–7.18 (m, 2H), 6.84–7.07 (m, 5H), 6.23 (dd, J = 2.8, 13.0 Hz, 1H), 6.13 (dd, J = 2.7, 9.0 Hz, 1H), 4.00–4.15 (m, 1H), 3.74–3.95 (m, 4H), 2.72 (s, 3H), 2.37–2.63 (m, 2H), 2.21 (t, J = 7.5 Hz, 2H), 1.02 (d, J = 6.6 Hz, 6H). ^{13}C NMR (75 MHz, CDCl_3): δ 173.6, 168.2, 160.1, 156.9, 149.5 (d, J = 9.8 Hz), 147.0, 137.3 (d, J = 8.3 Hz), 131.0, 129.9, 128.6, 126.4, 122.9, 121.1, 118.9, 110.6, 107.2 (d, J = 17.3 Hz), 102.2 (d, J =

25.5 Hz), 59.4, 50.8, 48.4, 43.0, 31.6, 20.8, 19.3. LCMS, m/z 509.4 (100) $[\text{M} + \text{H}]^+$.

N-[6-(4-Chloro-3-fluoro-*N*-isopropyl-anilino)-3-pyridyl]-2-[*N*-methyl-2-(2-oxopyrrolidin-1-yl)anilino]acetamide (**57**). General Method A was followed using **68** (15.0 mg, 0.053 mmol) and **169** (16.3 mg, 0.063 mmol) to afford **79** as a gray solid (24.3 mg, 94%). ^1H NMR (300 MHz, CDCl_3): δ 9.19 (s, 1H), 7.57 (t, J = 8.9 Hz, 1H), 7.23–7.32 (m, 2H), 7.03–7.22 (m, 5H), 6.90 (d, J = 8.3 Hz, 2H), 6.22–6.40 (m, 2H), 4.20 (td, J = 6.6, 13.1 Hz, 1H), 3.75–3.90 (m, 4H), 2.81 (s, 3H), 2.49–2.61 (m, 2H), 2.36 (s, 3H), 2.20 (quin, J = 7.5 Hz, 2H), 1.12 (d, J = 6.6 Hz, 6H). ^{13}C NMR (75 MHz, CDCl_3): δ 174.7, 168.1, 155.1 (d, J = 241.5 Hz), 148.4, 147.1 (d, J = 9.0 Hz), 140.4, 135.3, 131.8, 130.0, 129.1, 128.7, 127.7, 124.6 (d, J = 3.8 Hz), 123.7, 120.0, 115.2 (d, J = 12.0 Hz), 111.4, 103.2 (d, J = 24.0 Hz), 60.3, 50.7, 48.1, 42.5, 31.2, 20.9, 19.1. LCMS, m/z 489.4 (100) $[\text{M} + \text{H}]^+$. HRMS m/z : $[\text{M} + \text{H}]^+$ calculated for $\text{C}_{29}\text{H}_{33}\text{FN}_4\text{O}_2$, 489.2660; found 489.2653.

N-[4-(4-Chloro-3-fluoro-*N*-isopropyl-anilino)-2-fluoro-phenyl]-2-[*N*-methyl-2-(2-oxopyrrolidin-1-yl)anilino]acetamide (**58**). General Method A was followed using **68** (20 mg, 0.070 mmol) and **172** (22.9 mg, 0.077 mmol) to afford **58** as a gray solid (27.9 mg, 75%). ^1H NMR (300 MHz, CDCl_3): δ 9.56 (s, 1H), 7.88 (t, J = 8.9 Hz, 1H), 7.28–7.34 (m, 1H), 7.07–7.24 (m, 4H), 6.66–6.79 (m, 2H), 6.48 (dd, J = 2.6, 12.2 Hz, 1H), 6.38 (dd, J = 2.3, 8.9 Hz, 1H), 4.06–4.32 (m, 1H), 3.77–3.99 (m, 4H), 2.83 (s, 3H), 2.50–2.67 (m, 2H), 2.24 (quin, J = 7.5 Hz, 2H), 1.14 (d, J = 6.6 Hz, 6H). ^{13}C NMR (75 MHz, CDCl_3): δ 174.5, 168.5, 158.5 (d, J = 244.5 Hz), 154.5 (d, J = 247.5 Hz), 148.0, 147.7 (d, J = 9.0 Hz), 140.7 (d, J = 8.2 Hz), 131.8, 130.3, 127.7 (d, J = 18.8 Hz), 127.8 (d, J = 9.0 Hz), 124.6 (d, J = 2.3 Hz), 123.8, 123.2 (d, J = 2.3 Hz), 122.6 (d, J = 11.3 Hz), 119.9, 114.6, 114.3 (d, J = 23.3 Hz), 110.5 (d, J = 75.2 Hz), 106.2 (d, J = 24.8 Hz), 77.4, 77.2, 76.6, 60.1, 50.7, 48.7, 42.8, 31.3, 20.8, 19.1. LCMS, m/z 527.2 (100) $[\text{M} + \text{H}]^+$. HRMS m/z : $[\text{M} + \text{H}]^+$ calculated for $\text{C}_{28}\text{H}_{29}\text{ClF}_2\text{N}_4\text{O}_2$, 527.2020; found 527.2024.

N-[4-(4-Cyano-*N*-isopropyl-anilino)-2-fluoro-phenyl]-2-[*N*-methyl-2-(2-oxopyrrolidin-1-yl)anilino]acetamide (**59**). General Method A was followed using **68** (10.0 mg, 0.035 mmol) and **175** (9.5 mg, 0.035 mmol) to afford **59** as an off white solid (4.9 mg, 28%). ^1H NMR (300 MHz, CDCl_3): δ 9.72 (br. s., 1H), 7.90–8.07 (m, 1H), 7.30–7.42 (m, 3H), 7.05–7.24 (m, 3H), 6.78–6.90 (m, 2H), 6.52 (d, J = 9.07 Hz, 2H), 4.30 (td, J = 6.6, 13.2 Hz, 1H), 3.91 (t, J = 6.7 Hz, 4H), 2.84 (s, 3H), 2.61 (t, J = 8.0 Hz, 2H), 2.27 (quin, J = 7.5 Hz, 2H), 1.16 (d, J = 6.6 Hz, 6H). LCMS, m/z 500.4 (100) $[\text{M} + \text{H}]^+$. HRMS m/z : $[\text{M} + \text{H}]^+$ calculated for $\text{C}_{29}\text{H}_{30}\text{FN}_5\text{O}_2$, 500.2456; found 500.2448.

N-[6-(*N*-Ethyl-4-methyl-anilino)-3-pyridyl]-2-[*N*-methyl-2-(2-oxopyrrolidin-1-yl)anilino]acetamide (**60**). General Method A was followed using **68** (15 mg, 0.053 mmol) and **178** (14 mg, 0.063 mmol) to afford **60** as a white solid (16.7 mg, 69%). ^1H NMR (300 MHz, CDCl_3): δ 9.85 (s, 1H), 8.38 (d, J = 2.2 Hz, 1H), 7.62 (dd, J = 2.7, 9.1 Hz, 1H), 7.13–7.25 (m, 4H), 6.95–7.10 (m, 4H), 6.30 (d, J = 9.1 Hz, 1H), 3.75–4.04 (m, 6H), 2.78 (s, 3H), 2.51–2.62 (m, 2H), 2.35 (s, 3H), 2.25 (quin, J = 7.5 Hz, 2H), 1.16 (t, J = 7.0 Hz, 3H). ^{13}C NMR (75 MHz, CDCl_3): δ 173.6, 167.9, 155.4, 147.2, 142.9, 140.0, 135.1, 131.1, 130.3, 130.1, 128.5, 127.3, 126.5, 125.6, 122.9, 119.1, 108.7, 59.2, 50.7, 44.8, 42.9, 31.5, 21.0, 19.3, 13.1. LCMS, m/z 458.4 (100) $[\text{M} + \text{H}]^+$. HRMS m/z : $[\text{M} + \text{H}]^+$ calculated for $\text{C}_{27}\text{H}_{31}\text{N}_5\text{O}_2$, 458.2551; found 458.2541.

N-[6-(*N*-Isopropyl-4-methyl-anilino)-3-pyridyl]-2-[*N*-methyl-2-(2-oxopyrrolidin-1-yl)anilino]acetamide (**61**). General Method A was followed using **68** (12.0 mg, 0.042 mmol) and **180** (12 mg, 0.050 mmol) to afford **61** as a gray solid (14.7 mg, 74%). ^1H NMR (300 MHz, CDCl_3): δ 9.79 (s, 1H), 8.35 (d, J = 2.5 Hz, 1H), 7.54 (dd, J = 2.7, 9.2 Hz, 1H), 7.12–7.25 (m, 4H), 6.92–7.11 (m, 4H), 5.90 (d, J = 9.2 Hz, 1H), 5.14 (td, J = 6.7, 13.5 Hz, 1H). ^{13}C NMR (75 MHz, CDCl_3): δ 173.7, 167.9, 156.1, 147.3, 139.6, 138.5, 136.8, 131.3, 131.2, 130.4, 130.2, 128.5, 126.5, 125.0, 122.9, 119.1, 108.7, 59.2, 50.7, 45.9, 42.8, 31.5, 21.1, 21.1, 19.3. LCMS, m/z 472.2 (100) $[\text{M} + \text{H}]^+$. HRMS m/z : $[\text{M} + \text{H}]^+$ calculated for $\text{C}_{28}\text{H}_{33}\text{N}_5\text{O}_2$, 472.2707; found 472.2699.

N-[6-(3-Fluoro-*N*-isopropyl-4-methyl-anilino)-3-pyridyl]-2-[*N*-methyl-2-(2-oxopyrrolidin-1-yl)anilino]acetamide (**62**). General Method A was followed using **68** (15.0 mg, 0.053 mmol) and **183** (15 mg, 0.058 mmol) to afford **62** as a gray solid (22.2 mg, 86%). ¹H NMR (300 MHz, CDCl₃): δ 9.86 (s, 1H), 8.39 (d, *J* = 2.2 Hz, 1H), 7.60 (dd, *J* = 2.5, 9.11 Hz, 1H), 7.13–7.27 (m, 3H), 6.99–7.13 (m, 2H), 6.75–6.85 (m, 2H), 5.97 (d, *J* = 9.2 Hz, 1H), 5.03–5.22 (m, 1H), 3.77–4.03 (m, 4H), 2.79 (s, 3H), 2.54–2.64 (m, 2H), 2.20–2.36 (m, 5H), 1.11 (d, *J* = 6.7 Hz, 6H). ¹³C NMR (75 MHz, CDCl₃): δ 173.6, 167.9, 161.5 (d, *J* = 245.3 Hz), 155.6, 147.2, 140.6 (d, *J* = 9.0 Hz), 139.8, 131.7 (d, *J* = 6.0 Hz), 131.1, 130.3, 128.5, 126.7 (d, *J* = 3.0 Hz), 126.5, 125.6, 123.6 (d, *J* = 17.3 Hz), 122.8, 119.0, 117.9, 117.7, 108.9, 59.1, 50.7, 46.2, 42.9, 31.5, 21.1, 19.3, 14.2 (d, *J* = 3.8 Hz). LCMS, *m/z* 490.2 (100) [M + H]⁺. HRMS *m/z*: [M + H]⁺ calculated for C₂₈H₃₂FN₃O₂, 490.2613; found 490.2605.

N-[6-(4-Chloro-3-fluoro-*N*-isopropyl-anilino)-3-pyridyl]-2-[*N*-methyl-2-(2-oxopyrrolidin-1-yl)anilino]acetamide (**63**). General Method A was followed using **68** (9.0 mg, 0.032 mmol) and **186** (8.2 mg, 0.029 mmol) to afford **63** as a light purple solid (15.1 mg, 94%). ¹H NMR (300 MHz, CDCl₃): δ 9.98 (s, 1H), 8.44 (d, *J* = 2.5 Hz, 1H), 7.68 (dd, *J* = 2.6, 9.1 Hz, 1H), 7.41 (t, *J* = 8.4 Hz, 1H), 7.14–7.27 (m, 2H), 6.99–7.14 (m, 2H), 6.80–6.96 (m, 2H), 6.08 (d, *J* = 9.1 Hz, 1H), 5.06 (quin, *J* = 6.8 Hz, 1H), 3.79–4.04 (m, 4H), 2.79 (s, 3H), 2.61 (t, *J* = 8.0 Hz, 2H), 2.28 (quin, *J* = 7.5 Hz, 2H), 1.13 (d, *J* = 6.7 Hz, 6H). ¹³C NMR (75 MHz, CDCl₃): δ 173.6, 168.1, 158.4 (d, *J* = 249.0 Hz), 154.9, 147.1, 142.5 (d, *J* = 8.3 Hz), 140.0, 131.1, 130.9, 130.3, 128.6, 126.8, 126.7, 126.7, 126.5, 122.9, 119.0, 118.7 (d, *J* = 17.3 Hz), 118.4 (d, *J* = 21.0 Hz), 109.9, 59.0, 50.7, 46.8, 43.0, 31.5, 21.1, 19.3. LCMS, *m/z* 510.3 (100) [M + H]⁺. HRMS *m/z*: [M + H]⁺ calculated for C₂₇H₂₉ClFN₃O₂, 510.2067; found 510.2062.

N-[6-(4-Cyano-*N*-isopropyl-anilino)-3-pyridyl]-2-[*N*-methyl-2-(2-oxopyrrolidin-1-yl)anilino]acetamide (**64**). General Method A was followed using **68** (20 mg, 0.070 mmol) and **189** (21 mg, 0.084 mmol) to afford **64** as an off white solid (17.8 mg, 49%). ¹H NMR (300 MHz, CDCl₃): δ 10.29 (s, 1H), 8.67 (d, *J* = 2.6 Hz, 1H), 7.98 (dd, *J* = 2.7, 8.8 Hz, 1H), 7.45–7.52 (m, 2H), 7.14–7.26 (m, 2H), 7.00–7.11 (m, 2H), 6.80–6.88 (m, 2H), 6.58 (d, *J* = 8.7 Hz, 1H), 4.63–4.77 (m, 1H), 3.93 (br. s., 4H), 2.79 (s, 3H), 2.63 (t, *J* = 8.1 Hz, 2H), 2.30 (t, *J* = 7.6 Hz, 2H), 1.17 (d, *J* = 6.73 Hz, 6H). ¹³C NMR (75 MHz, CDCl₃): δ 173.6, 168.6, 152.2, 149.5, 146.8, 141.1, 133.3, 131.1, 131.0, 129.9, 128.6, 126.4, 123.0, 121.8, 119.7, 118.9, 117.7, 103.9, 76.6, 58.9, 50.8, 48.4, 43.3, 31.6, 21.0, 19.3. LCMS, *m/z* 483.2 (100) [M + H]⁺. HRMS *m/z*: [M + H]⁺ calculated for C₂₈H₃₀N₆O₂, 483.2503; found 483.2496.

1-(2-Aminophenyl)pyrrolidin-2-one (**65**). A pressure tube was charged with 2-bromoaniline (2.0 g, 12 mmol), copper iodide (0.22 g, 1.2 mmol), 2-pyrrolidinone (1.1 mL, 14 mmol), potassium carbonate (3.2 g, 23 mmol), *N,N'*-dimethylethylenediamine (0.12 mL, 1.2 mmol), and toluene (7 mL). The tube was sealed and the mixture was heated at 80 °C for 72 h. The resulting mixture was partitioned between EtOAc (10 mL) and H₂O (10 mL). The organic phase was separated, dried over anhydrous MgSO₄, filtered, and concentrated. The reaction was then concentrated in vacuo and the crude material purified by column chromatography eluting with 100% heptane to 100% EtOAc to afford **65** as a solid (605 mg, 30%). ¹H NMR (300 MHz, CDCl₃): δ 7.03–7.13 (m, 2H), 6.75–6.88 (m, 2H), 3.98 (br. s., 2H), 3.78–3.88 (m, 2H), 2.53–2.68 (m, 2H), 2.13–2.37 (m, 2H). LCMS, *m/z* 177 (100) [M + H]⁺.

tert-Butyl 2-[2-(2-oxopyrrolidin-1-yl)anilino]acetate (**66**). *tert*-Butyl bromoacetate (0.20 mL, 1.4 mmol) was added to a stirred solution of **65** (200 mg, 1.1 mmol) and K₂CO₃ (470 mg, 3.4 mmol) in MeCN (3 mL) and stirred at reflux for 16 h. The reaction was then filtered through diatomaceous earth, washed with EtOAc (20 mL) and concentrated. The crude material was then purified by column chromatography eluting with a gradient of 100% DCM to 30% EtOAc/DCM to afford **66** as an oil (330 mg, 100%). ¹H NMR (300 MHz, CDCl₃): δ 7.15–7.23 (m, 1H), 7.09 (dd, *J* = 1.5, 7.8 Hz, 1H), 6.72–6.84 (m, 1H), 6.61 (dd, *J* = 1.08, 8.17 Hz, 1H), 4.62 (br. s., 1H), 3.72–3.84 (m, 4H), 2.57–2.69 (m, 2H), 2.20–2.33 (m, 2H), 1.47–1.53 (m, 9H). LCMS, *m/z* 291 (100) [M + H]⁺.

2-[2-(2-Oxopyrrolidin-1-yl)anilino]acetic acid hydrochloride (**67**). **66** (210 mg, 0.72 mmol) was dissolved in 4 M HCl in 1,2-dioxane and stirred for 5 h. The reaction was then concentrated to afford **67** as a solid (180 mg, 92%). ¹H NMR (300 MHz, MeOD): δ 7.78–7.92 (m, 2H), 7.56–7.72 (m, 2H), 5.36 (s, 2H), 4.56 (t, *J* = 7.3 Hz, 2H), 3.47 (t, *J* = 7.7 Hz, 2H), 2.96 (quin, *J* = 7.5 Hz, 2H). LCMS, *m/z* 235.2 (100) [M + H]⁺.

1-(2-Nitrophenyl)piperidin-2-one (**71**). General Method B: Sodium hydride (255 mg, 6.38 mmol) was added to a stirred solution of 2-piperidone (253 mg, 2.55 mmol) in DMF (10 mL) and stirred for 30 min. 1-Fluoro-2-nitro-benzene (0.226 mL, 2.12 mmol) was then added, and the reaction mixture heated at 90 °C for 24 h. 10% citric acid (5 mL) was added to the reaction mixture for quenching and then this was neutralized with saturated NaHCO₃ (pH 7). The aqueous was extracted with EtOAc (2 × 20 mL). The organic layers were combined and washed with H₂O (20 mL), dried over MgSO₄, filtered, and concentrated. The crude material was then purified by column chromatography eluting with a gradient of 100% DCM to 5% MeOH/DCM to afford **71** as a solid (175 mg, 37%). ¹H NMR (300 MHz, CDCl₃): δ 8.01 (dd, *J* = 1.4, 8.2 Hz, 1H), 7.62–7.73 (m, 1H), 7.46 (dt, *J* = 1.4, 7.8 Hz, 1H), 7.35 (dd, *J* = 1.4, 7.9 Hz, 1H), 3.71 (t, *J* = 6.1 Hz, 2H), 2.48–2.61 (m, 2H), 1.88–2.10 (m, 4H). LCMS, *m/z* 221.2 (100) [M + H]⁺.

1-(2-Aminophenyl)piperidin-2-one (**75**). General method C: **71** (175 mg, 0.80 mmol) and Pd/C (10 wt % loading, 17.5 mg) were dissolved in MeOH (10 mL) and stirred under H₂ atmosphere for 4 h. This was then filtered through diatomaceous earth and washed with EtOH and concentrated to afford **75** as an oil (134 mg, 88%). ¹H NMR (300 MHz, CDCl₃): δ 7.03–7.19 (m, 2H), 6.79–6.89 (m, 2H), 3.30–3.78 (m, 4H), 2.52–2.72 (m, 2H), 1.97 (d, *J* = 4.7 Hz, 4H). LCMS, *m/z* 191.2 (100) [M + H]⁺.

2-[2-(2-Oxo-1-piperidyl)anilino]acetic acid (**73**). Ethyl 2-bromoacetate (0.086 mL, 0.77 mmol) was added to a stirred solution of the mixture of **72** (134 mg, 0.70 mmol) and K₂CO₃ (243 mg, 1.76 mmol) in MeCN (3 mL) and stirred at reflux for 16 h. The reaction was then filtered, washed with EtOAc (20 mL) and concentrated. The crude material was then purified by column chromatography eluting with a gradient of 100% DCM to 15% EtOAc/DCM to afford ethyl 2-[2-(2-oxo-1-piperidyl)anilino]acetate (100 mg, 51%). This was then dissolved in 1:1 MeOH/H₂O (5 mL) and lithium hydroxide monohydrate (44.5 mg, 1.06 mmol) added and stirred for 2 h. The reaction was then acidified to pH 5 with 10% citric acid and concentrated. The residue was then dissolved in EtOAc (10 mL) and H₂O (10 mL). The organic layers were separated, dried and concentrated to afford **73** as a white solid (85 mg, 49%). ¹H NMR (300 MHz, MeOD): δ 7.12–7.22 (m, 1H), 7.03 (dd, *J* = 1.3, 7.7 Hz, 1H), 6.73 (t, *J* = 7.6 Hz, 1H), 6.65 (d, *J* = 8.0 Hz, 1H), 3.91 (d, *J* = 4.9 Hz, 2H), 3.46–3.68 (m, 2H), 2.44–2.65 (m, 2H), 1.86–2.08 (m, 4H). LCMS, *m/z* 249.2 (100) [M + H]⁺.

1-(2-Aminophenyl)pyridin-2-one (**74**). Pyridin-2-ol (1.5 g, 16 mmol), 2-iodoaniline (6.9 g, 32 mmol), K₂CO₃ (2.18 g, 15.8 mmol), copper iodide (300 mg, 1.58 mmol) and DMF (20 mL) and stirred at mixture at 130 °C under N₂ for 16 h. The reaction was then cooled and solvent evaporated under reduced pressure. The crude was then dissolved in EtOAc (50 mL) and washed with H₂O (3 × 50 mL), dried with anhydrous MgSO₄, and concentrated. The crude material was then purified by column chromatography eluting with a gradient of 100% heptane to 60% EtOAc/DCM to afford **74**. ¹H NMR (300 MHz, CDCl₃): δ 8.23 (dd, *J* = 4.9, 1.7 Hz, 1 H) 7.68 (ddd, *J* = 8.3, 7.2, 2.0 Hz, 1 H) 6.96–7.09 (m, 3 H) 6.84–6.91 (m, 2 H) 6.76–6.83 (m, 1 H) 3.77 (br. s., 2 H). LCMS, *m/z* 187.2 (100) [M + H]⁺.

2-[2-(2-Oxo-1-pyridyl)anilino]acetic acid hydrochloride (**75**). General Method D: **74** (342 mg, 1.83 mmol), *tert*-butyl bromoacetate (0.334 mL, 2.26 mmol), and K₂CO₃ (780 mg, 5.7 mmol) in DMF (5 mL) and stirred at 80 °C for 24 h. The reaction was then filtered through diatomaceous earth, washed with EtOAc (20 mL), and concentrated. The crude material was then purified by column chromatography eluting with a gradient of 100% DCM to 20% EtOAc to *tert*-butyl 2-[2-(2-oxo-1-pyridyl)anilino]acetate as a solid (198 mg, 36%). ¹H

NMR (300 MHz, CDCl_3): δ 8.22 (dd, J = 4.89, 1.93 Hz, 1H), 7.63–7.73 (m, 1H), 7.06–7.16 (m, 1H), 6.95–7.05 (m, 2H), 6.92 (d, J = 8.4 Hz, 1H), 6.72–6.79 (m, 1H), 6.65 (dd, J = 8.0, 1.2 Hz, 1H), 4.69 (t, J = 5.1 Hz, 1H), 3.82 (d, J = 5.6 Hz, 2H), 1.45 (s, 9H). LCMS, m/z 301 (100) $[\text{M} + \text{H}]^+$. 50 mg of the aforementioned protected intermediate was then dissolved in 4 M HCl in dioxane (1 mL) and stirred for 16 h. This was then concentrated to afford **75** as a white solid (47 mg, 100%). ^1H NMR (300 MHz, $\text{DMSO}-d_6$) δ 8.09 (d, J = 1.9 Hz, 1H), 7.75–7.81 (m, 1H), 7.16–7.32 (m, 2H), 6.65–6.79 (m, 2H), 6.52 (t, J = 2.1 Hz, 1H), 3.89 (s, 2H). LCMS, m/z 291.2 (100) $[\text{M} + \text{H}]^+$.

2-(2-Nitrophenyl)-1,2-thiazolidine 1,1-dioxide (76). General Method B was followed using 1,2-thiazolidine 1,1-dioxide (210 mg, 1.7 mmol), and 1-fluoro-2-nitrobenzene (200 mg, 1.42 mmol) to afford **76** as a solid (170 mg, 50%). ^1H NMR (300 MHz, CDCl_3): δ 7.88–7.99 (m, 1H), 7.59–7.75 (m, 2H), 7.47–7.59 (m, 1H), 3.83 (t, J = 6.8 Hz, 2H), 3.32 (t, J = 7.5 Hz, 2H), 2.60 (quin, J = 7.2 Hz, 2H). LCMS, m/z 243.2 (100) $[\text{M} + \text{H}]^+$.

2-(1,1-Dioxo-1,2-thiazolidin-2-yl)aniline (77). General Method C was followed using **76** (173 mg, 0.71 mol) to afford **77** as an oil (150 mg, 99%). ^1H NMR (300 MHz, CDCl_3): δ 7.31–7.25 (m, 1H), 7.25 (s, 1H), 7.15 (t, J = 7.2 Hz, 1H), 6.81 (d, J = 7.7 Hz, 2H), 3.69 (q, J = 6.9 Hz, 2H), 3.27–3.46 (m, 4H), 2.55 (quin, J = 7.2 Hz, 2H). LCMS, m/z 213.2 (100) $[\text{M} + \text{H}]^+$.

2-[2-(1,1-Dioxo-1,2-thiazolidin-2-yl)anilino]acetic acid (78). Ethyl 2-bromoacetate (0.0865 mL, 0.777 mmol) was added to a stirred solution of the mixture of 2-(1,1-dioxo-1,2-thiazolidin-2-yl)aniline (150 mg, 0.71 mmol) and K_2CO_3 (240 mg, 1.8 mmol) in MeCN (3 mL) and stirred at reflux for 16 h. The reaction was then filtered, washed with EtOAc (20 mL) and concentrated. The crude material was then purified by column chromatography eluting with a gradient of 100% DCM to 15% EtOAc/DCM to afford ethyl 2-[2-(1,1-dioxo-1,2-thiazolidin-2-yl)anilino]acetate (75 mg, 36%). 36 mg of this was then dissolved in 1:1 MeOH/ H_2O (5 mL) and lithium hydroxide monohydrate (44.5 mg, 1.06 mmol) added and stirred for 2 h. The reaction was then acidified to pH 5 with 10% citric acid and concentrated. The residue was then dissolved in EtOAc (10 mL) and H_2O (10 mL). The organics were separated, dried and concentrated to afford **78** as a white solid. ^1H NMR (300 MHz, CDCl_3): δ 7.33 (dd, J = 1.3, 7.9 Hz, 1H), 7.22–7.27 (m, 1H), 6.82 (t, J = 7.6 Hz, 1H), 6.63 (d, J = 7.6 Hz, 1H), 4.01 (s, 2H), 3.70 (t, J = 6.7 Hz, 2H), 3.34–3.44 (m, 2H), 2.47–2.64 (m, 2H). LCMS, m/z 271.2 (100) $[\text{M} + \text{H}]^+$.

2-(2-Nitrophenyl)thiazinane 1,1-dioxide (79). General Method B was followed using thiazinane 1,1-dioxide (200 mg, 1.5 mmol) and 1-fluoro-2-nitrobenzene (150 mg, 1.1 mmol) to afford **79** as a solid (110 mg, 40%). ^1H NMR (300 MHz, CDCl_3): δ 7.85 (d, J = 8.0 Hz, 1H), 7.57–7.68 (m, 2H), 7.40–7.57 (m, 1H), 3.83 (br. s., 1H), 3.70 (app d, J = 19.8 Hz, 1H), 3.13–3.28 (m, 2H), 2.26–2.39 (m, 2H), 2.05 (s, 1H), 1.81–2.02 (m, 1H). LCMS, m/z 257.2 (100) $[\text{M} + \text{H}]^+$.

2-(1,1-Dioxothiazinan-2-yl)aniline (80). General Method C was followed using **79** (109 mg, 0.43 mmol) to afford **80** as an oil (82 mg, 85%). ^1H NMR (300 MHz, CDCl_3): δ 7.35 (d, J = 7.8 Hz, 1H), 7.16–7.25 (m, 1H), 7.10 (t, J = 6.1 Hz, 1H), 6.96 (t, J = 7.6 Hz, 1H), 3.69–3.82 (m, 1H), 3.34–3.60 (m, 3H), 3.07–3.34 (m, 2H), 2.20–2.52 (m, 3H), 1.86–2.07 (m, 2H). LCMS, m/z 227.2 (100) $[\text{M} + \text{H}]^+$.

2-[2-(1,1-Dioxothiazinan-2-yl)anilino]acetic acid hydrochloride (81). General Method D was followed using **80** (82 mg, 0.36 mmol) and *tert*-butyl bromoacetate (0.064 mL, 0.43 mmol) to afford **81** as a solid (100 mg, 86%). ^1H NMR (300 MHz, MeOD): δ 7.49 (d, J = 8.2 Hz, 1H), 7.38 (t, J = 7.8 Hz, 1H), 7.07 (d, J = 7.6 Hz, 2H), 4.05–4.28 (m, 2H), 3.74–3.92 (m, 1H), 3.41–3.55 (m, 2H), 3.35–3.41 (m, 1H), 2.28–2.44 (m, 2H), 1.81–2.19 (m, 2H). LCMS, m/z 285.2 (100) $[\text{M} + \text{H}]^+$.

3-(2-Nitrophenyl)oxazolidin-2-one (82). General Method B was followed using 1-fluoro-2-nitrobenzene (0.61 mL, 5.74 mmol) and 2-oxazolidinone (500 mg, 5.7 mmol) to afford **82** as a solid (708 mg, 59%). ^1H NMR (300 MHz, CDCl_3): δ 7.06–7.18 (m, 2H), 6.76–

6.88 (m, 2H), 4.55 (t, J = 7.9 Hz, 2H), 3.78–4.16 (m, 4H). LCMS, m/z 209.2 (100) $[\text{M} + \text{H}]^+$.

3-(2-Aminophenyl)oxazolidin-2-one (83). General Method C was followed using **82** (708 mg, 3.4 mmol) to afford **83** as an oil (614 mg, 100%). ^1H NMR (300 MHz, CDCl_3): δ 7.08–7.19 (m, 2H), 6.74–6.91 (m, 2H), 4.55 (t, J = 7.9 Hz, 2H), 3.77–4.15 (m, 4H). LCMS, m/z 179.2 (100) $[\text{M} + \text{H}]^+$.

2-Chloro-N-[4-(4-methylphenoxy)phenyl]acetamide (84). 2-Chloroacetyl chloride (0.0958 mL, 1.20 mmol) was added dropwise to a stirred solution of 4-(4-methylphenoxy)aniline (200 mg, 1.00 mmol) and DIPEA (0.42 mL, 3.0 mmol) in DCM (20 mL) at 0 °C and allowed to warm to 20 °C. The reaction was then stirred for a further 4 h and then washed with 5% citric acid (20 mL), saturated NaHCO_3 (20 mL), brine (20 mL), dried with anhydrous MgSO_4 , filtered, and concentrated to afford **84** (233 mg, 84%). ^1H NMR (300 MHz, CDCl_3): δ 8.09 (br. s., 1 H) 7.47 (d, J = 9.0 Hz, 2 H) 7.14 (d, J = 8.4 Hz, 3 H) 6.99 (d, J = 8.9 Hz, 3 H) 6.91 (d, J = 8.4 Hz, 3 H) 4.04 (s, 2 H) 2.34 (s, 3H). LCMS, m/z 320.2 (100) $[\text{M} + \text{H}]^+$, 322.2.

1-(2-Nitrophenyl)pyrrolidine (85). Pyrrolidine (0.7 mL, 8.51 mmol) and K_2CO_3 (1.2 g, 8.51 mmol) were dissolved in MeCN (15 mL) and stirred. 1-Fluoro-2-nitrobenzene (605 mg, 8.5 mmol) was then added and the reaction stirred under reflux for 3 h. The reaction was then concentrated in vacuo and H_2O (20 mL) added. The product was extracted from the aqueous with DCM (3 \times 20 mL). The organic layers were combined and washed with brine (2 \times 20 mL), dried with anhydrous MgSO_4 , filtered, and concentrated to afford **85** as a solid (0.78 g, 95%). ^1H NMR (300 MHz, CDCl_3): δ 7.75 (dd, J = 1.6, 8.3 Hz, 1H), 7.37 (ddd, J = 1.7, 7.0, 8.6 Hz, 1H), 6.91 (dd, J = 1.0, 8.6 Hz, 1H), 6.72 (ddd, J = 1.2, 7.1, 8.2 Hz, 1H), 3.14–3.31 (m, 4H), 1.92–2.08 (m, 4H). LCMS, m/z 193.2 (100) $[\text{M} + \text{H}]^+$.

2-Pyrrolidin-1-ylaniline (86). General Method F: 1-(2-Nitrophenyl)pyrrolidine (0.78 g, 4.1 mmol) and zinc (1.3 g, 20 mmol) were dissolved in a 1:1 mixture of saturated NH_4Cl and EtOH (20 mL) and stirred at 20 °C for 2 h. The reaction was then filtered through diatomaceous earth and concentrated. The residue was dissolved in EtOAc (10 mL), washed with saturated NaHCO_3 (10 mL), brine (10 mL), dried with MgSO_4 , filtered, and concentrated to afford **86** as an oil (600 mg, 91%). ^1H NMR (300 MHz, CDCl_3): δ 7.01 (dd, J = 1.4, 8.1 Hz, 1H), 6.85–6.93 (m, 1H), 6.71–6.79 (m, 2H), 3.86 (br. s., 2H), 3.01–3.10 (m, 4H), 1.89–1.98 (m, 4H). LCMS, m/z 163.2 (100) $[\text{M} + \text{H}]^+$.

2-(2-Pyrrolidin-1-ylanilino)acetic acid (87). General Method D was followed using **86** (100 mg, 0.62 mmol) and *tert*-butyl bromoacetate (0.15 mL, 0.62 mmol) to afford **87** as a solid (81 mg, 44%). ^1H NMR (300 MHz, MeOD): δ 7.55 (dd, J = 1.1, 8.1 Hz, 1H), 7.36–7.46 (m, 1H), 6.92–7.10 (m, 2H), 4.04 (s, 2H), 3.85 (t, J = 7.1 Hz, 4H), 2.33 (td, J = 3.7, 6.9 Hz, 4H). LCMS, m/z 221.2 (100) $[\text{M} + \text{H}]^+$.

1-(2-Nitrophenyl)pyrazole (88). General Method B was followed using pyrazole (1.9 g, 28 mmol) and 1-fluoro-2-nitrobenzene (1.49 mL, 14.2 mmol) to afford **88** as a solid (1.9 g, 72%). ^1H NMR (300 MHz, CDCl_3): δ 7.89 (dd, J = 1.2, 8.0 Hz, 1H), 7.75 (dd, J = 2.1, 9.0 Hz, 2H), 7.66–7.71 (m, 1H), 7.57–7.63 (m, 1H), 7.49–7.56 (m, 1H), 6.52 (t, J = 2.1 Hz, 1H). LCMS, m/z 190.2 (100) $[\text{M} + \text{H}]^+$.

2-Pyrazol-1-ylaniline (89). General Method C was followed using **88** (1.93 g, 10.2 mmol) to afford **89** as an oil (1.61 g, 99%). ^1H NMR (300 MHz, CDCl_3): δ 7.74 (dd, J = 1.9, 8.2 Hz, 2H), 7.09–7.23 (m, 2H), 6.72–6.91 (m, 2H), 6.46 (t, J = 2.1 Hz, 1H), 4.69 (br s, 2H). LCMS, m/z 160.2 (100) $[\text{M} + \text{H}]^+$.

2-(2-Pyrazol-1-ylanilino)acetic acid dihydrochloride (90). 2-Pyrazol-1-ylaniline (300 mg, 1.88 mmol), *tert*-butyl bromoacetate (0.334 mL, 2.26 mmol), and K_2CO_3 (780 mg, 5.7 mmol) in DMF (5 mL) and stirred at 80 °C for 24 h. The reaction was then filtered through diatomaceous earth, washed with EtOAc (20 mL) and concentrated. The crude material was then purified by column chromatography eluting with a gradient of 100% DCM to 15% EtOAc to afford *tert*-butyl 2-(2-pyrazol-1-ylanilino)acetate as a solid (340 mg, 65%). ^1H NMR (300 MHz, CDCl_3): δ 7.80 (d, J = 1.7 Hz, 1H), 7.72 (d, J = 2.3 Hz, 1H), 7.17–7.26 (m, 2H), 6.77 (t, J = 7.6 Hz, 1H), 6.64 (d, J = 8.1 Hz, 1H), 6.47 (t, J = 2.1 Hz, 1H), 6.30 (br. s., 1H), 3.85 (d, J = 5.3 Hz, 2H), 1.48 (s, 9H). MS, m/z 274.4 (100) $[\text{M} + \text{H}]^+$. 50 mg of the

aforementioned protected intermediate was then dissolved in 4 M HCl in dioxane (1 mL) and stirred for 16 h. This was then concentrated to afford **90** as a white solid (45 mg, 64%). ¹H NMR (300 MHz, DMSO-*d*₆): δ 8.09 (d, *J* = 1.9 Hz, 1H), 7.75–7.81 (m, 1H), 7.16–7.32 (m, 2H), 6.65–6.79 (m, 2H), 6.52 (t, *J* = 2.1 Hz, 1H), 3.89 (s, 2H). LCMS, *m/z* 291.2 (100) [M + H]⁺.

1-(2-Nitrophenyl)-1,2,4-triazole (91). To a stirred solution of 1-fluoro-2-nitrobenzene (0.747 mL, 7.09 mmol) in DMSO (10 mL), was added 1,2,4-triazole (538 mg, 7.80 mmol) and heated to 80 °C for 4 h. H₂O (20 mL) was added to the reaction mixture and extracted with EtOAc (2 × 20 mL). The organic layer was dried with MgSO₄, filtered, and concentrated. The crude material was then purified by column chromatography eluting with a gradient of 100% DCM to 5% MeOH/DCM to afford **91** as a solid (360 mg, 27%). ¹H NMR (300 MHz, CDCl₃): δ 8.42 (s, 1H) 8.14 (s, 1H) 8.05 (dd, *J* = 8.0, 1.4 Hz, 1H) 7.78 (dd, *J* = 7.7, 1.4 Hz, 1H) 7.70 (dd, *J* = 7.9, 1.4 Hz, 1H) 7.61 (dd, *J* = 7.8, 1.3 Hz, 1H). LCMS, *m/z* 191.2 (100) [M + H]⁺.

2-(1,2,4-Triazol-1-yl)aniline (92). General Method C was followed using **91** (363 mg, 1.91 mmol) to afford **92** as an oil (304 mg, 99%). ¹H NMR (300 MHz, CDCl₃): δ 8.37 (s, 1H) 8.17 (s, 1H) 7.15–7.25 (m, 2H) 6.75–6.91 (m, 2H) 4.52 (br. s., 2H). LCMS, *m/z* 161.2 (100) [M + H]⁺.

5-Methoxy-1-(2-nitrophenyl)pyrazole (93). General Method B was followed using 5-methoxy-1H-pyrazole (180 mg, 1.8 mmol) and 1-fluoro-2-nitrobenzene (0.15 mL, 1.42 mmol) to afford **93** as an oil (276 mg, 89%). ¹H NMR (300 MHz, CDCl₃): δ 7.77–7.85 (m, 1H), 7.58–7.70 (m, 1H), 7.51–7.58 (m, 2H), 7.37–7.46 (m, 1H), 5.94 (d, *J* = 2.7 Hz, 1H), 3.91 (s, 3H). LCMS, *m/z* 220.2 (100) [M + H]⁺.

2-(5-Methoxypyrazol-1-yl)aniline (94). General Method C was followed using **93** (276 mg, 1.26 mmol) to afford **94** as an oil (220 mg, 82%). ¹H NMR (300 MHz, CDCl₃): δ 7.51 (d, *J* = 2.5 Hz, 1H), 7.04–7.18 (m, 2H), 6.71–6.87 (m, 2H), 5.85 (d, *J* = 2.4 Hz, 1H), 4.68 (br. s., 2H), 3.95 (s, 3H). LCMS, *m/z* 190.2 (100) [M + H]⁺.

2-[N-Methyl-2-(2-oxopyrrolidin-1-yl)anilino]acetic acid hydrochloride (68). Iodomethane (0.13 mL, 2.1 mmol) was added to a stirred solution of **66** (120 mg, 0.41 mmol) and K₂CO₃ (170 mg, 1.2 mmol) in DMF (2 mL) and stirred at 30 °C overnight. The reaction was then filtered, washed with EtOAc (20 mL) and concentrated. The crude material was then purified by column chromatography eluting with a gradient of 100% DCM to 30% EtOAc to afford *tert*-butyl 2-(2-pyrazol-1-ylanilino)acetate as an oil (110 mg, 83%). The aforementioned intermediate was then dissolved in 4 M HCl in 1,2-dioxane and stirred for 2 h and then concentrated to afford **68** (99 mg, 100%) as a solid. ¹H NMR (300 MHz, CDCl₃): δ 7.16–7.24 (m, 2H), 6.98–7.11 (m, 2H), 3.87 (t, *J* = 7.1 Hz, 2H), 3.63 (s, 2H), 2.81 (s, 3H), 2.48–2.60 (m, 2H), 2.17 (quin, *J* = 7.6 Hz, 2H). LCMS, *m/z* 249.2 (100) [M + H]⁺.

2-[N-Ethyl-2-(2-oxopyrrolidin-1-yl)anilino]acetic acid hydrochloride (69). The procedure used for **69** was followed using **66** (80 mg, 0.28 mmol) and iodoethane (0.111 mL, 1.38 mmol) to afford **69** as a solid (34 mg, 41%). ¹H NMR (300 MHz, MeOD): δ 7.60–7.74 (m, 1H), 7.35–7.57 (m, 3H), 4.44 (s, 2H), 3.99 (t, *J* = 7.1 Hz, 2H), 3.71 (q, *J* = 7.2 Hz, 2H), 2.61 (t, *J* = 8.0 Hz, 2H), 2.26 (quin, *J* = 7.5 Hz, 2H), 1.27 (t, *J* = 7.2 Hz, 3H). LCMS, *m/z* 263.2 (100) [M + H]⁺.

1-Benzoyloxy-2-iodo-benzene (95). 2-Iodophenol (1.0 g, 4.5 mmol), bromomethylbenzene (0.81 mL, 6.8 mmol), and K₂CO₃ (1.88 g, 13.6 mmol) in acetone (20 mL) was stirred at reflux for 4 h. The reaction was then filtered through diatomaceous earth and concentrated. The crude material was then purified by column chromatography eluting with a gradient of 100% heptane to 20% EtOAc to afford **95** as an oil (640 mg, 45%). ¹H NMR (300 MHz, CDCl₃): δ 7.81 (dd, *J* = 7.8, 1.6 Hz, 1H), 7.48–7.55 (m, 2H), 7.28–7.45 (m, 4H), 6.88 (dd, *J* = 8.2, 1.03 Hz, 1H), 6.74 (td, *J* = 7.6, 1.26 Hz, 1H), 5.17 (s, 2H). LCMS, *m/z* 311.2 (100) [M + H]⁺.

1-(2-Benzoyloxyphenyl)pyrrolidin-2-one (96). **95** (639 mg, 2.06 mmol), K₂CO₃ (280 mg, 2.1 mmol), 2-pyrrolidinone (0.47 mL, 6.2 mmol), and copper (260 mg, 4.1 mmol) were heated neat at 165 °C for 16 h. The reaction was then quenched with H₂O (40 mL) and mixture extracted with EtOAc (2 × 20 mL). The organics were

washed with 5% citric acid (20 mL), H₂O (20 mL), brine (20 mL), dried with anhydrous MgSO₄, filtered, and concentrated. The crude material was then purified by column chromatography eluting with a gradient of 100% DCM to 100% EtOAc to afford **96** as an oil (370 mg, 68%). ¹H NMR (300 MHz, CDCl₃): δ 7.28–7.45 (m, 6H), 7.23 (d, *J* = 1.7 Hz, 1H), 6.98–7.06 (m, 2H), 5.10 (s, 2H), 3.77 (t, *J* = 7.0 Hz, 2H), 2.41–2.62 (m, 2H), 2.14 (quin, *J* = 7.5 Hz, 2H). LCMS, *m/z* 268.2 (100) [M + H]⁺.

1-(2-Hydroxyphenyl)pyrrolidin-2-one (97). **96** (370 mg, 1.4 mmol) and Pd/C (10 wt % loading, 40 mg) were dissolved in EtOH and stirred under H₂ atmosphere for 12 h. This was then filtered through diatomaceous earth and washed with EtOH and concentrated to afford **97** as solid crystals (1.61 g, 99%). ¹H NMR (300 MHz, CDCl₃): δ 8.57 (br. s., 1H), 7.11–7.24 (m, 1H), 6.98–7.11 (m, 2H), 6.82–6.98 (m, 1H), 3.95 (t, *J* = 7.0 Hz, 2H), 2.61–2.73 (m, 2H), 2.27 (quin, *J* = 7.5 Hz, 2H). LCMS, *m/z* 178.2 (100) [M + H]⁺.

***tert*-Butyl 2-[2-(2-oxopyrrolidin-1-yl)phenoxy]acetate (98).** **97** (0.25 g, 1.4 mmol), *tert*-butyl bromoacetate (0.31 mL, 2.1 mmol), and K₂CO₃ (573 mg, 4.15 mmol) in acetone (20 mL) was stirred at reflux for 4 h. The reaction was then filtered through diatomaceous earth and concentrated. The crude material was then purified by column chromatography eluting with a gradient of 100% heptane to 20% EtOAc to afford **98** as a solid (400 mg, 99% yield). ¹H NMR (300 MHz, CDCl₃): δ 7.31 (dd, *J* = 7.8, 1.7 Hz, 1H), 7.20–7.25 (m, 1H) 7.03 (td, *J* = 7.6, 1.0 Hz, 1H), 6.84 (d, *J* = 8.3 Hz, 1H), 4.53 (s, 2H), 3.88 (t, *J* = 7.0 Hz, 2H), 2.57 (t, *J* = 8.0 Hz, 2H), 2.20 (quin, *J* = 7.5 Hz, 2H), 1.49 (s, 9H). LCMS, *m/z* 292.2 (100) [M + H]⁺.

2-[2-(2-Oxopyrrolidin-1-yl)phenoxy]acetic acid (117). **116** (399 mg, 1.37 mmol) was dissolved in 4 M HCl in 1,2-dioxane (3 mL) and stirred for 5 h. The reaction was then concentrated to afford **117** as a solid (320 mg, 100%). ¹H NMR (300 MHz, CDCl₃): δ 7.19–7.36 (m, 2H), 6.96–7.13 (m, 2H), 4.70 (s, 2H), 3.87 (t, *J* = 7.1 Hz, 2H), 2.54 (t, *J* = 8.0 Hz, 2H), 2.14–2.31 (m, 2H). LCMS, *m/z* 236.2 (100) [M + H]⁺.

2-Bromo-N-[4-(4-methylphenoxy)phenyl]propanamide (100). 2-Bromopropanoyl bromide (0.16 mL, 1.5 mmol) was added dropwise to a stirred solution of 4-(4-methylphenoxy)aniline (200 mg, 1.0 mmol) and triethylamine (0.42 mL, 3.0 mmol) in DCM (10 mL) and stirred for 30 min. The reaction mixture was then washed with 1 M HCl (10 mL), saturated NaHCO₃ (10 mL), brine (10 mL), dried with anhydrous MgSO₄, filtered, and concentrated to afford **100** as a solid (330 mg, 98%). ¹H NMR (300 MHz, CDCl₃): δ 8.03 (br. s., 1H), 7.41–7.54 (m, 2H), 7.09–7.19 (m, *J* = 8.2 Hz, 2H), 6.94–7.05 (m, 2H), 6.86–6.94 (m, 2H), 4.56 (q, *J* = 7.0 Hz, 1H), 2.34 (s, 3H), 1.98 (d, *J* = 7.0 Hz, 3H). LCMS, *m/z* 334.2 (100) [M + H]⁺, 336.2.

2-Bromo-2-methyl-N-[4-(4-methylphenoxy)phenyl]propanamide (101). The procedure used for **100** was followed using 2-bromo-2-methyl-propanoyl bromide (0.11 mL, 0.90 mmol) and 4-(4-methylphenoxy)aniline (150 mg, 0.75 mmol) to afford **101** as a solid (258 mg, 98%). ¹H NMR (300 MHz, CDCl₃): δ 8.43 (br. s., 1H), 7.43–7.53 (m, 2H), 7.09–7.19 (m, *J* = 8.5 Hz, 2H), 6.95–7.06 (m, 2H), 6.90 (d, *J* = 8.4 Hz, 2H), 2.34 (s, 3H), 2.06 (s, 6H).

N,4-Dimethyl-N-(4-nitrophenyl)aniline (102). General Method G: Sodium hydride (150 mg, 3.7 mmol) was added to a stirred solution of N,4-dimethylaniline (0.31 mL, 2.5 mmol) in DMF (3 mL) and stirred for 10 min. 1-Fluoro-4-nitrobenzene (0.26 mL, 2.5 mmol) was then added and the reaction stirred for 18 h at 90 °C. The reaction was then quenched with 10% citric acid (1 mL) and concentrated. The residue was dissolved in EtOAc (10 mL) and washed successively with saturated NaHCO₃ (10 mL), brine (10 mL), dried with anhydrous MgSO₄ and concentrated. The crude material was then purified by column chromatography eluting with a gradient of 100% heptane to 30% DCM/heptane to afford **102** as a solid (172 mg, 17%). ¹H NMR (300 MHz, CDCl₃): δ 7.97–8.13 (m, 2H), 7.25–7.33 (m, 2H), 7.11 (d, *J* = 8.3 Hz, 2H), 6.55–6.71 (m, 2H), 3.39 (s, 3H), 2.41 (s, 3H). LCMS, *m/z* 243.2 (100) [M + H]⁺.

N,4-Methyl-N,4-(*p*-tolyl)benzene-1,4-diamine (103). General Method C was followed using **102** (172 mg, 0.71 mmol) to afford **103** as an oil (148 mg, 98%). ¹H NMR (300 MHz, CDCl₃): δ 6.88–7.23 (m,

4H), 6.48–6.87 (m, 4H), 3.14 (br. s., 3H), 2.16–2.37 (m, 3H). LCMS, m/z 213.2 (100) $[M + H]^+$.

N-[4-(4-Methylbenzoyl)phenyl]-2-[*N*-methyl-2-(2-oxopyrrolidin-1-yl)-anilino]acetamide (**104**). General Method A was followed using **68** (65 mg, 0.228 mmol) and (4-aminophenyl)-(p-tolyl)methanone (63 mg, 0.297 mmol) to afford **104** as a solid (45 mg, 45%). ^1H NMR (300 MHz, CDCl_3): δ 10.27 (s, 1H), 7.81–7.93 (m, 2H), 7.59–7.81 (m, 4H), 7.15–7.26 (m, 3H), 7.00–7.13 (m, 2H), 3.91 (br. s., 4H), 2.79 (s, 3H), 2.55–2.69 (m, 2H), 2.43 (s, 3H), 2.20–2.35 (m, 2H). LCMS, m/z 442.2 (100) $[M + H]^+$.

4-[1-(p-Tolyl)ethyl]aniline (**105**). 4'-Methylacetophenone (200 mg, 1.49 mmol) and p-Toluenesulfonyl hydrazide (416 mg, 2.24 mmol) were dissolved in 1,4-dioxane (3 mL) and stirred at 80 °C for 2 h in a reaction tube. K_2CO_3 (618 mg, 4.47 mmol) and (4-aminophenyl)-boronic acid hydrochloride (388 mg, 2.24 mmol) were added to the reaction mixture were then added and the reaction was refluxed at 110 °C for 5 h. The reaction was then cooled to 40 °C and concentrated. The residue was dissolved in DCM (20 mL) and washed successively with saturated NaHCO_3 (10 mL), brine (10 mL), dried with anhydrous MgSO_4 and concentrated. The crude material was then purified by column chromatography eluting with a gradient of 100% heptane to 50% EtOAc/heptane to afford **105** as an oil (79 mg, 25%). ^1H NMR (300 MHz, $\text{DMSO}-d_6$): δ 7.01–7.12 (m, 4H), 6.86 (m, J = 8.4 Hz, 2H), 6.46 (m, J = 8.4 Hz, 2H), 4.82 (s, 2H), 3.89 (q, J = 7.1 Hz, 1H), 2.23 (s, 3H), 1.46 (d, J = 7.18 Hz, 3H). LCMS, m/z 212.2 (100) $[M + H]^+$.

4-[1-Methyl-1-(p-tolyl)ethyl]aniline (**106**). Aniline (0.049 mL, 0.54 mmol), 1-isopropenyl-4-methyl-benzene (140 mg, 1.1 mmol), sodium acetate (110 mg, 1.3 mmol), and hexafluoroisopropanol (2.8 mL, 27 mmol) were added to a pressure tube and purged with N_2 . Following this, the vial was heated at 80 °C for 12 h. The mixture was cooled to 20 °C, and the solvent was evaporated under reduced pressure. The crude material was then purified by column chromatography eluting with a gradient of 100% DCM to 5% EtOAc/DCM to afford **106** as a solid (45 mg, 37%). ^1H NMR (300 MHz, CDCl_3): δ 7.11–7.17 (m, 2H), 7.00–7.11 (m, 4H), 6.56–6.66 (m, 2H), 3.57 (br. s., 2H), 2.32 (s, 3H), 1.64 (s, 6H). LCMS, m/z 226.4 (100) $[M + H]^+$.

4-Methyl-N-(4-nitrophenyl)aniline (**70**). 4-Methylaniline (0.95 mL, 9.3 mmol) and 1-fluoro-4-nitro-benzene (2.97 mL, 28.0 mmol) were dissolved in DMSO (10 mL) were stirred at 130 °C for 12 h. The reaction was then diluted in EtOAc (40 mL) and washed with cold 1 M HCl solution (20 mL), saturated NaHCO_3 (20 mL), brine (20 mL), dried with anhydrous MgSO_4 and concentrated. The crude material was then purified by column chromatography eluting with a gradient of 100% heptane to 100% DCM to afford **70** as a solid (1.68 g, 79%). ^1H NMR (300 MHz, CDCl_3): δ 8.06–8.16 (m, 2H), 7.21 (m, J = 8.2 Hz, 2H), 7.12 (m, J = 8.4 Hz, 2H), 6.79–6.90 (m, 2H), 2.37 (s, 3H). LCMS, m/z 229.2 (100) $[M + H]^+$.

N-Ethyl-4-methyl-N-(4-nitrophenyl)aniline (**107**). General Method H: Sodium hydride (35 mg, 0.88 mmol) was added to a stirred solution of **106** (100 mg, 0.44 mmol) in DMF (10 mL) and stirred for 10 min. Iodoethane (0.070 mL, 0.88 mmol) was then added and the reaction mixture heated at 40 °C for 24 h. 10% citric acid (5 mL) was added to the reaction mixture for quenching and then this was neutralized with saturated NaHCO_3 . The aqueous was extracted with EtOAc (2 \times 20 mL). The organic layers were combined and washed with H_2O (20 mL), dried over anhydrous MgSO_4 , filtered, and concentrated. The crude material was then purified by column chromatography eluting with a gradient of 100% heptane to 100% DCM to afford **107** as a solid (95 mg, 84%). ^1H NMR (300 MHz, CDCl_3): δ 8.00–8.09 (m, 2H), 7.29–7.27 (m, 2H), 7.09 (d, J = 8.3 Hz, 2H), 6.53–6.62 (m, J = 9.4 Hz, 2H), 3.80 (q, J = 7.2 Hz, 2H), 2.41 (s, 3H), 0.83–0.90 (m, 3H). LCMS, m/z 257.2 (100) $[M + H]^+$.

*N*4-Ethyl-N4-(p-tolyl)benzene-1,4-diamine (**108**). General Method F was followed using **107** (95 mg, 0.37 mmol) to afford **108** as an oil (75 mg, 89%). ^1H NMR (300 MHz, CDCl_3): δ 6.90–7.01 (m, 4H), 6.72–6.62 (m, 4H), 3.66–3.48 (m, 4H), 2.25 (s, 3H), 0.84–0.91 (m, 3H). LCMS, m/z 227.2 (100) $[M + H]^+$.

4-Methyl-N-(4-nitrophenyl)-*N*-propyl-aniline (**109**). General Method H was followed using **70** (95 mg, 0.37 mmol) and 1-iodopropane

(0.064 mL, 0.66 mmol) to afford **109** as an oil (48 mg, 81%). ^1H NMR (300 MHz, CDCl_3): δ 7.99–8.07 (m, 2H), 7.27 (d, J = 8.1 Hz, 2H), 7.09 (d, J = 8.3 Hz, 2H), 6.53–6.60 (m, 2H), 3.60–3.73 (m, 2H), 2.41 (s, 3H), 1.73 (d, J = 7.7 Hz, 2H), 0.96 (t, J = 7.4 Hz, 3H). LCMS, m/z 271.2 (100) $[M + H]^+$.

*N*4-Propyl-N4-(p-tolyl)benzene-1,4-diamine (**110**). General Method F was followed using **109** (48 mg, 0.18 mmol) to afford **110** as an oil (25.2 mg, 59%). ^1H NMR (300 MHz, CDCl_3): δ 7.02–7.21 (m, 3H), 6.88–7.02 (m, 2H), 6.71–6.88 (m, 3H), 3.50–3.63 (m, 2H), 2.3 (s, 3H), 1.65 (s, 2H) 0.92 (td, J = 7.3, 3.6 Hz, 3H). LCMS, m/z 241.4 (100) $[M + H]^+$.

N-Isopropyl-4-methyl-N-(4-nitrophenyl)aniline (**111**). General Method H was followed using **70** (95 mg, 0.37 mmol) and 2-iodopropane (111 mg, 0.66 mmol) to afford **111** as an oil (41 mg, 69%). ^1H NMR (300 MHz, CDCl_3): δ 7.97–8.06 (m, 2H), 7.29 (d, J = 8.2 Hz, 2H), 6.99 (d, J = 8.3 Hz, 2H), 6.43–6.50 (m, 2H), 4.39 (td, J = 6.6, 13.2 Hz, 1H), 2.43 (s, 3H), 1.19 (d, J = 6.6 Hz, 6H). LCMS, m/z 271.2 (100) $[M + H]^+$.

*N*4-Isopropyl-N4-(p-tolyl)benzene-1,4-diamine (**112**). General Method F was followed using **111** (41 mg, 0.15 mmol) to afford **112** as an oil (35 mg, 96%). ^1H NMR (300 MHz, CDCl_3): δ 6.96 (d, J = 8.4 Hz, 2H), 6.81–6.92 (m, J = 8.5 Hz, 2H), 6.65–6.75 (m, 2H), 6.53 (d, J = 8.6 Hz, 2H), 4.23 (td, J = 6.6, 13.1 Hz, 1H), 3.65 (br. s., 2H), 2.23 (s, 3H), 1.12 (d, J = 6.6 Hz, 6H). LCMS, m/z 241.2 (100) $[M + H]^+$.

N-Cyclopentyl-4-methyl-N-(4-nitrophenyl)aniline (**113**). General Method H was followed using **70** (95 mg, 0.37 mmol) and bromocyclopentane (0.13 mL, 1.3 mmol) to afford **113** as an oil (63 mg, 49%). ^1H NMR (300 MHz, CDCl_3): δ 7.95–8.06 (m, 2H), 7.30 (s, 3H), 7.00 (d, J = 8.2 Hz, 2H), 6.45–6.51 (m, 2H), 4.20–4.43 (m, 1H), 2.43 (s, 3H), 1.98–2.12 (m, 2H), 1.57–1.66 (m, 4H), 1.32–1.50 (m, 2H). LCMS, m/z 297.2 (100) $[M + H]^+$.

*N*1-Cyclopentyl-N1-(p-tolyl)benzene-1,4-diamine (**114**). General Method C was followed using **113** (63 mg, 0.21 mmol) to afford **114** as an oil (57 mg, 97%). ^1H NMR (300 MHz, CDCl_3): δ 6.96 (d, J = 8.4 Hz, 2H), 6.80–6.92 (m, 2H), 6.69 (d, J = 8.5 Hz, 2H), 6.51–6.63 (m, 2H), 4.17 (t, J = 7.6 Hz, 1H), 2.24 (s, 3H), 1.87–1.99 (m, 2H), 1.39–1.57 (m, 6H). LCMS, m/z 267.4 (100) $[M + H]^+$.

N-Isobutyl-4-methyl-N-(4-nitrophenyl)aniline (**115**). General Method H was followed using **70** (100 mg, 0.44 mmol) and 1-bromo-2-methylpropane (0.14 mL, 1.3 mmol) to afford **115** as an oil (110 mg, 88%). ^1H NMR (300 MHz, CDCl_3): δ 7.98–8.09 (m, 2H), 7.29 (d, J = 3.6 Hz, 2H), 7.08–7.17 (m, 2H), 6.54–6.68 (m, 2H), 3.58 (d, J = 7.5 Hz, 2H), 2.42 (s, 3H), 2.08 (td, J = 6.9, 13.7 Hz, 1H), 0.99 (d, J = 6.64 Hz, 6H). LCMS, m/z 285.2 (100) $[M + H]^+$.

*N*1-Isobutyl-N1-(p-tolyl)benzene-1,4-diamine (**116**). General Method C was followed using **115** (110 mg, 0.39 mmol) to afford **116** as an oil (97 mg, 98%). ^1H NMR (300 MHz, CDCl_3): δ 7.06–7.27 (m, 4H), 6.87–7.06 (m, 2H), 6.77 (d, J = 9.1 Hz, 2H), 3.45 (d, J = 7.2 Hz, 2H), 2.33 (br. s. 3H), 1.92–2.09 (m, 1H), 0.88–1.00 (m, 6H). LCMS, m/z 255.4 (100) $[M + H]^+$.

N-Butyl-4-methyl-N-(4-nitrophenyl)aniline (**117**). General Method H was followed using **70** (50 mg, 0.22 mmol) and 1-bromobutane (0.071 mL, 0.66 mmol) to afford **117** as an oil (50.1 mg, 80%). ^1H NMR (300 MHz, CDCl_3): δ 7.99–8.10 (m, 2H), 7.26–7.33 (m, 2H), 7.09 (d, J = 8.3 Hz, 2H), 6.51–6.61 (m, 2H), 3.64–3.78 (m, 2H), 2.41 (s, 3H), 1.59–1.80 (m, 2H), 1.31–1.45 (m, 2H), 0.95 (t, J = 7.3 Hz, 3H). LCMS, m/z 285.2 (100) $[M + H]^+$.

*N*1-Butyl-N1-(p-tolyl)benzene-1,4-diamine (**118**). General Method C was followed using **117** (50.1 mg, 0.18 mmol) to afford **118** as an oil (44 mg, 99%). ^1H NMR (300 MHz, CDCl_3): δ 6.94 (d, J = 8.6 Hz, 2H), 6.98 (d, J = 8.5 Hz, 2H), 6.65 (d, J = 8.6 Hz, 2H), 6.69 (d, J = 8.6 Hz, 2H), 3.52–3.60 (m, 2H), 2.25 (s, 3H), 1.55–1.67 (m, 2H), 1.35 (dd, J = 7.4, 15.0 Hz, 2H), 0.92 (t, J = 7.4 Hz, 3H). LCMS, m/z 255.2 (100) $[M + H]^+$.

4-Methyl-N-(4-nitrophenyl)-*N*-sec-butyl-aniline (**119**). General Method H was followed using **70** (48 mg, 0.21 mmol) and 2-bromobutane (0.069 mL, 0.66 mmol) to afford **119** as an oil (19.3 mg, 32%). ^1H NMR (300 MHz, CDCl_3): δ 8.01 (m, J = 9.5 Hz, 2H), 7.30 (s, 2H), 7.01 (d, J = 8.3 Hz, 2H), 6.46 (m, J = 9.51 Hz, 2H), 3.98–4.18 (m, 1H), 2.43 (s, 3H), 1.71 (dt, J = 13.7, 6.6 Hz, 1H),

1.28–1.46 (m, 1H), 1.17 (d, $J = 6.6$ Hz, 3H), 1.00 (t, $J = 7.4$ Hz, 3H). LCMS, m/z 285.2 (100) $[M + H]^+$.

N1-Butyl-N1-(*p*-tolyl)benzene-1,4-diamine (120). General Method C was followed using **119** (19.3 mg, 0.18 mmol) to afford **120** as an oil (16 mg, 93%). ^1H NMR (300 MHz, CDCl_3): δ 6.95 (d, $J = 8.5$ Hz, 2H), 6.84–6.91 (m, 2H), 6.65–6.75 (m, 2H), 6.48–6.58 (m, 2H), 3.86–3.97 (m, 1H), 2.23 (s, 3H), 1.56–1.80 (m, 2H), 1.12 (d, $J = 6.6$ Hz, 2H), 0.96 (t, $J = 7.4$ Hz, 3H).

N4-(4-Chlorophenyl)-N4-methyl-benzene-1,4-diamine (121). General Method G was followed using 4-chloro-*N*-methyl-aniline (200 mg, 1.4 mmol) and 1-fluoro-4-nitrobenzene (200 mg, 1.4 mmol) to afford *N*-(4-chlorophenyl)-*N*-methyl-4-nitroaniline as a crude oil (83.6 mg, 22%). LCMS, m/z 263.2 (100) $[M + H]^+$. General Method F was then followed using this intermediate to afford **121** as an oil (69 mg, 20% overall). ^1H NMR (300 MHz, CDCl_3): δ 7.12 (d, $J = 8.9$ Hz, 2H), 6.94–7.01 (m, 2H), 6.66 (d, $J = 8.9$ Hz, 3H), 6.72 (d, $J = 8.5$ Hz, 2H), 3.65 (br. s., 2H), 3.22 (s, 3H). LCMS, m/z 233.2 (100) $[M + H]^+$.

2-Fluoro-4-methyl-N-(4-nitrophenyl)aniline (122). The procedure used for **70** was followed using 2-fluoro-4-methyl-aniline (0.40 g, 3.2 mmol) and 1-fluoro-4-nitrobenzene (0.339 mL, 3.20 mmol) to afford **122** as a solid (16.2 mg, 2%). ^1H NMR (300 MHz, CDCl_3): δ 8.09–8.21 (m, 2H), 6.95–7.07 (m, 2H), 6.84–6.95 (m, 2H), 2.39 (s, 3H).

2-Fluoro-N,4-dimethyl-N-(4-nitrophenyl)aniline (123). General Method H was followed using **122** (16 mg, 0.065 mmol) and iodomethane (0.0162 mL, 0.26 mmol) to afford **123** as an oil (9.1 mg, 53%). ^1H NMR (300 MHz, CDCl_3): δ 8.05–8.14 (m, 2H) 7.16 (t, $J = 8.0$ Hz, 1H) 7.05 (m, $J = 9.5$ Hz, 2H) 6.60 (m, $J = 9.2$ Hz, 2H) 3.36 (s, 3H) 2.41 (s, 3H). LCMS, m/z 261.2 (100) $[M + H]^+$.

N1-(2-Fluoro-4-methyl-phenyl)-N1-methyl-benzene-1,4-diamine (124). General Method F was followed using **123** (9.1 mg, 0.035 mmol) to afford **124** as an oil (8.0 mg, 99%). ^1H NMR (300 MHz, CDCl_3): δ 7.04 (t, $J = 8.48$ Hz, 1H) 6.84–6.96 (m, 2H) 6.68 (s, 4H) 3.14–3.25 (m, 3H) 2.33 (s, 3H). LCMS, m/z 231.2 (100) $[M + H]^+$.

3-Fluoro-4-methyl-N-(4-nitrophenyl)aniline (143). The procedure used for **10** was followed using 3-fluoro-4-methyl-aniline (0.40 g, 3.2 mmol) and 1-fluoro-4-nitrobenzene (0.339 mL, 3.20 mmol) to afford **143** as a solid (162 mg, 21%). 8.06–8.20 (m, 2H), 7.19 (t, $J = 8.21$ Hz, 1H), 6.84–6.99 (m, 4H), 6.27 (br. s., 1H), 2.28 (s, 3H).

3-Fluoro-N,4-dimethyl-N-(4-nitrophenyl)aniline (126). General Method H was followed using **125** (40 mg, 0.065 mmol) and iodomethane (0.041 mL, 0.65 mmol) to afford **126** as an oil (33.9 mg, 80%). ^1H NMR (300 MHz, CDCl_3): δ 8.03–8.13 (m, 2H), 7.26 (t, $J = 8.4$ Hz, 1H), 6.87–6.95 (m, 2H), 6.66–6.74 (m, 2H). LCMS, m/z 261.2 (100) $[M + H]^+$.

N4-(3-Fluoro-4-methyl-phenyl)-N4-methyl-benzene-1,4-diamine (127). General Method F was followed using **126** (33.9 mg, 0.13 mmol) to afford **127** as an oil (29 mg, 97%). ^1H NMR (300 MHz, CDCl_3): δ 6.96 (d, $J = 8.4$ Hz, 4H) 6.72 (d, $J = 7.6$ Hz, 2H) 6.39 (s, 1H) 6.43 (s, 1H) 3.20 (br. s., 4H) 2.16 (s, 3H). LCMS, m/z 231.2 (100) $[M + H]^+$.

3-Chloro-N,4-dimethyl-N-(4-nitrophenyl)aniline (128). General Method G was followed using 3-chloro-*N*,4-dimethyl-aniline hydrochloride (330 mg, 1.7 mmol) and 1-fluoro-4-nitrobenzene (0.18 mL, 1.7 mmol) to afford **128** as a solid (200 mg, 42%). ^1H NMR (300 MHz, CDCl_3): δ 8.03–8.18 (m, 2H), 7.29–7.35 (m, 1H), 7.24 (d, $J = 2.2$ Hz, 1H), 7.04 (dd, $J = 2.2, 8.1$ Hz, 1H), 6.69 (d, $J = 9.3$ Hz, 2H), 3.38 (s, 3H), 2.42 (s, 3H). LCMS, m/z 277.2 (100) $[M + H]^+$.

N4-(3-Chloro-4-methyl-phenyl)-N4-methyl-benzene-1,4-diamine (129). General Method F was followed using **128** (199 mg, 0.719 mmol) to afford **129** as an oil (162 mg, 91%). ^1H NMR (300 MHz, CDCl_3): δ 6.90–7.05 (m, 3H), 6.73–6.89 (m, 3H), 6.50–6.66 (m, 1H), 3.21 (s, 3H), 2.28 (s, 3H). LCMS, m/z 247.2 (100) $[M + H]^+$.

N4-(3,4-Dichlorophenyl)-N4-methyl-benzene-1,4-diamine (130). General Method G was followed using 3,4-dichloro-*N*-methyl-aniline (330 mg, 1.9 mmol) and 1-fluoro-4-nitrobenzene (0.20 mL, 1.9 mmol) to afford 3,4-dichloro-*N*-methyl-*N*-(4-nitrophenyl)aniline as a solid (423.2 mg, 76%). LCMS, m/z 297.0 (100) $[M + H]^+$. General Method F was followed using this intermediate to afford **130** as an oil

(371 mg, 74% overall). ^1H NMR (300 MHz, CDCl_3): δ 7.17 (d, $J = 8.9$ Hz, 1H), 6.97 (d, $J = 8.6$ Hz, 2H), 6.74–6.84 (m, 3H), 6.53 (dd, $J = 2.3, 8.9$ Hz, 1H), 3.21 (s, 3H). LCMS, m/z 267.2 (100) $[M + H]^+$.

4-Chloro-3-fluoro-N-(4-nitrophenyl)aniline (131). General Method G was followed using 4-chloro-3-fluoro-aniline (1.2 g, 8.5 mmol) and 1-fluoro-4-nitrobenzene (0.451 mL, 4.25 mmol) (with heating increased to 100 °C for 48 h) to afford **131** as a solid (605 mg, 53%). ^1H NMR (300 MHz, $\text{DMSO}-d_6$): δ 9.52 (s, 1H), 8.14 (d, $J = 9.1$ Hz, 2H), 7.48–7.60 (m, 1H), 7.27 (dd, $J = 11.1, 2.5$ Hz, 1H), 7.04–7.21 (m, 4H).

4-Chloro-3-fluoro-N-methyl-N-(4-nitrophenyl)aniline (132). General Method H was followed using **131** (55 mg, 0.21 mmol) and iodomethane (0.064 mL, 1.03 mmol) to afford **132** as an oil (41 mg, 71%). ^1H NMR (300 MHz, CDCl_3): δ 8.05–8.16 (m, 2H), 7.45 (t, $J = 8.4$ Hz, 1H), 6.88–7.14 (m, 2H), 6.72–6.85 (m, 2H), 3.41 (s, 3H). LCMS, m/z 281.2 (100) $[M + H]^+$.

N1-(4-Chloro-3-fluoro-phenyl)-N1-methyl-benzene-1,4-diamine (133). General Method F was followed using **132** (41 mg, 0.15 mmol) to afford **133** as an oil (36 mg, 98%). ^1H NMR (300 MHz, CDCl_3): δ 7.15 (t, $J = 8.6$ Hz, 1H), 6.96–7.08 (m, 4H), 6.44–6.63 (m, 2H), 3.17–3.27 (m, 3H). LCMS, m/z 250.2 (100) $[M + H]^+$.

3,4-Difluoro-N-methyl-N-(4-nitrophenyl)aniline (134). General Method G was followed using 3,4-difluoro-*N*-methyl-aniline (100 mg, 0.71 mmol) and 1-fluoro-4-nitrobenzene (0.075 mL, 0.71 mmol) to afford **134** as a solid (99.7 mg, 53%). ^1H NMR (300 MHz, CDCl_3): δ 8.05–8.15 (m, $J = 9.3$ Hz, 2H), 7.19–7.25 (m, 1H), 7.04–7.13 (m, 1H), 6.96–7.04 (m, 1H), 6.66–6.74 (m, $J = 9.3$ Hz, 2H), 3.39 (s, 3H). LCMS, m/z 265.2 (100) $[M + H]^+$.

N4-(3,4-Difluorophenyl)-N4-methyl-benzene-1,4-diamine (135). General Method F was followed using **134** (99.7 mg, 0.38 mmol) to afford **135** as an oil (85.4 mg, 97%). ^1H NMR (300 MHz, CDCl_3): δ 6.85–7.04 (m, 3H), 6.72 (d, $J = 8.6$ Hz, 2H), 6.49 (ddd, $J = 2.9, 6.8, 13.6$ Hz, 1H), 6.28–6.40 (m, 1H), 3.18 (s, 3H). LCMS, m/z 235.2 (100) $[M + H]^+$.

5-Methyl-N-(4-nitrophenyl)pyridin-2-amine (136). General Method G was followed using 6-amino-3-picoline (200 mg, 1.9 mmol) and 1-fluoro-4-nitrobenzene (0.20 mL, 1.9 mmol) to afford **136** as a solid (156 mg, 36%). ^1H NMR (300 MHz, CDCl_3): δ 8.11–8.24 (m, 3H), 7.46–7.56 (m, 3H), 6.86–6.96 (m, 1H), 2.31 (s, 3H). LCMS, m/z 230.2 (100) $[M + H]^+$.

N,5-Dimethyl-N-(4-nitrophenyl)pyridin-2-amine (137). General Method H was followed using **136** (155 mg, 0.676 mmol) and iodomethane (0.211 mL, 3.38 mmol) to afford **137** as an oil (22.7 mg, 13%). ^1H NMR (300 MHz, CDCl_3): δ 8.26 (s, 1H), 8.12–8.21 (m, $J = 9.3$ Hz, 2H), 7.49 (dd, $J = 2.4, 8.5$ Hz, 1H), 7.08–7.16 (m, $J = 9.2$ Hz, 2H), 7.03 (d, $J = 8.5$ Hz, 1H), 3.58 (s, 3H), 2.34 (s, 3H). LCMS, m/z 244.2 (100) $[M + H]^+$.

N4-Methyl-N4-(5-methyl-2-pyridyl)benzene-1,4-diamine (138). General Method F was followed using **137** (22.7 mg, 0.093 mmol) to afford **138** as an oil (19.5 mg, 98%). ^1H NMR (300 MHz, CDCl_3): δ 8.02 (s, 1H), 7.13 (dd, $J = 2.2, 8.7$ Hz, 1H), 6.99–7.06 (m, 2H), 6.68–6.77 (m, 2H), 6.34 (d, $J = 8.7$ Hz, 1H), 3.72 (br. s., 2H), 3.40 (s, 3H), 2.18 (s, 3H). LCMS, m/z 214.2 (100) $[M + H]^+$.

6-Methyl-N-(4-nitrophenyl)pyridin-3-amine (139). 5-Amino-2-methylpyridine (260 mg, 2.4 mmol), 1-bromo-4-nitrobenzene (400 mg, 2.00 mmol), cesium carbonate (1.61 g, 4.95 mmol), $\text{Pd}(\text{OAc})_2$ (22.2 mg, 0.100 mmol) *rac*-BINAP (123 mg, 0.199 mmol) were dissolved in DMF (7 mL) and purged with N_2 for 10 min. The reaction was then stirred at 100 °C for 16 h. The reaction was then concentrated and dissolved in EtOAc (10 mL) and filtered through diatomaceous earth that was washed with more EtOAc (10 mL). The organic layers were washed with saturated NaHCO_3 (10 mL), brine (10 mL), dried with anhydrous MgSO_4 , filtered, and concentrated. The crude material was then purified by column chromatography eluting with a gradient of 100% heptane to 100% EtOAc/heptane to afford **139** as a solid (389 mg, 86%). ^1H NMR (300 MHz, CDCl_3): δ 8.53 (s, 1H), 8.09–8.21 (m, 2H), 7.62 (d, $J = 8.3$ Hz, 1H), 7.24 (s, 1H), 6.97 (m, $J = 8.9$ Hz, 2H), 2.57–2.67 (m, 3H). LCMS, m/z 230.2 (100) $[M + H]^+$.

N,6-Dimethyl-N-(4-nitrophenyl)pyridin-3-amine (140). General Method H was followed using **139** (101 mg, 0.436 mmol) and

iodomethane (0.086 mL, 1.37 mmol) to afford **140** as an oil (29.0 mg, 27%). ¹H NMR (300 MHz, CDCl₃): δ 8.42 (d, *J* = 2.6 Hz, 1H), 8.08–8.14 (m, 2H), 7.51 (dd, *J* = 2.7, 8.3 Hz, 1H), 7.27–7.30 (s, 1H), 6.70–6.80 (m, *J* = 9.33 Hz, 2H), 3.43 (s, 3H), 2.65 (s, 3H). LCMS, *m/z* 244.2 (100) [M + H]⁺.

N1-Methyl-N1-(6-methyl-3-pyridyl)benzene-1,4-diamine (141). General Method C was followed using **140** (29 mg, 0.119 mmol) to afford **141** as an oil (25.0 mg, 98%). ¹H NMR (300 MHz, CDCl₃): δ 8.05 (d, *J* = 2.2 Hz, 1H), 6.88–7.01 (m, 4H), 6.69 (d, *J* = 8.6 Hz, 2H), 3.22 (s, 3H), 2.45 (s, 3H). LCMS, *m/z* 214.2 (100) [M + H]⁺.

3-Fluoro-4-nitro-N-(p-tolyl)aniline (142). 2,6-Dimethylpyridine (0.126 mL, 1.09 mmol), 3-fluoro-4-nitroaniline (170 mg, 1.09 mmol), copper(II) acetate (19.8 mg, 0.109 mmol) and myristic acid (0.050 mL, 0.22 mmol) were suspended in toluene (2 mL) and stirred at ambient temperature (22 °C) for 24 h. The mixture was then filtered through diatomaceous earth, washed with EtOAc (10 mL) and concentrated. The crude material was then purified by column chromatography eluting with a gradient of 100% heptane to 20% EtOAc/heptane to afford **142** as a solid (29.9 mg, 11%). ¹H NMR (300 MHz, CDCl₃): δ 7.96–8.06 (m, 1H), 7.23 (m, *J* = 8.2 Hz, 2H), 7.11 (m, *J* = 8.3 Hz, 2H), 6.61–6.66 (m, 1H), 6.60 (s, 1H), 2.38 (s, 3H). LCMS, *m/z* 247.2 (100) [M + H]⁺.

3-Fluoro-N-methyl-4-nitro-N-(p-tolyl)aniline (143). General Method H was followed using **160** (29.9 mg, 0.12 mmol) and iodomethane (0.030 mL, 0.49 mmol) to afford **143** as an oil (17.9 mg, 57%). ¹H NMR (300 MHz, CDCl₃): δ 7.90–8.01 (m, 1H), 7.30 (s, 2H), 7.10 (d, *J* = 8.3 Hz, 2H), 6.25–6.44 (m, 2H), 3.37 (s, 3H), 2.41 (s, 3H). LCMS, *m/z* 261.2 (100) [M + H]⁺.

2-Fluoro-N4-methyl-N4-(p-tolyl)benzene-1,4-diamine (144). General Method F was followed using **143** (17.9 mg, 0.69 mmol) to afford **144** as an oil (15.8 mg, 100%). ¹H NMR (300 MHz, CDCl₃): δ 7.03–7.13 (m, 2H), 6.83–6.95 (m, 3H), 6.57–6.74 (m, 2H), 3.22 (s, 3H), 2.31 (s, 3H). LCMS, *m/z* 231.2 (100) [M + H]⁺.

2-Chloro-N4-(4-chlorophenyl)-N4-methyl-benzene-1,4-diamine (145). General Method G was followed using 4-chloro-N-methyl-aniline hydrochloride (0.50 g, 2.8 mmol) and 2-chloro-4-fluoro-1-nitrobenzene (0.54 g, 3.1 mmol) to afford 3-chloro-N-(4-chlorophenyl)-N-methyl-4-nitro-aniline as an oil (219 mg, 26%). LCMS, *m/z* 297.0 (100) [M + H]⁺, 299.2. General Method F was followed using this intermediate to afford **145** as an oil (136 mg, 18% overall). ¹H NMR (300 MHz, CDCl₃): δ 7.11–7.16 (m, 3H), 6.85–6.93 (m, 1H), 6.76 (d, *J* = 9.0 Hz, 1H), 6.68 (d, *J* = 9.0 Hz, 2H), 6.51–6.57 (m, 1H), 3.20 (s, 3H). LCMS, *m/z* 267.2 (100) [M + H]⁺, 269.0.

2-Fluoro-4-nitro-N-(p-tolyl)aniline (146). 4-Methylaniline (0.38 mL, 3.8 mmol) and 1,2-difluoro-4-nitrobenzene (0.226 mL, 1.89 mmol) in DMSO (2 mL) were stirred in a microwave reactor for 15 min at 130 °C (90W power). The reaction was then diluted in EtOAc (20 mL) and washed with 1 M HCl (10 mL), saturated NaHCO₃ (10 mL), brine (10 mL), dried with anhydrous MgSO₄ and concentrated. The crude material was then purified by column chromatography eluting with a gradient of 100% heptane to 100% DCM to afford **146** as an oil (373 mg, 80%). ¹H NMR (300 MHz, CDCl₃): δ 7.90–8.04 (m, 2H), 7.20–7.26 (m, 2H), 7.01–7.17 (m, 3H), 6.32 (br. s., 1H), 2.39 (s, 3H). LCMS, *m/z* 247.2 (100) [M + H]⁺.

2-Fluoro-N-methyl-4-nitro-N-(p-tolyl)aniline (147). General Method H was followed using **146** (100 mg, 0.44 mmol) and iodomethane (0.101 mL, 1.62 mmol) to afford **147** as an oil (59.7 mg, 56%). ¹H NMR (300 MHz, CDCl₃): δ 7.85–7.99 (m, 2H), 7.11–7.19 (m, 2H), 6.93–7.05 (m, 3H), 3.43 (d, *J* = 1.6 Hz, 3H), 2.35 (s, 3H). LCMS, *m/z* 261.2 (100) [M + H]⁺.

2-Fluoro-N1-methyl-N1-(p-tolyl)benzene-1,4-diamine (148). General Method F was followed using **147** (59.7 mg, 0.23 mmol) to afford **148** as an oil (52 mg, 98%). ¹H NMR (300 MHz, CDCl₃): δ 6.96–7.13 (m, 3 H) 6.53–6.73 (m, 4 H) 3.21 (s, 3 H) 2.26 (s, 3 H). LCMS, *m/z* 231.2 (100) [M + H]⁺.

2-Chloro-N-(4-chlorophenyl)-N-methyl-4-nitro-aniline (149). General Method G was followed using 4-chloro-N-methyl-aniline hydrochloride (0.33 g, 1.88 mmol) and 2-chloro-1-fluoro-4-nitrobenzene (0.33 g, 1.88 mmol) to afford **149** as an oil (18 mg, 3%). ¹H NMR (300 MHz, CDCl₃): δ 8.33 (d, *J* = 2.6 Hz, 1H), 8.15 (dd, *J* = 2.6, 8.9

Hz, 1H), 7.36 (d, *J* = 8.9 Hz, 1H), 7.19–7.26 (m, 2H), 6.70–6.77 (m, 2H), 3.35 (s, 3H). LCMS, *m/z* 297.2 (100) [M + H]⁺.

2-Chloro-N1-(4-chlorophenyl)-N1-methyl-benzene-1,4-diamine (150). General Method F was followed using **149** (16 mg, 0.061 mmol) to afford **150** as an oil (13.5 mg, 83%). ¹H NMR (300 MHz, CDCl₃): δ 7.08–7.17 (m, 3H), 7.02 (d, *J* = 2.3 Hz, 1H), 6.82 (dd, *J* = 2.4, 8.4 Hz, 1H), 6.48 (d, *J* = 9.0 Hz, 2H), 3.19 (s, 3H). LCMS, *m/z* 267.2 (100) [M + H]⁺, 269.2.

N-Methyl-6-nitro-N-(p-tolyl)pyridin-3-amine (151). The procedure used for **139** was followed using *N*,4-dimethylaniline (0.17 mL, 1.2 mmol) and 5-bromo-2-nitro-pyridine (80 mg, 0.39 mmol) to afford **151** as a solid (33.5 mg, 35%). ¹H NMR (300 MHz, CDCl₃): δ 8.09 (d, *J* = 9.2 Hz, 1H), 7.96 (d, *J* = 3.0 Hz, 1H), 7.30 (d, *J* = 9.1 Hz, 1H), 7.12 (d, *J* = 8.3 Hz, 2H), 7.02 (dd, *J* = 3.1, 9.16 Hz, 1H), 3.42 (s, 3H), 2.41 (s, 3H). LCMS, *m/z* 244.2 (100) [M + H]⁺.

NS-Methyl-NS-(p-tolyl)pyridine-2,5-diamine (152). General Method F was followed using **151** (33.5 mg, 0.14 mmol) to afford **152** as a semi solid (29 mg, 99%). ¹H NMR (300 MHz, CDCl₃): δ 7.94 (d, *J* = 2.5 Hz, 1H), 7.22–7.27 (m, 1H), 6.97–7.07 (m, *J* = 8.3 Hz, 2H), 6.65–6.76 (m, *J* = 8.6 Hz, 2H), 6.51 (d, *J* = 8.7 Hz, 1H), 4.36 (br. s., 2H), 3.22 (s, 3H), 2.27 (s, 3H). LCMS, *m/z* 214.2 (100) [M + H]⁺.

N-Methyl-5-nitro-N-(p-tolyl)pyridin-2-amine (153). A solution of the 2-chloro-5-nitro-pyridine (250 mg, 1.58 mmol), *N*,4-dimethylaniline hydrochloride (249 mg, 1.58 mmol) and triethylamine (0.659 mL, 4.73 mmol) in anhydrous DMF (20 mL) under argon was heated at 100 °C for 14 h. The DMF was removed in vacuo and the residue was then taken up in EtOAc (20 mL) and the organics washed with 1 N HCl (20 mL) and brine (20 mL) dried with anhydrous MgSO₄, filtered, and concentrated. The crude material was then purified by column chromatography eluting with a gradient of 100% heptane to 60% EtOAc/heptane to afford **153** as a solid (361 mg, 94%). ¹H NMR (300 MHz, CDCl₃): δ 9.13 (d, *J* = 2.8 Hz, 1H), 8.03 (dd, *J* = 2.8, 9.5 Hz, 1H), 7.3 (d, *J* = 8.1 Hz, 2H), 7.15 (d, *J* = 8.3 Hz, 2H), 6.34 (d, *J* = 9.5 Hz, 1H), 3.58 (s, 3H), 2.42 (s, 3H). LCMS, *m/z* 244.2 (100) [M + H]⁺.

N2-Methyl-N2-(p-tolyl)pyridine-2,5-diamine (154). General Method F was followed using **153** (361 mg, 1.48 mmol) to afford **154** as a solid (312 mg, 99%). ¹H NMR (300 MHz, CDCl₃): δ 7.82 (d, *J* = 29 Hz, 1H), 7.15–7.13 (m, 2H), 7.08–7.05 (m, 2H), 6.86 (dd, *J* = 2.96, 8.80 Hz, 1H), 6.50–6.58 (m, 1H), 3.39 (s, 3H), 2.34 (s, 3H). LCMS, *m/z* 214.2 (100) [M + H]⁺.

1-(5-Fluoro-2-nitro-phenyl)pyrrolidin-2-one (155). 2,4-Difluoro-1-nitrobenzene (0.690 mL, 6.29 mmol) was added to a stirred solution of K₂CO₃ (1.74 g, 12.6 mmol) and 2-pyrrolidinone (0.716 mL, 9.43 mmol) in DMF (10 mL) at 0 °C. The reaction was then stirred at 80 °C for 72 h. The reaction mixture was then concentrated and dissolved in EtOAc (20 mL), which was then washed with H₂O (2 × 10 mL), brine (20 mL), dried with anhydrous MgSO₄, filtered, and concentrated. The crude material was then purified by column chromatography eluting with a gradient of 100% DCM to 30% EtOAc/DCM to afford **155** as an oil (611 mg, 43%). ¹H NMR (300 MHz, CDCl₃): δ 8.03 (dd, *J* = 5.5, 9.0 Hz, 1H), 7.02–7.15 (m, 2H), 3.89 (t, *J* = 7.0 Hz, 2H), 2.57 (t, *J* = 7.9 Hz, 2H), 2.30 (quin, *J* = 7.5 Hz, 2H). LCMS, *m/z* 225.2 (100) [M + H]⁺. LCMS, *m/z* 225.2 (100) [M + H]⁺.

1-(2-Amino-5-fluoro-phenyl)pyrrolidin-2-one (156). General Method F was followed using **155** (611 mg, 2.73 mmol) to afford **156** as an oil (471 mg, 88%). ¹H NMR (300 MHz, CDCl₃): δ 6.80–6.93 (m, 2H), 6.74–6.80 (m, 1H), 3.79–3.90 (m, 2H), 2.54–2.71 (m, 2H), 2.27 (quin, *J* = 7.5 Hz, 2H). LCMS, *m/z* 195.2 (100) [M + H]⁺.

2-[4-Fluoro-N-methyl-2-(2-oxopyrrolidin-1-yl)anilino]acetic acid hydrochloride (157). 1-(2-Amino-5-fluoro-phenyl)pyrrolidin-2-one (250 mg, 1.3 mmol), *tert*-butyl bromoacetate (0.23 mL, 1.5 mmol) and K₂CO₃ (360 mg, 2.6 mmol) in MeCN (2 mL) were stirred at 80 °C for 90 h. The reaction was then concentrated and dissolved in EtOAc (10 mL), which was washed successively with H₂O (10 mL) and brine (10 mL). The organics were then dried with anhydrous MgSO₄, filtered, and concentrated. The crude material was then purified by column chromatography eluting with a gradient of 100% heptane to 50% EtOAc/heptane to afford *tert*-butyl 2-[4-fluoro-2-(2-oxopyrroli-

din-1-yl)anilino]acetate as an oil (87 mg, 22%). ¹H NMR (300 MHz, CDCl₃): δ 6.78–6.98 (m, 2H), 6.54 (dd, *J* = 5.1, 9.0 Hz, 1H), 4.53 (br. s., 1H), 3.69–3.88 (m, 4H), 2.52–2.75 (m, 2H), 2.27 (t, *J* = 7.5 Hz, 2H), 1.49 (s, 9H). LCMS, *m/z* 309.2 (100) [*M* + *H*]⁺. The intermediate was then dissolved in DMF (1 mL) and K₂CO₃ (71.2 mg, 0.51 mmol) added. Iodomethane (0.032 mL, 0.51 mmol) was then added and the reaction stirred at 35 °C for 72 h. The reaction was then concentrated and dissolved in EtOAc (10 mL), which was washed successively with H₂O (10 mL), brine (10 mL), dried with anhydrous MgSO₄, filtered, and concentrated. The crude material was then purified by column chromatography eluting with a gradient of 100% heptane to 45% EtOAc/heptane to afford *tert*-butyl 2-[4-fluoro-*N*-methyl-2-(2-oxopyrrolidin-1-yl)anilino]acetate as an oil (47 mg, 11%). ¹H NMR (300 MHz, CDCl₃): δ 6.86–7.13 (m, 3H), 3.89 (t, *J* = 7.1 Hz, 2H), 3.57 (s, 2H), 2.78 (s, 3H), 2.48–2.58 (m, 2H), 2.12–2.24 (m, 2H), 1.45 (s, 9H). LCMS, *m/z* 323.2 (100) [*M* + *H*]⁺. The aforementioned intermediate was then dissolved in 4 M HCl in dioxane (1 mL) and stirred at 40 °C for 3 h and then concentrated to afford **157** as a solid (36.4, 9.3% overall). ¹H NMR (300 MHz, MeOD): δ 7.67–7.80 (m, 1H), 7.19–7.38 (m, 2H), 4.36 (d, *J* = 4.4 Hz, 2H), 3.99 (t, *J* = 6.7 Hz, 2H), 3.26 (s, 3H), 2.52–2.66 (m, 2H), 2.18–2.37 (m, 2H). LCMS, *m/z* 267.2 (100) [*M* + *H*]⁺.

1-(4-Fluoro-2-nitro-phenyl)pyrrolidin-2-one (158). The procedure used for **155** was followed using 1,4-difluoro-2-nitro-benzene (561 mg, 3.52 mmol) and pyrrolidin-2-one (0.269 mL, 3.52 mmol) to afford **158** as a solid (55 mg, 7%). ¹H NMR (300 MHz, CDCl₃): δ 7.74 (dd, *J* = 1.8, 7.7 Hz, 1H), 7.31–7.41 (m, 2H), 3.87 (t, *J* = 6.9 Hz, 2H), 2.49–2.59 (m, 2H), 2.21–2.34 (m, 2H).

1-(2-Amino-4-fluoro-phenyl)pyrrolidin-2-one (159). General Method F was followed using **158** (55 mg, 0.245 mmol) to afford **159** as an oil (25 mg, 52%). ¹H NMR (300 MHz, CDCl₃): δ 7.01 (dd, *J* = 5.8, 9.1 Hz, 1H), 6.43–6.56 (m, 2H), 3.75–3.81 (m, 2H), 2.54–2.62 (m, 2H), 2.20–2.26 (m, 2H). LCMS, *m/z* 195.2 (100) [*M* + *H*]⁺.

2-[5-Fluoro-*N*-methyl-2-(2-oxopyrrolidin-1-yl)anilino]acetic acid hydrochloride (160). The procedure used for **157** was followed using *tert*-butyl bromoacetate (0.022 mL, 0.16 mmol) and iodomethane (0.024 mL, 0.386) to afford **160** as a solid (55 mg, 7%). ¹H NMR (300 MHz, MeOD): δ 7.20 (dd, *J* = 8.7, 6.2 Hz, 1H), 7.04 (dd, *J* = 10.8, 2.6 Hz, 1H), 6.84 (td, *J* = 8.2, 2.7 Hz, 1H), 3.87–3.95 (m, 2H), 3.81 (t, *J* = 7.0 Hz, 2H), 2.97 (s, 3H), 2.54 (t, *J* = 8.1 Hz, 2H), 2.20 (quin, *J* = 7.5 Hz, 2H). LCMS, *m/z* 267.2 (100) [*M* + *H*]⁺.

1-(5-Amino-2-pyridyl)pyrrolidin-2-one (161). The procedure used for **65** was followed using 2-bromopyridin-3-amine (0.50 g, 2.9 mmol) and 2-pyrrolidinone (0.33 mL, 4.3 mmol) to afford **161** as an oil (375 mg, 73%). ¹H NMR (300 MHz, CDCl₃): δ 7.94 (app s, 1H), 7.14–7.21 (m, 1H), 7.05–7.14 (m, 1H), 4.14 (t, *J* = 7.1 Hz, 2H), 2.67 (t, *J* = 8.0 Hz, 2H), 2.20–2.35 (m, 2H). LCMS, *m/z* 178.2 (100) [*M* + *H*]⁺.

***tert*-Butyl *N*-[2-(2-oxopyrrolidin-1-yl)-3-pyridyl]carbamate (162).** A solution of **161** (100 mg, 0.56 mmol), Boc anhydride (180 mg, 0.85 mmol), and triethylamine (110 mg, 1.1 mmol) in a 3:1 mixture of 1,4-dioxane/H₂O (8 mL) was stirred for 120 h at 20 °C. The solvent was then concentrated and 1 M HCl was added to reach pH 5. The precipitate was filtered and dried to afford **162** as a solid (107 mg, 69%). ¹H NMR (300 MHz, CDCl₃): δ 8.12–8.26 (m, 2H), 8.03 (br. s., 1H), 7.22 (dd, *J* = 8.2, 4.7 Hz, 1H), 4.11–4.17 (m, 2H), 2.64–2.76 (m, 2H), 2.26 (t, *J* = 7.5 Hz, 2H), 1.52 (s, 9H). LCMS, *m/z* 278.2 (100) [*M* + *H*]⁺.

1-[3-(Methylamino)-2-pyridyl]pyrrolidin-2-one bis trifluoroacetic acid (163). Sodium hydride (14 mg, 0.36 mmol) was added to a stirred solution of **162** (50 mg, 0.18 mmol) in dry THF (1 mL) and stirred for 10 min. Iodomethane (0.034 mL, 0.541 mmol) was then added and the reaction stirred at 20 °C for 2 h. The reaction was then quenched with 10% citric acid (1 mL) and concentrated. The reaction was then diluted in EtOAc (20 mL) and washed with 1 M HCl (10 mL), saturated NaHCO₃ (10 mL), brine (10 mL), dried with anhydrous MgSO₄ and concentrated. The crude material was then purified by column chromatography eluting with a gradient of 100% DCM to 100% EtOAc to afford *tert*-butyl *N*-methyl-*N*-[2-(2-oxopyrrolidin-1-yl)-3-pyridyl]carbamate as an oil (38 mg, 72%). ¹H

NMR (300 MHz, CDCl₃): δ 8.14 (dd, *J* = 1.5, 4.6 Hz, 1H), 7.43 (dd, *J* = 1.4, 8.2 Hz, 1H), 7.21 (dd, *J* = 4.7, 8.2 Hz, 1H), 4.17 (q, *J* = 7.1 Hz, 2H), 3.80–3.95 (m, 4H), 2.93 (s, 3H), 2.57 (t, *J* = 8.1 Hz, 2H), 2.21 (quin, *J* = 7.5 Hz, 2H), 1.26 (t, *J* = 7.1 Hz, 3H). LCMS, *m/z* 292.2 (100) [*M* + *H*]⁺. This was then stirred in 1:1 TFA/DCM (2 mL) for 3 h and then concentrated to afford **163** as an oil (56 mg, 72%). ¹H NMR (300 MHz, CDCl₃): δ 8.08 (t, *J* = 2.9 Hz, 1H), 7.56 (d, *J* = 3.4 Hz, 2H), 4.16 (d, *J* = 5.2 Hz, 2H), 2.98 (s, 3H), 2.74 (t, *J* = 7.9 Hz, 2H), 2.38 (t, *J* = 7.4 Hz, 2H). LCMS, *m/z* 192.2 (100) [*M* + *H*]⁺.

2-[Methyl-2-(2-oxopyrrolidin-1-yl)-3-pyridyl]amino]acetic acid (164). **163** (54 mg, 0.13 mmol), ethyl 2-bromoacetate (0.017 mL, 0.15 mmol), and K₂CO₃ (71 mg, 0.52 mmol) in MeCN (2 mL) was stirred at 50 °C for 72 h. The reaction was then filtered through diatomaceous earth, washed with EtOAc (20 mL) and concentrated. The crude material was then purified by column chromatography eluting with a gradient of 100% DCM to 20% MeOH/DCM to afford ethyl 2-[methyl-2-(2-oxopyrrolidin-1-yl)-3-pyridyl]amino]acetate as an oil (9.0 mg, 25%). ¹H NMR (300 MHz, CDCl₃): δ 8.14 (dd, *J* = 4.6, 1.5 Hz, 1H), 7.43 (dd, *J* = 8.2, 1.4 Hz, 1H), 7.21 (dd, *J* = 8.2, 4.7 Hz, 1H), 4.17 (q, *J* = 7.1 Hz, 2H), 3.82–3.92 (m, 4H), 2.90–2.98 (m, 3H), 2.57 (t, *J* = 8.1 Hz, 2H), 2.21 (quin, *J* = 7.5 Hz, 3H), 1.26 (t, *J* = 7.1 Hz, 3H). LCMS, *m/z* 278.2 (100) [*M* + *H*]⁺. This was then dissolved in a 1:1 mixture of EtOH/10% LiOH (2 mL) and stirred at 20 °C for 2 h. The reaction was concentrated and diluted with H₂O, made pH 6 with 10% citric acid and extracted with EtOAc (10 mL). This was dried with anhydrous MgSO₄, filtered, and concentrated to afford **164** (5.0 mg, 16%). ¹H NMR (300 MHz, MeOD): δ 8.04 (d, *J* = 3.8 Hz, 1H), 7.58 (dd, *J* = 1.3, 8.3 Hz, 1H), 7.33 (dd, *J* = 4.6, 8.2 Hz, 1H), 3.75–3.93 (m, 4H), 2.92 (s, 3H), 2.51–2.60 (m, 2H), 2.19–2.29 (m, 2H). LCMS, *m/z* 250.2 (100) [*M* + *H*]⁺.

4-Chloro-3-fluoro-*N*-isopropyl-*N*-(4-nitrophenyl)aniline (165). General Method H was followed using **131** (405 mg, 1.52 mmol) and 2-iodopropane (0.61 mL, 6.1 mmol) to afford **165** as an oil (53 mg, 11%). ¹H NMR (300 MHz, CDCl₃): δ 8.01–8.09 (m, 2H), 7.53 (t, *J* = 8.3 Hz, 1H), 6.97 (dd, *J* = 2.3, 9.5 Hz, 1H), 6.86–6.93 (m, 1H), 6.48–6.58 (m, 2H), 4.41 (td, *J* = 6.6, 13.2 Hz, 1H), 1.21 (d, *J* = 6.6 Hz, 6H).

***N*4-(4-Chloro-3-fluoro-phenyl)-*N*4-isopropyl-benzene-1,4-diamine (166).** General Method F was followed using **165** (52.0 mg, 0.168 mmol) to afford **166** as an oil (43.9 mg, 94%). ¹H NMR (300 MHz, CDCl₃): δ 7.04 (t, *J* = 8.8 Hz, 1H), 6.82–6.92 (m, 2H), 6.69–6.79 (m, 2H), 6.18–6.33 (m, 2H), 4.15 (td, *J* = 6.5, 13.1 Hz, 1H), 3.74 (br. s., 2H), 1.12 (d, *J* = 6.6 Hz, 6H). LCMS, *m/z* 279.2 (100) [*M* + *H*]⁺.

3-Fluoro-4-nitro-*N*-(*p*-tolyl)aniline (167). 3-Fluoro-4-nitro-aniline (300 mg, 1.92 mmol) and 1-bromo-4-methyl-benzene (362 mg, 2.11 mmol), Pd(OAc)₂ (22 mg, 0.096 mmol), Xantphos (111 mg, 0.19 mmol) and cesium carbonate (1.25 g, 3.84 mmol) were dissolved in dioxane (10 mL) in a pressure tube under N₂ atmosphere. The reaction was then heated at 100 °C for 16 h. The reaction was then filtered through diatomaceous earth and concentrated. The residue was dissolved in EtOAc (10 mL), washed with saturated NaHCO₃ (10 mL), brine (10 mL), dried with MgSO₄, filtered, and concentrated. The crude material was then purified by column chromatography eluting with a gradient of 100% heptane to 50% EtOAc/heptane to afford **167** as a solid (118.3 mg, 25%). ¹H NMR (300 MHz, CDCl₃): δ 8.03 (d, *J* = 8.9 Hz, 1H), 7.23 (d, *J* = 8.4 Hz, 2H), 7.11 (d, *J* = 8.3 Hz, 2H), 6.61–6.66 (m, 1H), 6.59 (s, 1H), 2.38 (s, 3H). LCMS, *m/z* 247.2 (100) [*M* + *H*]⁺.

3-Fluoro-*N*-isopropyl-4-nitro-*N*-(*p*-tolyl)aniline (168). General Method H was followed using **167** (118 mg, 0.479 mmol) and 2-iodopropane (0.144 mL, 1.44 mmol) to afford **168** as a solid (88 mg, 64%). ¹H NMR (300 MHz, CDCl₃): δ 7.81–8.02 (m, 1H), 7.30 (d, *J* = 8.2 Hz, 2H), 6.98 (d, *J* = 8.3 Hz, 2H), 6.16–6.31 (m, 2H), 4.32 (dt, *J* = 13.2, 6.7 Hz, 1H), 2.44 (s, 3H), 1.18 (d, *J* = 6.6 Hz, 6H). LCMS, *m/z* 289.2 (100) [*M* + *H*]⁺.

2-Fluoro-*N*4-isopropyl-*N*4-(*p*-tolyl)benzene-1,4-diamine (169). General Method F was followed using **168** (88 mg, 0.305 mmol) to afford **169** as an oil (78 mg, 99%). ¹H NMR (300 MHz, CDCl₃): δ 7.01 (d,

$J = 8.4$ Hz, 2H), 6.55–6.80 (m, 5H), 4.21 (dt, $J = 13.2$, 6.5 Hz, 1H), 2.27 (s, 3H), 1.13 (d, $J = 6.6$ Hz, 6H). LCMS, m/z 259.2 (100) $[M + H]^+$.

N-(4-Chloro-3-fluoro-phenyl)-3-fluoro-4-nitro-aniline (**170**). The procedure used for **167** was followed using 3-fluoro-4-nitro-aniline (500 mg, 3.20 mmol) and 4-bromo-1-chloro-2-fluoro-benzene (671 mg, 3.20 mmol) to afford **170** as a solid (650 mg, 71%). ^1H NMR (300 MHz, CDCl_3): δ 8.07 (t, $J = 8.9$ Hz, 1H), 7.42 (t, $J = 8.4$ Hz, 1H), 7.03 (dd, $J = 2.6$, 9.9 Hz, 1H), 6.96 (d, $J = 9.0$ Hz, 1H), 6.66–6.78 (m, 2H), 6.30 (br. s., 1H). LCMS, m/z 285.2 (100) $[M + H]^+$.

N-(4-Chloro-3-fluoro-phenyl)-3-fluoro-*N*-isopropyl-4-nitro-aniline (**171**). General Method H was followed using **170** (200 mg, 0.703 mmol) and 2-iodopropane (0.281 mL, 2.81 mmol) to afford **171** as a solid (106.7 mg, 46%). ^1H NMR (300 MHz, CDCl_3): δ 7.81–8.03 (m, 1H), 7.48–7.63 (m, 1H), 6.86–7.01 (m, 2H), 6.20–6.33 (m, 2H), 4.27–4.40 (m, 1H), 1.21 (d, $J = 6.6$ Hz, 6H). LCMS, m/z 327.2 (100) $[M + H]^+$.

N-(4-Chloro-3-fluoro-phenyl)-2-fluoro-*N*¹-isopropyl-benzene-1,4-diamine (**172**). General Method F was followed using **171** (106.7 mg, 0.327 mmol) to afford **172** as an oil (94 mg, 97%). ^1H NMR (300 MHz, CDCl_3): δ 7.81–8.03 (m, 1H), 7.48–7.63 (m, 1H), 6.86–7.01 (m, 2H), 6.20–6.33 (m, 2H), 4.27–4.40 (m, 1H), 1.21 (d, $J = 6.6$ Hz, 6H). LCMS, m/z 297.2 (100) $[M + H]^+$.

4-(3-Fluoro-4-nitro-anilino)benzonitrile (**173**). The procedure used for **167** was followed using 3-fluoro-4-nitro-aniline (300 mg, 1.92 mmol) and 4-bromobenzonitrile (385 mg, 2.11 mmol) to afford **173** as a solid (372.4 mg, 75%). ^1H NMR (300 MHz, CDCl_3): δ 8.03–8.15 (m, 1H), 7.63–7.71 (m, 2H), 7.24 (d, $J = 8.7$ Hz, 2H), 6.83–6.97 (m, 2H), 6.60 (s, 1H). LCMS, m/z 258.2 (100) $[M + H]^+$.

4-(3-Fluoro-*N*-isopropyl-4-nitro-anilino)benzonitrile (**174**). General Method H was followed using **173** (250 mg, 0.972 mmol) and 2-iodopropane (0.293 mL, 2.92 mmol) to afford **174** as a solid (42.9 mg, 15%). ^1H NMR (300 MHz, CDCl_3): δ 7.76–8.06 (m, 3H), 7.24–7.21 (s, 2H), 6.25–6.35 (m, 1H), 5.99–6.17 (m, 1H), 4.34–4.46 (m, 1H), 1.21 (dd, $J = 2.9$, 6.6 Hz, 6H). LCMS, m/z 300.2 (100) $[M + H]^+$.

4-(4-Amino-3-fluoro-*N*-isopropyl-anilino)benzonitrile (**175**). General Method F was followed using **174** (40 mg, 0.134 mmol) to afford **175** as an oil (29 mg, 81%). ^1H NMR (300 MHz, CDCl_3): δ 7.31–7.40 (m, 2H), 6.64–6.92 (m, 2H), 6.51 (d, $J = 9.1$ Hz, 3H), 4.27 (qd, $J = 6.4$, 12.9 Hz, 1H), 3.86 (br. s., 2H), 1.06–1.23 (m, 6H). LCMS, m/z 270.2 (100) $[M + H]^+$.

5-Nitro-*N*-(*p*-tolyl)pyridin-2-amine (**176**). The procedure used for **153** was followed using 2-chloro-5-nitro-pyridine (500 mg, 3.15 mmol) and 4-methylaniline (491 mg, 4.58 mmol) to afford **176** as a solid (675.3 mg, 93%). ^1H NMR (300 MHz, $\text{DMSO}-d_6$) δ 10.06 (s, 1H), 9.02 (d, $J = 2.8$ Hz, 1H), 8.27 (dd, $J = 2.87$, 9.3 Hz, 1H), 7.40–7.73 (m, $J = 8.4$ Hz, 2H), 7.08–7.25 (m, $J = 8.4$ Hz, 2H), 6.86 (d, $J = 9.3$ Hz, 1H), 2.29 (s, 3H). LCMS, m/z 230.2 (100) $[M + H]^+$.

N-Ethyl-5-nitro-*N*-(*p*-tolyl)pyridin-2-amine (**177**). General Method H was followed using **176** (179 mg, 0.781 mmol) and iodoethane (0.188 mL, 2.34 mmol) to afford **177** as an oil (175 mg, 87%). ^1H NMR (300 MHz, CDCl_3): δ 9.11 (d, $J = 2.7$ Hz, 1H), 7.99 (dd, $J = 9.5$, 2.7 Hz, 1H), 7.31 (m, $J = 8.1$ Hz, 2H), 7.11 (m, $J = 8.3$ Hz, 2H), 6.18 (d, $J = 9.5$ Hz, 1H), 4.08 (q, $J = 7.1$ Hz, 2H), 2.43 (s, 3H), 1.25 (t, $J = 7.1$ Hz, 3H). LCMS, m/z 258.2 (100) $[M + H]^+$.

*N*2-Ethyl-*N*2-(*p*-tolyl)pyridine-2,5-diamine (**178**). General Method C was followed using **177** (175 mg, 0.68 mmol) to afford **178** as an oil (153.1 mg, 98%). ^1H NMR (300 MHz, CDCl_3): δ 7.80 (d, $J = 2.87$ Hz, 1H), 7.12–7.20 (m, $J = 8.17$ Hz, 2H), 7.02–7.10 (m, $J = 8.35$ Hz, 2H), 6.84 (dd, $J = 2.92$, 8.84 Hz, 1H), 6.40 (d, $J = 8.80$ Hz, 1H), 3.93 (q, $J = 7.00$ Hz, 2H), 2.35 (s, 3H), 1.19 (t, $J = 7.00$ Hz, 3H). LCMS, m/z 228.2 (100) $[M + H]^+$.

N-Isopropyl-5-nitro-*N*-(*p*-tolyl)pyridin-2-amine (**179**). General Method H was followed using **176** (104 mg, 0.454 mmol) and 2-iodopropane (0.14 mL, 1.4 mmol) to afford **179** as an oil (122 mg, 99%). ^1H NMR (300 MHz, CDCl_3): δ 9.11 (d, $J = 2.9$ Hz, 1H), 7.94 (dd, $J = 9.6$, 2.8 Hz, 1H), 7.32 (m, $J = 8.0$ Hz, 2H), 7.02 (m, $J = 8.3$ Hz, 2H), 5.89 (d, $J = 9.5$ Hz, 1H), 5.40 (dt, $J = 13.5$, 6.8 Hz, 1H),

2.44 (s, 3H), 1.17 (d, $J = 6.8$ Hz, 6H). LCMS, m/z 272.2 (100) $[M + H]^+$.

*N*2-Isopropyl-*N*2-(*p*-tolyl)pyridine-2,5-diamine (**180**). General Method F was followed using **179** (122 mg, 0.45 mmol) to afford **180** as an oil (105 mg, 97%). ^1H NMR (300 MHz, CDCl_3): δ 7.78 (d, $J = 2.9$ Hz, 1H), 7.21 (d, $J = 8.0$ Hz, 3H), 7.01 (d, $J = 8.2$ Hz, 3H), 6.77 (dd, $J = 8.9$, 3.0 Hz, 1H), 5.95 (d, $J = 8.9$ Hz, 1H), 5.04 (d, $J = 6.6$ Hz, 1H), 2.39 (s, 3H), 1.12 (d, $J = 6.7$ Hz, 6H). LCMS, m/z 242.2 (100) $[M + H]^+$.

N-(3-Fluoro-4-methyl-phenyl)-5-nitro-pyridin-2-amine (**181**). A solution of 2-chloro-5-nitro-pyridine (0.900 g, 5.68 mmol), 3-fluoro-4-methyl-aniline (0.888 g, 7.10 mmol) and K_2CO_3 (3.0 mL, 16 mmol) in anhydrous DMF (2 mL) under argon was heated at 120 °C for 16 h. The reaction was then concentrated in vacuo and the residue was dissolved in EtOAc (20 mL), washed with H_2O (20 mL), brine (20 mL), dried with anhydrous MgSO_4 , filtered, and concentrated. The crude material was then purified by column chromatography eluting with a gradient of 100% heptane to 50% EtOAc/heptane to afford **181** as a solid (470 mg, 33%). ^1H NMR (300 MHz, CDCl_3): δ 9.09 (d, $J = 2.7$ Hz, 1H), 8.30 (dd, $J = 9.3$, 2.7 Hz, 1H), 7.16–7.23 (m, 2H), 7.03 (d, $J = 10.4$ Hz, 1H), 6.79 (d, $J = 9.4$ Hz, 1H), 2.30 (d, $J = 1.8$ Hz, 3H). LCMS, m/z 248.2 (100) $[M + H]^+$.

N-(3-Fluoro-4-methyl-phenyl)-*N*-isopropyl-5-nitro-pyridin-2-amine (**182**). General Method H was followed using **181** (130 mg, 0.526 mmol) and 2-iodopropane (0.158 mL, 1.58 mmol) to afford **182** as a solid (120.1 mg, 79%). ^1H NMR (300 MHz, CDCl_3): δ 9.11 (d, $J = 2.8$ Hz, 1H), 7.98 (dd, $J = 9.6$, 2.7 Hz, 1H), 7.33 (t, $J = 8.2$ Hz, 1H), 6.78–6.88 (m, 2H), 5.95 (d, $J = 9.6$ Hz, 1H), 5.31–5.47 (m, 1H), 2.37 (d, $J = 1.8$ Hz, 3H), 1.18 (d, $J = 6.7$ Hz, 6H). LCMS, m/z 290.2 (100) $[M + H]^+$.

*N*2-(3-Fluoro-4-methyl-phenyl)-*N*2-isopropyl-pyridine-2,5-diamine (**183**). General Method F was followed using **182** (120 mg, 0.414 mmol) to afford **183** as an oil (105 mg, 98%). ^1H NMR (300 MHz, CDCl_3): δ 7.82 (d, $J = 2.8$ Hz, 1H), 7.15–7.23 (m, 1H), 6.90 (d, $J = 10.1$ Hz, 1H), 6.67–6.86 (m, 3H), 6.12 (d, $J = 9.0$ Hz, 1H), 4.88–5.07 (m, 1H), 2.24–2.35 (m, 3H), 1.15–1.20 (m, 6H). LCMS, m/z 260.0 (100) $[M + H]^+$.

N-(4-Chloro-3-fluoro-phenyl)-5-nitro-pyridin-2-amine (**184**). The procedure used for **181** was followed using 2-chloro-5-nitro-pyridine (1.08 g, 6.81 mmol) and 4-chloro-3-fluoro-aniline (0.826 g, 5.68 mmol) to afford **184** as a solid (123 mg, 8.1%). ^1H NMR (300 MHz, CDCl_3): δ 9.14 (d, $J = 2.6$ Hz, 1H), 8.33 (dd, $J = 2.8$, 9.2 Hz, 1H), 7.55 (dd, $J = 2.5$, 10.6 Hz, 1H), 7.41 (t, $J = 8.4$ Hz, 1H), 7.13 (d, $J = 7.5$ Hz, 2H), 6.78 (d, $J = 9.2$ Hz, 1H). LCMS, m/z 268.2 (100) $[M + H]^+$.

N-(4-Chloro-3-fluoro-phenyl)-*N*-isopropyl-5-nitro-pyridin-2-amine (**185**). General Method H was followed using **184** (44.5 mg, 0.167 mmol) and 2-iodopropane (0.664 mL, 0.665 mmol) to afford **185** as a solid (32 mg, 62%). ^1H NMR (300 MHz, CDCl_3): δ 9.11 (d, $J = 2.8$ Hz, 1H), 8.03 (dd, $J = 9.5$, 2.8 Hz, 1H), 7.53–7.65 (m, 1H), 6.88–7.07 (m, 3H), 5.97 (d, $J = 9.4$ Hz, 1H), 5.39 (t, $J = 6.6$ Hz, 1H), 1.19 (d, $J = 6.7$ Hz, 6H). LCMS, m/z 310.2 (100) $[M + H]^+$.

*N*2-(4-Chloro-3-fluoro-phenyl)-*N*2-isopropyl-pyridine-2,5-diamine (**186**). General Method F was followed using **185** (32 mg, 0.103 mmol) to afford **186** as an oil (28 mg, 97%). ^1H NMR (300 MHz, CDCl_3): δ 7.90 (d, $J = 2.9$ Hz, 1H), 7.30–7.25 (m, 1H), 6.93 (dd, $J = 8.7$, 3.0 Hz, 1H), 6.69 (dd, $J = 11.3$, 2.5 Hz, 1H), 6.57–6.65 (m, 1H), 6.41 (d, $J = 8.6$ Hz, 1H), 4.68 (quin, $J = 6.7$ Hz, 1H), 3.66 (s, 2H), 1.17 (d, $J = 6.7$ Hz, 6H). LCMS, m/z 280.2 (100) $[M + H]^+$.

4-[(5-Nitro-2-pyridyl)amino]benzonitrile (**187**). The procedure used for **167** was followed using 5-nitropyridin-2-amine (250 mg, 1.8 mmol) and 4-bromobenzonitrile (360 mg, 2.00 mmol) to afford **187** as a crude oil (139.7 mg, 32%). ^1H NMR (300 MHz, CDCl_3): δ 7.76–7.88 (m, 1H), 7.72 (d, $J = 8.7$ Hz, 1H), 7.63 (d, $J = 8.8$ Hz, 1H), 7.43–7.55 (m, 2H), 7.33 (dd, $J = 14.2$, 8.2 Hz, 1H), 6.94–7.08 (m, 1H), 6.83–6.94 (m, 1H). LCMS, m/z 241.2 (100) $[M + H]^+$.

4-[Isopropyl-(5-nitro-2-pyridyl)amino]benzonitrile (**188**). General Method H was followed using **187** (139.7 mg, 0.482 mmol) and 2-iodopropane (0.174 mL, 1.74 mmol) to afford **188** as an oil (82.3 mg, 50%). ^1H NMR (300 MHz, CDCl_3): δ 9.12 (d, $J = 2.7$ Hz, 1H), 8.04

(dd, $J = 9.5, 2.8$ Hz, 1 H) 7.85 (d, $J = 8.5$ Hz, 2H), 7.32 (d, $J = 8.4$ Hz, 2H), 5.94 (d, $J = 9.4$ Hz, 1H), 5.33–5.45 (m, 1H), 1.20 (d, $J = 6.8$ Hz, 6H). LCMS, m/z 283.2 (100) $[M + H]^+$.

4-[(*S*-Amino-2-pyridyl)-isopropyl-amino]benzonitrile (**189**). General Method F was followed using **188** (82.3 mg, 0.292 mmol) to afford **189** as an oil (73.0 mg, 99%). ^1H NMR (300 MHz, CDCl_3): δ 8.06 (d, $J = 3.0$ Hz, 1 H), 7.35–7.44 (m, 2H), 7.07 (dd, $J = 8.4, 3.1$ Hz, 1H), 6.85 (d, $J = 8.4$ Hz, 1H), 6.49–6.61 (m, 2 H), 4.39 (quin, $J = 6.6$ Hz, 1H), 3.78 (br. s., 2H), 1.19–1.23 (m, 6H). LCMS, m/z 253.2 (100) $[M + H]^+$.

***P. falciparum* 3D7 Asexual Stage Growth Assay.** This is a platform assay conducted by the Screening Facility at the Walter and Eliza Hall Institute and follows a previously described protocol that determines *P. falciparum* 3D7 asexual parasite growth after 72 h of compound exposure by measuring LDH activity.⁴⁶ Benchmark control compounds, chloroquine EC_{50} 30 nM; mefloquine EC_{50} 24 nM.

Human HepG2 Growth Assay. This is a platform assay conducted by the Screening Facility at the Walter and Eliza Hall Institute and follows a previously described protocol that determines human HepG2 cell growth following 48 h exposure to the compound by measuring Cell TiterGlo luminescence.^{46,47} Benchmark control compound, bortezomib EC_{50} 0.007 nM.

Uninfected Red Blood Cell Lysis Assay. Generation of a Standard Curve. In a 96-well plate, uninfected red blood cells (uRBCs) were serially diluted in a supplemented RPMI-1640 medium (2-fold serial dilution; 16% to 0.031% hematocrit). The uRBC samples were frozen at -80°C and thawed at room temperature to lyse the cells. The plate was centrifuged (1000 rpm, 4 min), and 50 μL of lysate was collected from the surface of each well and transferred to a new 96-well plate. Released hemoglobin was quantified by measuring the absorbance at 540 nm (OD540) of the lysate samples using a Multiskan GO Spectrophotometer (Thermo Scientific).

Quantification of WEHI-326-Induced Hemolysis. In a 96-well plate, uRBCs were diluted to 2% hematocrit in supplemented RPMI-1640 medium and treated with serially diluted WEHI-326 (2-fold serial dilution; 1000 nM to 0.488 nM) or with a DMSO vehicle control. After 4 h of incubation at 37°C , cells were pelleted by centrifugation (1000 rpm, 4 min) and 50 μL of supernatant from each well was transferred to a new 96-well plate. Hemolysis was quantified by measuring the OD540 of hemoglobin released into the culture medium as described above.

In Vitro ADME. Aqueous solubility at pH 7.4, metabolic stability in human liver microsomes and rat hepatocytes and eLogD are platform assays conducted by TCG Lifesciences using previously described protocols.⁴⁸

Minimum Inoculum of Resistance (MIR) Assay. This is a platform assay undertaken by the Fidock laboratory and follows a standardized protocol.^{20,48} Parasite culture: *P. falciparum* asexual blood stage (ABS) parasites were cultured at 3% hematocrit in human O+ RBCs in RPMI-1640 media, supplemented with 25 mM HEPES, 50 mg/L hypoxanthine, 2 mM L-glutamine, 0.21% sodium bicarbonate, 0.5% (wt/vol) AlbumaxII (Invitrogen) and 10 $\mu\text{g}/\text{mL}$ gentamycin, in modular incubator chambers (Billups-Rothenberg) at 5% O_2 , 5% CO_2 and 90% N_2 at 37°C . Dd2 parasites were obtained from T. Wellems (NIAID, NIH). Dd2-B2 is a genetically homogeneous line that was cloned from Dd2 by limiting dilution in the Fidock lab.

Compound susceptibility assays: Compound stocks were made at 10 mM and 1 mM in dimethyl sulfoxide (DMSO) and stored at -80°C . All in vitro studies were done such that the final DMSO concentration was $<0.5\%$. To define the IC_{50} and IC_{90} of ABS parasites, we exposed Dd2-B2 ring-stage cultures at 0.3% parasitemia and 1% hematocrit for 72 h to a range of ten drug concentrations that were 2-fold serially diluted in duplicates, along with drug-free controls. Parasite survival was assessed by flow cytometry on an iQue flow cytometer (Sartorius) using SYBR Green and MitoTracker Deep Red FM (Life Technologies) as nuclear stain and vital dyes, respectively. Inocula of 3.3×10^6 parasites were plated in each well of a 24-well plate (to cover parasite numbers up to 7.9×10^8). Selections were initiated at 0.5% parasitemia and 3% hematocrit in 2 mL

volumes per well. Cultures were monitored for complete parasite clearance for the first 7 days by microscopic examination of Giemsa-stained thin blood smears. Once parasite levels fell below 0.2%, they were noted as clear. After clearance, fresh drug media was replenished in the cultures twice a week. Cultures were passaged once a week by replacing 40% of the culture with media and fresh RBCs according to the concentrations described above. Selections were monitored three times a week over 60 days by flow cytometry to screen for parasite recrudescence. Cultures that remained negative on day 60 were stopped. With recrudescence cultures, three wells were randomly chosen and expanded for phenotypic dose–response analysis (as described above), whole-genome sequencing, and cryopreservation.

Whole Genome Sequencing of MIR Recrudescence Populations. Whole-genome sequencing was performed as previously described.⁴⁸ Whole-genome sequencing data that support the findings of this study have been deposited in the European Nucleotide Archive (ENA) at EMBL-EBI under accession number: PRJEB81692 (<https://www.ebi.ac.uk/ena/browser/view/PRJEB81692>).

Antimalarial Resistome Barcode Sequencing (AReBar) Assay. Parasite culture was performed as above. The parasite pool comprises 52 barcoded lines with distinct resistance mutations, the majority derived from in vitro resistance selections, as well as wildtype Dd2 and 3D7 (shown in Table S6). Barcode tagging was performed by CRISPR insertion at the nonessential *pf* gene locus (PF3D7_0709700) of a 101 bp barcode cassette,²⁵ and the lines pooled in equal proportion. Prior to commencing the assay, a 72h SYBR-green assay was performed to obtain EC_{50} values for WEHI-326 (33) against Dd2 and 3D7, which were initially determined to be 0.0033 and 0.0072 μM respectively. The lowest EC_{50} value (Dd2) was used to set the compound concentration used against the AReBar pool. Triplicate 200 μL cultures of the pooled lines were exposed to $3 \times \text{EC}_{50}$ of WEHI-326 (33), or an untreated control, and growth over the 14 day assay was measured by flow cytometry (Cytotflex, Beckman Coulter) after staining with $1 \times$ SYBR green/200 nM Mitotracker Deep Red. Cultures were replenished with fresh media and compound every 2–3 days, and maintained between 0.3 and 5% parasitemia. Cultures were harvested at day 14, lysed by saponin (0.01%) and the parasite pellets washed twice with PBS and resuspended in $\sim 30 \mu\text{L}$ of PBS. Barcode amplification and indexing were performed as described in Carrasquilla et al.,²⁵ with PCR amplification of the barcode cassette performed directly on 5 μL of parasite pellet using CloneAmp HiFi PCR premix. Products from PCR1 were indexed in a second PCR, 25 ng of each sample was combined and diluted to 4 nM for Illumina MiSeq sequencing with 150 bp paired-end reads. FASTQ files were generated using tools on Illumina BaseSpace and barcode counts were analyzed using the R package DESeq2.⁴⁹ Barcodes differentially represented compared with control were determined as having a Log2 fold change (LFC) > 2.5 and $p = 0.001$ (Wald test).

Homology Model of *P. falciparum* ROM8. The homology model of *P. falciparum* ROM8 was created using SWISS-MODEL software⁵⁰ to identify *Escherichia coli* GlpG (PDB: 6XRP)³⁴ as the highest homologous X-ray structure based on the protein sequence of *P. falciparum* 3D7 ROM8 (PF3D7_1411200). The resulting output for the model of *P. falciparum* ROM8 was transformed, and mutations were mapped and visualized using PyMol Molecular Graphics System software (version 2.5.0). Amino acids 1–506 and 696–738 were excluded for clarity.

Homology Model of *P. falciparum* CSC1. The homology model of *P. falciparum* CSC1 was created using SWISS-MODEL software⁵⁰ to identify *Arabidopsis thaliana* OSCA (PDB: 8GRN)³⁷ as the highest homologous X-ray structure based on the protein sequence of *P. falciparum* 3D7 CSC1 (PF3D7_1250200). The pdb for the model of *P. falciparum* CSC1 was transformed, and mutations were mapped and visualized using PyMol Molecular Graphics System software (version 2.5.0). Amino acids 181–686 and 966–1039 were excluded for clarity.

MMV020512-Resistant Asexual Stage Assays. MMV020512-resistant *P. falciparum* 3D7 parasite populations 3D7-Pop A, D, and E were generated as previously described.³⁰ Compounds were evaluated against resistant parasites using the lactate dehydrogenase

(LDH) assay format. Briefly, parasite populations were exposed to a serial dilution of compound for 72 h. Parasites were frozen (-78°C) and thawed to lyse cells, and lactate dehydrogenase assay mix added (0.1 M Tris pH 9.0, 20 g/L lactic acid, pH 7.5, 0.2% Triton-X100, 0.5 g/L acetylpyridine adenine dinucleotide (APAD, Sigma), 200 $\mu\text{g}/\text{mL}$ nitroblue tetrazolium (NBT; Sigma), 1 $\mu\text{g}/\text{mL}$ phenazine ethosulfate (PES; Sigma)). Absorbance (650 nm) was measured and % parasitemia determined using the formula: growth inhibition (%) = $(1 - (\text{average}(\text{sample}) - \text{average}(\text{uRBC})) / (\text{average}(\text{DMSO}) - \text{average}(\text{uRBC}))) \times 100$. EC_{50} values were determined using a nonlinear regression (log(inhibitor) vs response, variable slope) in GraphPad Prism.

Parasite Reduction Ratio Assay. This is a platform assay undertaken by TCG Lifesciences and is based on previously described protocols.^{42,46} Briefly, *P. falciparum* 3D7 parasites were treated with the selected drug at a concentration corresponding to $10\times \text{EC}_{50}$ for 120 h. The compound was renewed daily over the entire treatment period. Samples of parasites were taken from the treated culture every 24 h (0 for the control of the initial number of parasites, followed by 24, 48, 72, 96, and 120 h time points), the drug was washed out and drug-free parasites were cultured in 96-well plates by adding fresh erythrocytes and new culture media. To quantify the number of viable parasites after treatment, a 3-fold serial dilution was used with the above-mentioned samples after removing the compound. Parasites were cultured in microtiter plates to allow all wells with viable parasites, to render detectable parasitaemia. Four independent serial dilutions were done with each sample to correct experimental variations. After 22 days of culturing, samples were taken to examine growth. Additional sampling was done after 28 days to confirm growth/no growth. The number of viable parasites was determined by counting the number of wells with growth, which was determined with an LDH assay with a 72 h incubation time as follows: 70 μL of freshly reaction mix was prepared containing: 143 mM sodium L-lactate, 143 μM 3-acetylpyridine adenine dinucleotide (APAD), 178.75 μM nitro blue tetrazolium chloride (NBT), diaphorase (2.83 U/mL), 0.7% Tween 20, 100 mM Tris-HCl pH 8.0. The mix was added to each well of the incubation plate mentioned above. Plates were shaken to ensure mixing. Plates are placed in an incubator at 21°C for 20 min and absorbance at 650 nm was recorded using a plate reader (Spectramax M5). The experimental number of viable parasites after each treatment was back-calculated by using formula X^{n-1} where n was the number of wells able to render growth and X the dilution factor (when $n = 0$ number of viable parasites is estimated as zero). The number of initial parasites (no treatment) was calculated similarly and used to calculate a normalization factor to correct the deviation of the experimental determination from the theoretical number of initial parasites (10^5 , 100 μL from 10^6 parasites/mL inoculum). The normalization factor was used to correct all the experimental data for a starting number of parasites equal to 10^5 and enables comparison between different experiments. Additional parameters were calculated such as lag phase (time needed to observe the maximal killing effect of the drug being tested), PRR (parasite reduction ratio; such as the reduction in the number of parasites by the drug in a parasite life cycle) and PCT99.9% (parasite clearance time; the time required to kill 99.9% of the initial population).

Egress and Invasion Assays. Conducted as described previously¹⁵ using transgenic *P. falciparum* 3D7 parasites expressing an exported bioluminescent nanoluciferase enzyme.⁵¹ Briefly, Percoll-purified late-stage schizonts (>40 h postinvasion) at 1% hematocrit and 2% parasitaemia were treated with serially diluted WEHI-326 or WEHI-328 for 4 h. Cell-free culture medium, containing nanoluciferase released during merozoite egress, was collected and remaining unruptured schizonts were eliminated by sorbitol lysis. Cells were washed 2–3 times in complete RPMI to remove compounds and sorbitol. Parasites were grown at 37°C for a further 24 h before being frozen and thawed to lyse the cells and release nanoluciferase. To quantify egress or invasion, 5 μL of cell-free supernatant (collected after the 4 h drug treatment window) or 5 μL of cell lysate (collected 24 h after drug washout), respectively, was added to 45 μL Nano-Glo

substrate diluted 1:1000 in incomplete RPMI medium. The bioluminescent signal intensity was measured in relative light units (RLU) using a CLARIOstar luminometer (BMG Labtech). A background control, consisting of Percoll-purified schizonts that were refrigerated at 4°C during the 4 h treatment window before being treated with sorbitol and incubated at 37°C for 24 h. Percentage egress and invasion were calculated as follows, using the RLU of cell-free supernatant or cell lysate samples, respectively: % egress or invasion = $(\text{RLU}_{\text{compound treated}} - \text{mean RLU}_{\text{background}}) / (\text{mean RLU}_{\text{untreated}} - \text{mean RLU}_{\text{background}}) \times 100$.

Gametocyte Viability Assay. This is a platform assay in the Birkholtz laboratory at the University of Pretoria and uses a previously described protocol.⁴³ Briefly, gametocytogenesis was induced with synchronized NF54-Pfs16-GFP-luc or 3D7elo1-pfs16-CBG99 *P. falciparum* asexual ring stage parasites⁵² using nutrient starvation and decreased hematocrit. Stage II/III gametocytes were exposed to 50 mM N-acetyl glucosamine on days 1–4 to remove remaining asexual parasites and harvested on days 5–6, while stage V gametocytes, were exposed to 50 mM N-acetyl glucosamine on days 3–7 and harvested at day 13. Stage II–III and stage V gametocytes were exposed to serially diluted compound for 48 h. Luciferase activity was determined using 30 μL of parasite lysate with the addition of 30 μL of luciferin mix (Promega Luciferase Assay System) at room temperature and bioluminescence was measured using a GloMax-Multi Detection System with Instinct software. % inhibition was determined using bioluminescence of compound treated versus control viable gametocytes and the EC_{50} was calculated using nonlinear curve fitting and four parametric equations (Graph-Pad Prism).

Dual Gamete Formation Assay. This is a platform assay in the Delves laboratory at the London School of Hygiene and Tropical Medicine (LSHTM) and uses the previously described protocol.⁴⁴ Briefly, compounds are incubated with *P. falciparum* NF54 stage V gametocytes for 48 h in 384-well plates before gamete formation is triggered by a drop in temperature and the addition of xanthurenic acid. Thirty min post-triggering, male gamete exflagellation is recorded and quantified by automated microscopy. The plates are then incubated at 26°C for a further 24 h and then the female gamete formation of samples is assessed by live staining using a fluorophore-conjugated αPfs25 antibody specific for female gametes and quantified by automated microscopy.

Standard Membrane Feeding Assay. This model is conducted in the Wellcome Trust Human Malaria Transmission Facility at LSHTM following a previously described protocol.⁵³ Briefly, *P. falciparum* NF54 gametocytes were prepared for blood-feeding to mosquitoes according to the method previously described.⁵⁴ Gametocyte aliquots from a single NF54 culture were mixed in the membrane feeder reservoir with WEHI-326 at 500 nM or 100 nM, and methylene blue at 1 μM (positive control) or culture medium with DMSO (no-drug control). The concentration of DMSO during experimental mosquito feeds was at 1.0% v/v. Pools of 70–80 female *Anopheles stephensi* (SD500 strain) mosquitoes (2 to 5 days old) were allowed to feed on 500 μL of the respective culture-drug-DMSO mixture, presented to each pool of mosquitoes in a preheated water channel membrane feeder, until fully fed. Mosquitoes were placed in an incubator at standard conditions and midguts were dissected in 0.25% mercurochrome stain for oocyst counts by light microscopy 7–8 days postfeed. The statistical significance of observed differences was tested by the nonparametric Wilcoxon ranksum test.

Animal Ethics. Experiments involving rodents were performed in strict accordance with the recommendations of the Australian Government and National Health and Medical Research Council Australian code of practice for the care and use of animals for scientific purposes. The protocols were approved by the Animal Welfare Committee at Deakin University (approval no. G11/2023).

***P. berghei* 4-Day Mouse Model.** This model is conducted by the de Koning Ward laboratory at Deakin University following a previously described protocol.²⁰ Briefly, compound was suspended in a vehicle of 70% (v/v) Tween 80 and 30% (v/v) ethanol in distilled sterile water. Eight week old female Swiss mice at day 0 were infected

with 2×10^7 *P. berghei* ANKA-infected erythrocytes. At 2 h and days 1, 2, and 3 postinfection, mice were orally gavaged with 50 mg/kg of WEHI-326 (5 mice), 30 mg/kg artesunate (3 mice), or vehicle control (5 mice). Parasitemia levels in mice were determined on days 2, 3, and 4 by visualizing Giemsa-stained thin blood smears by microscopy.

Mouse Plasma Exposure. Animal ethics statement: The study was performed under protocol approved by the Institutional Animal Care Committee (IAEC) of TCG Lifesciences Pvt. Ltd. All animal procedures were conducted according to the guidelines of experimental animal care issued by the Committee for Control and Supervision of Experiments on Animals (CCSEA). The experiment was performed using 3 male CD1 mice (6–8 weeks) procured from Hylasco Bio-Technology (licensed breeder and supplier of Charles River Lab in India). Animals were housed under 12/12 h light–dark cycle, 22 ± 3 °C temp, $50 \pm 20\%$ humidity in the AAALAC accredited facility. Animals were allowed free access to food and water ad libitum and were acclimatized to laboratory conditions for 5–7 days prior to enrollment in the study. Method: Mouse plasma exposure was performed by TCG Lifesciences following a previously described protocol.⁵⁵ Briefly, the vehicle for WEHI-326 (33) was a homogeneous suspension of 5% DMSO, 95% HPBCD (20% in water). WEHI-326 (33) was administered by oral gavage at 20 mg/kg (dose volume 10 mL/kg). At 0.08, 0.25, 0.5, 1, 2, 4, 8, 24 h postdosing blood samples were collected, and pharmacokinetic parameters were analyzed and estimated using a NCA model in WinNonlin.

■ ASSOCIATED CONTENT

SI Supporting Information

The Supporting Information is available free of charge at <https://pubs.acs.org/doi/10.1021/acs.jmedchem.5c01471>.

P. falciparum wildtype and drug-resistant asexual and gametocyte and gamete dose–response curves, MIR and AReBar analyses and whole genome sequencing, mouse and transmission model data, and compound synthesis schemes and spectra (PDF)

Molecular formula strings (CSV)

Molecular structure (PDB)

Molecular structure (PDB)

■ AUTHOR INFORMATION

Corresponding Author

Brad E. Sleebs – The Walter and Eliza Hall Institute of Medical Research, Parkville 3052, Australia; Department of Medical Biology, The University of Melbourne, Parkville 3010, Australia; orcid.org/0000-0001-9117-1048; Email: sleebs@wehi.edu.au

Authors

William Nguyen – The Walter and Eliza Hall Institute of Medical Research, Parkville 3052, Australia; Department of Medical Biology, The University of Melbourne, Parkville 3010, Australia; orcid.org/0000-0002-3984-2390

Coralie Boulet – Burnet Institute, Melbourne, Victoria 3004, Australia; orcid.org/0000-0002-5476-7800

Madeline G. Dans – The Walter and Eliza Hall Institute of Medical Research, Parkville 3052, Australia; Department of Medical Biology, The University of Melbourne, Parkville 3010, Australia

Katie Loi – The Walter and Eliza Hall Institute of Medical Research, Parkville 3052, Australia

Kate E. Jarman – The Walter and Eliza Hall Institute of Medical Research, Parkville 3052, Australia; Department of

Medical Biology, The University of Melbourne, Parkville 3010, Australia

Claudia B. G. Barnes – Burnet Institute, Melbourne, Victoria 3004, Australia

Tomas Yeo – Department of Microbiology & Immunology and Center for Malaria Therapeutics and Antimicrobial Resistance, Columbia University Irving Medical Center, New York, New York 10032, United States

Tanaya Sheth – Department of Microbiology & Immunology and Center for Malaria Therapeutics and Antimicrobial Resistance, Columbia University Irving Medical Center, New York, New York 10032, United States

Partha Mukherjee – TCG Lifesciences, Kolkata, West Bengal 700091, India

Arnish Chakraborty – TCG Lifesciences, Kolkata, West Bengal 700091, India

Mufuiliat T. Famodimu – Department of Infection Biology, London School of Hygiene and Tropical Medicine, London WC1E 7HT, United Kingdom; orcid.org/0000-0002-8852-1040

Michael J. Delves – Department of Infection Biology, London School of Hygiene and Tropical Medicine, London WC1E 7HT, United Kingdom; orcid.org/0000-0001-8526-4782

Harry Pollard – Department of Infection Biology, London School of Hygiene and Tropical Medicine, London WC1E 7HT, United Kingdom

Colin J. Sutherland – Department of Infection Biology, London School of Hygiene and Tropical Medicine, London WC1E 7HT, United Kingdom

Rachael Coyle – Wellcome Genome Campus, Wellcome Sanger Institute, Hinxton CB10 1SA, United Kingdom; Biological Chemistry and Drug Discovery, Wellcome Centre for Anti-Infectives Research, University of Dundee, Dundee DD1 4HN, United Kingdom

Nicole Sevileno – Wellcome Genome Campus, Wellcome Sanger Institute, Hinxton CB10 1SA, United Kingdom

Nonlawat Boonyalai – Biological Chemistry and Drug Discovery, Wellcome Centre for Anti-Infectives Research, University of Dundee, Dundee DD1 4HN, United Kingdom

Marcus C. S. Lee – Wellcome Genome Campus, Wellcome Sanger Institute, Hinxton CB10 1SA, United Kingdom; Biological Chemistry and Drug Discovery, Wellcome Centre for Anti-Infectives Research, University of Dundee, Dundee DD1 4HN, United Kingdom

Tayla Rabie – Department of Biochemistry, Genetics and Microbiology, Institute for Sustainable Malaria Control, University of Pretoria, Pretoria 0028, South Africa

Lyn-Marié Birkholtz – Department of Biochemistry, Genetics and Microbiology, Institute for Sustainable Malaria Control, University of Pretoria, Pretoria 0028, South Africa

Delphine Baud – Medicines for Malaria Venture, Geneva 1215, Switzerland; orcid.org/0009-0005-6745-233X

Stephen Brand – Medicines for Malaria Venture, Geneva 1215, Switzerland

Mrittika Chowdury – School of Medicine, Deakin University, Waurn Ponds 3216, Australia; Institute for Mental and Physical Health and Clinical Translation, Deakin University, Geelong 3216, Australia

Tania F. de Koning-Ward – School of Medicine, Deakin University, Waurn Ponds 3216, Australia; Institute for Mental and Physical Health and Clinical Translation, Deakin University, Geelong 3216, Australia

David A. Fidock — Department of Microbiology & Immunology, Center for Malaria Therapeutics and Antimicrobial Resistance, and Division of Infectious Diseases, Department of Medicine, Columbia University Irving Medical Center, New York, New York 10032, United States

Paul R. Gilson — Burnet Institute, Melbourne, Victoria 3004, Australia; orcid.org/0000-0001-8778-6795

Complete contact information is available at:

<https://pubs.acs.org/10.1021/acs.jmedchem.5c01471>

Notes

The authors declare no competing financial interest.

ACKNOWLEDGMENTS

This work was funded by the National Health and Medical Research Council of Australia (Development Grant 2014427 to B.E.S. and A.F.C.; and Ideas Grant 2001073 to P.R.G. and W.N.; Synergy Grant 1185354 to P.R.G. and T.F.d.K.-W.), the Victorian State Government Operational Infrastructure Support and the Australian Government NHMRC IRIISS. D.A.F., M.C.S.L., L.M.B., and B.E.S. acknowledge the support of Medicines for Malaria Venture (RD-08-2800, RD-08-0015, RD-18-0005, RD-19-001, and RD-08-0003, respectively). M.T.F. is supported by a grant awarded to M.J.D. by the Medicines for Malaria Venture (RD-21-1003). M.J.D. is supported by an UKRI Medical Research Council Career Development Award (MR/V010034/1). Mosquito infection studies at LSHTM are supported by Wellcome Trust Biomedical Resources Grant (221363/Z/20/Z) awarded to C.J.S. We thank and acknowledge the Australian Red Cross Lifeblood & UK NHS Blood and Transplant for the provision of fresh red blood cells. L.M.B. thanks the South African National Research Foundation Research Chair Initiative (SARChI 84627). A.F.C. is a Howard Hughes International Scholar and an Australia Fellow of the NHMRC. B.E.S. is a Corin Centenary Fellow.

ABBREVIATIONS

ACT, artemisinin combination therapy; AReBar, antimalarial resistome barcoding; CRAC, calcium release-activated calcium channel; CSC1, calcium-permeable stress-gated cation channel 1; DGFA, dual gamete formation assay; GFP, green fluorescent protein; LDH, lactate dehydrogenase; MIR, minimum inoculum of resistance; OSCA1, hyperosmolality-gated Ca^{2+} permeable channel 1; PRR, parasite reduction ratio; PV, parasitophorous vacuole; RHBDL2, rhomboid-related protein 2; ROM8, rhomboid protease 8; SNP, single nucleotide polymorphism.

REFERENCES

- (1) Laurens, M. B. RTS,S/AS01 vaccine (Mosquirix): an overview. *Hum. Vaccin. Immunother.* **2020**, *16* (3), 480–489.
- (2) Dato, M. S.; Natama, H. M.; Somé, A.; Bellamy, D.; Traoré, O.; Rouamba, T.; Tahita, M. C.; Ido, N. F. A.; Yameogo, P.; Valia, D.; Millogo, A.; Ouedraogo, F.; Soma, R.; Sawadogo, S.; Sorgho, F.; Derra, K.; Rouamba, E.; Ramos-Lopez, F.; Cairns, M.; Provstgaard-Morys, S.; Aboagye, J.; Lawrie, A.; Roberts, R.; Valéa, L.; Sorgho, H.; Williams, R.; Glenn, G.; Fries, L.; Reimer, J.; Ewer, K. J.; Shaligram, U.; Hill, A. V. S.; Tinto, H. Efficacy and immunogenicity of R21/Matrix-M vaccine against clinical malaria after 2 years' follow-up in children in Burkina Faso: a phase 1/2b randomised controlled trial. *Lancet Infect. Dis.* **2022**, *22* (12), 1728–1736.
- (3) Duffey, M.; Shafer, R. W.; Timm, J.; Burrows, J. N.; Fotouhi, N.; Cockett, M.; Leroy, D. Combating antimicrobial resistance in malaria,

- HIV and tuberculosis. *Nat. Rev. Drug Discovery* **2024**, *23* (6), 461–479.
- (4) Ashley, E. A.; Dhorda, M.; Fairhurst, R. M.; Amaratunga, C.; Lim, P.; Suon, S.; Sreng, S.; Anderson, J. M.; Mao, S.; Sam, B.; Sopha, C.; Chuor, C. M.; Nguon, C.; Sovannarothe, S.; Pukrittayakamee, S.; Jittamala, P.; Chotivanich, K.; Chutasmit, K.; Suchatsoonthorn, C.; Runchaoren, R.; Hien, T. T.; Thuy-Nhien, N. T.; Thanh, N. V.; Phu, N. H.; Htut, Y.; Han, K. T.; Aye, K. H.; Mokuolu, O. A.; Olaosebikan, R. R.; Folaranmi, O. O.; Mayxay, M.; Khanthavong, M.; Hongvanthong, B.; Newton, P. N.; Onyamboko, M. A.; Fanello, C. I.; Tshefu, A. K.; Mishra, N.; Valecha, N.; Phyo, A. P.; Nosten, F.; Yi, P.; Tripura, R.; Borrmann, S.; Bashraheil, M.; Peshu, J.; Faiz, M. A.; Ghose, A.; Hossain, M. A.; Samad, R.; Rahman, M. R.; Hasan, M. M.; Islam, A.; Miotto, O.; Amato, R.; MacInnis, B.; Stalker, J.; Kwiatkowski, D. P.; Bozdech, Z.; Jeeyapant, A.; Cheah, P. Y.; Sakulthaew, T.; Chalk, J.; Intharabut, B.; Silamut, K.; Lee, S. J.; Vihokhern, B.; Kunasol, C.; Imwong, M.; Tarning, J.; Taylor, W. J.; Yeung, S.; Woodrow, C. J.; Flegg, J. A.; Das, D.; Smith, J.; Venkatesan, M.; Plowe, C. V.; Stepniewska, K.; Guerin, P. J.; Dondorp, A. M.; Day, N. P.; White, N. J. Spread of Artemisinin resistance in *Plasmodium falciparum* Malaria. *N. Engl. J. Med.* **2014**, *371* (5), 411–423.
 - (5) Uwimana, A.; Legrand, E.; Stokes, B. H.; Ndikumana, J.-L. M.; Warsame, M.; Umulisa, N.; Ngamije, D.; Munyaneza, T.; Mazarati, J.-B.; Munguti, K.; Campagne, P.; Criscuolo, A.; Arie, F.; Murindahabi, M.; Ringwald, P.; Fidock, D. A.; Mbituyumuremyi, A.; Menard, D. Emergence and clonal expansion of in vitro artemisinin-resistant *Plasmodium falciparum* kelch13 R561H mutant parasites in Rwanda. *Nat. Med.* **2020**, *26*, 1602–1608.
 - (6) Ashton, T. D.; Devine, S. M.; Möhrle, J. J.; Laleu, B.; Burrows, J. N.; Charman, S. A.; Creek, D. J.; Sleebs, B. E. The development process for discovery and clinical advancement of modern antimalarials. *J. Med. Chem.* **2019**, *62* (23), 10526–10562.
 - (7) Siqueira-Neto, J. L.; Wicht, K. J.; Chibale, K.; Burrows, J. N.; Fidock, D. A.; Winzeler, E. A. Antimalarial drug discovery: progress and approaches. *Nat. Rev. Drug Discovery* **2023**, *22* (10), 807–826.
 - (8) Burrows, J. N.; Duparc, S.; Gutteridge, W. E.; Hooft van Huijsduijnen, R.; Kaszubska, W.; Macintyre, F.; Mazzuri, S.; Möhrle, J. J.; Wells, T. N. C. New developments in anti-malarial target candidate and product profiles. *Malar. J.* **2017**, *16* (1), 26.
 - (9) Abd-Rahman, A. N.; Zaloumis, S.; McCarthy, J. S.; Simpson, J. A.; Commons, R. J. Scoping review of antimalarial drug candidates in phase I and II drug development. *Antimicrob. Agents Chemother.* **2022**, *66* (2), e01659–21.
 - (10) Andrews, M.; Baum, J.; Gilson, P. R.; Wilson, D. W. Bottoms up! Malaria parasite invasion the right way around. *Trends Parasitol.* **2023**, *39* (12), 1004–1013.
 - (11) Burns, A. L.; Dans, M. G.; Balbin, J. M.; de Koning-Ward, T. F.; Gilson, P. R.; Beeson, J. G.; Boyle, M. J.; Wilson, D. W. Targeting malaria parasite invasion of red blood cells as an antimalarial strategy. *FEMS Microbiol. Rev.* **2019**, *43* (3), 223–238.
 - (12) Dvorin, J. D.; Goldberg, D. E. Plasmodium egress across the parasite life cycle. *Annu. Rev. Microbiol.* **2022**, *76*, 67–90.
 - (13) Favuzza, P.; de Lera Ruiz, M.; Thompson, J. K.; Triglia, T.; Ngo, A.; Steel, R. W. J.; Vavrek, M.; Christensen, J.; Healer, J.; Boyce, C.; Guo, Z.; Hu, M.; Khan, T.; Murgolo, N.; Zhao, L.; Penington, J. S.; Reaksudan, K.; Jarman, K.; Dietrich, M. H.; Richardson, L.; Guo, K. Y.; Lopatnicki, S.; Tham, W. H.; Rottmann, M.; Papenfuss, T.; Robbins, J. A.; Boddey, J. A.; Sleebs, B. E.; Sabroux, H. J.; McCauley, J. A.; Olsen, D. B.; Cowman, A. F. Dual plasmepsin-targeting antimalarial agents disrupt multiple stages of the malaria parasite life cycle. *Cell Host Microbe* **2020**, *27* (4), 642–658.
 - (14) de Lera Ruiz, M. Invention of the dual plasmepsin IX/X inhibitor MK-7602—A promising next generation antimalarial agent from an efficient academic/industrial collaboration In *American Society of Tropical Medicine and Hygiene, Annual Meeting 2023*, Toronto, Ontario, Canada, October 18th–22th, 2023.
 - (15) Dans, M. G.; Weiss, G. E.; Wilson, D. W.; Sleebs, B. E.; Crabb, B. S.; de Koning-Ward, T. F.; Gilson, P. R. Screening the Medicines for Malaria Venture Pathogen Box for invasion and egress inhibitors

of the blood stage of *Plasmodium falciparum* reveals several inhibitory compounds. *Int. J. Parasitol.* **2020**, *50* (3), 235–252.

(16) Duffy, S.; Sykes, M. L.; Jones, A. J.; Shelper, T. B.; Simpson, M.; Lang, R.; Poulsen, S. A.; Sleebs, B. E.; Avery, V. M. Screening the Medicines for Malaria Venture Pathogen Box across multiple pathogens reclassifies starting points for open-source drug discovery. *Antimicrob. Agents Chemother.* **2017**, *61* (9), e00379–17.

(17) Dans, M. G.; Piirainen, H.; Nguyen, W.; Khurana, S.; Mehra, S.; Razook, Z.; Geoghegan, N. D.; Dawson, A. T.; Das, S.; Parkyn Schneider, M.; Jonsdottir, T. K.; Gabriela, M.; Gancheva, M. R.; Tonkin, C. J.; Mollard, V.; Goodman, C. D.; McFadden, G. I.; Wilson, D. W.; Rogers, K. L.; Barry, A. E.; Crabb, B. S.; de Koning-Ward, T. F.; Sleebs, B. E.; Kursula, I.; Gilson, P. R. Sulfonylpiperazine compounds prevent *Plasmodium falciparum* invasion of red blood cells through interference with actin-1/profilin dynamics. *PLoS Biol.* **2023**, *21* (4), No. e3002066.

(18) Nguyen, W.; Dans, M. G.; Ngo, A.; Gancheva, M. R.; Romeo, O.; Duffy, S.; de Koning-Ward, T. F.; Lowes, K. N.; Sabroux, H. J.; Avery, V. M.; Wilson, D. W.; Gilson, P. R.; Sleebs, B. E. Structure activity refinement of phenylsulfonyl piperazines as antimalarials that block erythrocytic invasion. *Eur. J. Med. Chem.* **2021**, *214*, 113253.

(19) Dans, M. G.; Boulet, C.; Watson, G. M.; Nguyen, W.; Dziekan, J. M.; Evelyn, C.; Reaksudsan, K.; Mehra, S.; Razook, Z.; Geoghegan, N. D.; Mlodzianowski, M. J.; Goodman, C. D.; Ling, D. B.; Jonsdottir, T. K.; Tong, J.; Famodimu, M. T.; Kristan, M.; Pollard, H.; Stewart, L. B.; Brandner-Garrod, L.; Sutherland, C. J.; Delves, M. J.; McFadden, G. I.; Barry, A. E.; Crabb, B. S.; de Koning-Ward, T. F.; Rogers, K. L.; Cowman, A. F.; Tham, W. H.; Sleebs, B. E.; Gilson, P. R. Aryl amino acetamides prevent *Plasmodium falciparum* ring development via targeting the lipid-transfer protein PfSTART1. *Nat. Commun.* **2024**, *15* (1), 5219.

(20) Nguyen, W.; Boulet, C.; Dans, M. G.; Loi, K.; Jarman, K. E.; Watson, G. M.; Tham, W. H.; Fairhurst, K. J.; Yeo, T.; Fidock, D. A.; Wittlin, S.; Chowdury, M.; de Koning-Ward, T. F.; Chen, G.; Yan, D.; Charman, S. A.; Baud, D.; Brand, S.; Jackson, P. F.; Cowman, A. F.; Gilson, P. R.; Sleebs, B. E. Activity refinement of aryl amino acetamides that target the *P. falciparum* STAR-related lipid transfer 1 protein. *Eur. J. Med. Chem.* **2024**, *270*, 116354.

(21) Thompson, R. A.; Isin, E. M.; Ogese, M. O.; Mettetal, J. T.; Williams, D. P. Reactive metabolites: current and emerging risk and hazard assessments. *Chem. Res. Toxicol.* **2016**, *29* (4), 505–533.

(22) St. Jean, D. J., Jr.; Fotsch, C. Mitigating heterocycle metabolism in drug discovery. *J. Med. Chem.* **2012**, *55* (13), 6002–6020.

(23) Ding, X. C.; Ubben, D.; Wells, T. N. C. A framework for assessing the risk of resistance for anti-malarials in development. *Malar. J.* **2012**, *11* (1), 292.

(24) Duffey, M.; Blasco, B.; Burrows, J. N.; Wells, T. N. C.; Fidock, D. A.; Leroy, D. Assessing risks of *Plasmodium falciparum* resistance to select next-generation antimalarials. *Trends Parasitol.* **2021**, *37* (8), 709–721.

(25) Carrasquilla, M.; Drammeh, N. F.; Rawat, M.; Sanderson, T.; Zenonos, Z.; Rayner, J. C.; Lee, M. C. S. Barcoding genetically distinct *Plasmodium falciparum* strains for comparative assessment of fitness and antimalarial drug resistance. *mBio* **2022**, *13* (5), No. e0093722.

(26) Meister, S.; Plouffe, D. M.; Kuhen, K. L.; Bonamy, G. M.; Wu, T.; Barnes, S. W.; Bopp, S. E.; Borboa, R.; Bright, A. T.; Che, J.; Cohen, S.; Dharia, N. V.; Gagaring, K.; Gettayacamin, M.; Gordon, P.; Groessl, T.; Kato, N.; Lee, M. C.; McNamara, C. W.; Fidock, D. A.; Nagle, A.; Nam, T. G.; Richmond, W.; Roland, J.; Rottmann, M.; Zhou, B.; Froissard, P.; Glynn, R. J.; Mazier, D.; Sattabongkot, J.; Schultz, P. G.; Tuntland, T.; Walker, J. R.; Zhou, Y.; Chatterjee, A.; Diagana, T. T.; Winzeler, E. A. Imaging of *Plasmodium* liver stages to drive next-generation antimalarial drug discovery. *Science* **2011**, *334* (6061), 1372–1377.

(27) Luth, M. R.; Godinez-Macias, K. P.; Chen, D.; Okombo, J.; Thathy, V.; Cheng, X.; Daggupati, S.; Davies, H.; Dhingra, S. K.; Economy, J. M.; Edgar, R. C. S.; Gomez-Lorenzo, M. G.; Istvan, E. S.; Jado, J. C.; LaMonte, G. M.; Melillo, B.; Mok, S.; Narwal, S. K.; Ndiaye, T.; Otlilie, S.; Palomo Diaz, S.; Park, H.; Peña, S.; Rocamora,

F.; Sakata-Kato, T.; Small-Saunders, J. L.; Summers, R. L.; Tumwebaze, P. K.; Vanaerschot, M.; Xia, G.; Yeo, T.; You, A.; Gamo, F. J.; Goldberg, D. E.; Lee, M. C. S.; McNamara, C. W.; Ndiaye, D.; Rosenthal, P. J.; Schreiber, S. L.; Serra, G.; De Siqueira-Neto, J. L.; Skinner-Adams, T. S.; Uhlemann, A. C.; Kato, N.; Lukens, A. K.; Wirth, D. F.; Fidock, D. A.; Winzeler, E. A. Systematic in vitro evolution in *Plasmodium falciparum* reveals key determinants of drug resistance. *Science* **2024**, *386* (6725), eadk9893.

(28) Gamo, F.-J.; Sanz, L. M.; Vidal, J.; de Cozar, C.; Alvarez, E.; Lavandera, J.-L.; Vanderwall, D. E.; Green, D. V. S.; Kumar, V.; Hasan, S.; Brown, J. R.; Peishoff, C. E.; Cardon, L. R.; Garcia-Bustos, J. F. Thousands of chemical starting points for antimalarial lead identification. *Nature* **2010**, *465*, 305–310.

(29) Sanz, L. M.; Jiménez-Díaz, M. B.; Crespo, B.; De-Cozar, C.; Almela, M. J.; Angulo-Barturen, I.; Castañeda, P.; Ibañez, J.; Fernández, E. P.; Ferrer, S.; Herreros, E.; Lozano, S.; Martínez, M. S.; Rueda, L.; Burrows, J. N.; García-Bustos, J. F.; Gamo, F. J. Cyclopropyl carboxamides, a chemically novel class of antimalarial agents identified in a phenotypic screen. *Antimicrob. Agents Chemother.* **2011**, *55* (12), 5740–5745.

(30) Boulet, C.; Barnes, C. B. G.; Nguyen, W.; Dans, M. G.; Razook, Z.; McCann, K.; Barry, A. E.; Crabb, B. S.; Sleebs, B. E.; Gilson, P. R. Aryl N-acetamides compounds exert antimalarial activity by acting as agonists of rhomboid protease PfROM8 and cation channel PfCSC1. *bioRxiv* **2025**, DOI: 10.1101/2025.03.18.644039.

(31) Lin, J. W.; Meireles, P.; Prudêncio, M.; Engelmann, S.; Annoura, T.; Sajid, M.; Chevalley-Maurel, S.; Ramasar, J.; Nahar, C.; Avramut, C. M.; Koster, A. J.; Matuschewski, K.; Waters, A. P.; Janse, C. J.; Mair, G. R.; Khan, S. M. Loss-of-function analyses defines vital and redundant functions of the *Plasmodium* rhomboid protease family. *Mol. Microbiol.* **2013**, *88* (2), 318–338.

(32) Ramaprasad, A.; Blackman, M. J. A scaleable inducible knockout system for studying essential gene function in the malaria parasite. *Nucleic Acids Res.* **2025**, *53* (4), gkae1274.

(33) Baker, R. P.; Wijetilaka, R.; Urban, S. Two *Plasmodium* rhomboid proteases preferentially cleave different adhesins implicated in all invasive stages of malaria. *PLoS Pathog.* **2006**, *2* (10), No. e113.

(34) Gandhi, S.; Baker, R. P.; Cho, S.; Stanchev, S.; Strisovsky, K.; Urban, S. Designed parasite-selective rhomboid inhibitors block invasion and clear blood-stage malaria. *Cell Chem. Biol.* **2020**, *27* (11), 1410–1424.e6.

(35) Zhang, M.; Wang, C.; Otto, T. D.; Oberstaller, J.; Liao, X.; Adapa, S. R.; Udenze, K.; Bronner, I. F.; Casandra, D.; Mayho, M.; Brown, J.; Li, S.; Swanson, J.; Rayner, J. C.; Jiang, R. H. Y.; Adams, J. H. Uncovering the essential genes of the human malaria parasite *Plasmodium falciparum* by saturation mutagenesis. *Science* **2018**, *360* (6388), eaap7847.

(36) Martin, R. E. The transportome of the malaria parasite. *Biol. Rev. Camb. Philos. Soc.* **2020**, *95* (2), 305–332.

(37) Zhang, M.; Shan, Y.; Cox, C. D.; Pei, D. A mechanical-coupling mechanism in OSCA/TMEM63 channel mechanosensitivity. *Nat. Commun.* **2023**, *14* (1), 3943.

(38) Vinothkumar, K. R.; Pierrat, O. A.; Large, J. M.; Freeman, M. Structure of rhomboid protease in complex with β -lactam inhibitors defines the S2' cavity. *Structure* **2013**, *21* (6), 1051–1058.

(39) Yang, J.; Carvalho, L. A. R.; Ji, S.; Chen, S.; Moreira, R.; Verhelst, S. H. L. 4-Oxo- β -lactams as novel inhibitors for rhomboid proteases. *Chembiochem* **2023**, *24* (21), No. e202300418.

(40) Han, Y.; Zhou, Z.; Jin, R.; Dai, F.; Ge, Y.; Ju, X.; Ma, X.; He, S.; Yuan, L.; Wang, Y.; Yang, W.; Yue, X.; Chen, Z.; Sun, Y.; Corry, B.; Cox, C. D.; Zhang, Y. Mechanical activation opens a lipid-lined pore in OSCA ion channels. *Nature* **2024**, *628* (8009), 910–918.

(41) Grieve, A. G.; Yeh, Y. C.; Chang, Y. F.; Huang, H. Y.; Zarcone, L.; Breuning, J.; Johnson, N.; Štríšovský, K.; Brown, M. H.; Parekh, A. B.; Freeman, M. Conformational surveillance of Orail1 by a rhomboid intramembrane protease prevents inappropriate CRAC channel activation. *Mol. Cell* **2021**, *81* (23), 4784–4798.

(42) Sanz, L. M.; Crespo, B.; De-Cózar, C.; Ding, X. C.; Llergo, J. L.; Burrows, J. N.; García-Bustos, J. F.; Gamo, F. J. *P. falciparum* in vitro

killing rates allow to discriminate between different antimalarial mode-of-action. *PLoS One* **2012**, *7* (2), No. e30949.

(43) Reader, J.; van der Watt, M. E.; Birkholtz, L. M. Streamlined and robust stage-specific profiling of gametocytocidal compounds against *Plasmodium falciparum*. *Front. Cell Infect. Microbiol.* **2022**, *12*, 926460.

(44) Delves, M. J.; Miguel-Blanco, C.; Matthews, H.; Molina, I.; Ruecker, A.; Yahiya, S.; Straschil, U.; Abraham, M.; León, M. L.; Fischer, O. J.; Rueda-Zubiaurre, A.; Brandt, J. R.; Cortés, Á.; Barnard, A.; Fuchter, M. J.; Calderón, F.; Winzeler, E. A.; Sinden, R. E.; Herreros, E.; Gamo, F. J.; Baum, J. A high throughput screen for next-generation leads targeting malaria parasite transmission. *Nat. Commun.* **2018**, *9* (1), 3805.

(45) Bower-Lepts, C.; Rawat, M.; Keith, W. C.; Girling, G.; Luth, M. R.; Carolino, K.; Boroviak, K.; Coyle, R.; Schwach, F.; Smidt, C.; Bushell, E.; Moliner-Cubel, S.; Gomez-Lorenzo, M. D.; Gamo, F.-J.; Winzeler, E. A.; Billker, O.; Lee, M. C. S.; Rayner, J. C., A novel chemogenomic screening platform for scalable antimalarial drug target identification. *bioRxiv* **2024**, DOI: 10.1101/2024.08.27.609875.

(46) Nguyen, W.; Dans, M. G.; Currie, I.; Awalt, J. K.; Bailey, B. L.; Lumb, C.; Ngo, A.; Favuzza, P.; Palandri, J.; Ramesh, S.; Penington, J.; Jarman, K. E.; Mukherjee, P.; Chakraborty, A.; Maier, A. G.; van Dooren, G. G.; Papenfuss, T.; Wittlin, S.; Churchyard, A.; Baum, J.; Winzeler, E. A.; Baud, D.; Brand, S.; Jackson, P. F.; Cowman, A. F.; Sleebs, B. E. 7-N-Substituted-3-oxadiazole quinolones with potent antimalarial activity target the cytochrome bc(1) complex. *ACS Infect. Dis.* **2023**, *9* (3), 668–691.

(47) Gilson, P. R.; Tan, C.; Jarman, K. E.; Lowes, K. N.; Curtis, J. M.; Nguyen, W.; Di Rago, A. E.; Bullen, H. E.; Prinz, B.; Duffy, S.; Baell, J. B.; Hutton, C. A.; Jousset Subroux, H.; Crabb, B. S.; Avery, V. M.; Cowman, A. F.; Sleebs, B. E. Optimization of 2-anilino 4-amino substituted qinazolines into potent antimalarial agents with oral *in vivo* activity. *J. Med. Chem.* **2017**, *60* (3), 1171–1188.

(48) Ashton, T. D.; Dans, M. G.; Favuzza, P.; Ngo, A.; Lehane, A. M.; Zhang, X.; Qiu, D.; Chandra Maity, B.; De, N.; Schindler, K. A.; Yeo, T.; Park, H.; Uhlemann, A. C.; Churchyard, A.; Baum, J.; Fidock, D. A.; Jarman, K. E.; Lowes, K. N.; Baud, D.; Brand, S.; Jackson, P. F.; Cowman, A. F.; Sleebs, B. E. Optimization of 2,3-dihydroquinazolinone-3-carboxamides as antimalarials targeting PfATP4. *J. Med. Chem.* **2023**, *66* (5), 3540–3565.

(49) Love, M. I.; Huber, W.; Anders, S. Moderated estimation of fold change and dispersion for RNA-seq data with DESeq2. *Genome Biol.* **2014**, *15* (12), 550.

(50) Waterhouse, A.; Bertoni, M.; Bienert, S.; Studer, G.; Tauriello, G.; Gumienny, R.; Heer, F. T.; de Beer, T. A. P.; Rempfer, C.; Bordoli, L.; Lepore, R.; Schwede, T. SWISS-MODEL: homology modelling of protein structures and complexes. *Nucleic Acids Res.* **2018**, *46* (W1), W296–w303.

(51) Hall, M. P.; Unch, J.; Binkowski, B. F.; Valley, M. P.; Butler, B. L.; Wood, M. G.; Otto, P.; Zimmerman, K.; Vidugiris, G.; Machleidt, T.; Robers, M. B.; Benink, H. A.; Eggers, C. T.; Slater, M. R.; Meisenheimer, P. L.; Klaubert, D. H.; Fan, F.; Encell, L. P.; Wood, K. V. Engineered luciferase reporter from a deep sea shrimp utilizing a novel imidazopyrazinone substrate. *ACS Chem. Biol.* **2012**, *7* (11), 1848–1857.

(52) Cevenini, L.; Camarda, G.; Michelini, E.; Siciliano, G.; Calabretta, M. M.; Bona, R.; Kumar, T. R.; Cara, A.; Branchini, B. R.; Fidock, D. A.; Roda, A.; Alano, P. Multicolor bioluminescence boosts malaria research: quantitative dual-color assay and single-cell imaging in *Plasmodium falciparum* parasites. *Anal. Chem.* **2014**, *86* (17), 8814–8821.

(53) Ashton, T. D.; Calic, P. P. S.; Dans, M. G.; Ooi, Z. K.; Zhou, Q.; Palandri, J.; Loi, K.; Jarman, K. E.; Qiu, D.; Lehane, A. M.; Maity, B. C.; De, N.; Giannangelo, C.; MacRaild, C. A.; Creek, D. J.; Mao, E. Y.; Gancheva, M. R.; Wilson, D. W.; Chowdury, M.; de Koning-Ward, T. F.; Famodimu, M. T.; Delves, M. J.; Pollard, H.; Sutherland, C. J.; Baud, D.; Brand, S.; Jackson, P. F.; Cowman, A. F.; Sleebs, B. E. Property and activity refinement of dihydroquinazolinone-3-carbox-

amides as orally efficacious antimalarials that target PfATP4. *J. Med. Chem.* **2024**, *67* (16), 14493–14523.

(54) Delves, M. J.; Straschil, U.; Ruecker, A.; Miguel-Blanco, C.; Marques, S.; Dufour, A. C.; Baum, J.; Sinden, R. E. Routine *in vitro* culture of *P. falciparum* gametocytes to evaluate novel transmission-blocking interventions. *Nat. Protoc.* **2016**, *11* (9), 1668–1680.

(55) Awalt, J. K.; Ooi, Z. K.; Ashton, T. D.; Mansouri, M.; Calic, P. P. S.; Zhou, Q.; Vasanthan, S.; Lee, S.; Loi, K.; Jarman, K.; Penington, J.; Qiu, D.; Lehane, A. M.; Mao, E. Y.; Gancheva, M. R.; Wilson, D. W.; Giannangelo, C.; MacRaild, C. A.; Creek, D. J.; Yeo, T.; Sheth, T.; Fidock, D. A.; Churchyard, A.; Baum, J.; Famodimu, M. T.; Delves, M. J.; Kristan, M.; Stewart, L. B.; Sutherland, C. J.; de Koning-Ward, T. F.; Baud, D.; Brand, S.; Jackson, P. F.; Cowman, A. F.; Dans, M. G.; Sleebs, B. E. Optimization and characterization of N-acetamide indoles as antimalarials that target PfATP4. *J. Med. Chem.* **2025**, *68* (8), 8933–8966.